



# LUND UNIVERSITY

## Glacial history of Northeast Greenland: cosmogenic nuclide constraints on chronology and ice dynamics

Håkanson, Lena

2008

[Link to publication](#)

### *Citation for published version (APA):*

Håkanson, L. (2008). *Glacial history of Northeast Greenland: cosmogenic nuclide constraints on chronology and ice dynamics*. [Doctoral Thesis (compilation), Quaternary Sciences]. Department of Geology, Lund University.

### *Total number of authors:*

1

### **General rights**

Unless other specific re-use rights are stated the following general rights apply:

Copyright and moral rights for the publications made accessible in the public portal are retained by the authors and/or other copyright owners and it is a condition of accessing publications that users recognise and abide by the legal requirements associated with these rights.

- Users may download and print one copy of any publication from the public portal for the purpose of private study or research.
- You may not further distribute the material or use it for any profit-making activity or commercial gain
- You may freely distribute the URL identifying the publication in the public portal

Read more about Creative commons licenses: <https://creativecommons.org/licenses/>

### **Take down policy**

If you believe that this document breaches copyright please contact us providing details, and we will remove access to the work immediately and investigate your claim.

LUND UNIVERSITY

PO Box 117  
221 00 Lund  
+46 46-222 00 00

# LUNDQUA Thesis 61

---

## Glacial history of Northeast Greenland: cosmogenic nuclide constraints on chronology and ice dynamics

*Lena Håkansson*

### **Avhandling**

Att med tillstånd från Naturvetenskapliga Fakulteten vid Lunds Universitet för avläggande av filosofie doktorsexamen, offentligen försvaras i Geologiska Institutionens föreläsningssal Pangea, Sölvegatan 12, fredagen den 11 april 2008 kl. 13.15.

---

**Lund 2008**  
**Lund University, Department of Geology, Quaternary Sciences**

<b>Organization</b> LUND UNIVERSITY  Department of Geology, Quaternary Sciences	<b>Document name</b> DOCTORAL DISSERTATION	
	<b>Date of issue</b> 14 March 2008	
	<b>Sponsoring organization</b>	
<b>Author(s)</b> Lena Håkansson		
<b>Title and subtitle</b> Glacial history of Northeast Greenland: cosmogenic nuclide constraints on chronology and ice dynamics		
<b>Abstract</b> <p>The aim of this thesis was to use cosmogenic exposure dating to investigating whether highly weathered landscapes in the Northeast Greenland fjord zone have developed during prolonged ice free conditions or have been preserved beneath cold-based ice. Previous work along the Northeast Greenland coast has presented two conflicting hypotheses for the extent of the Greenland Ice Sheet during the last glacial maximum (LGM). Land-based investigations have suggested that low gradient outlet glaciers were restricted to fjord troughs and terminated at the inner continental shelf. In contrast, marine studies have recently indicated that the margin of the Greenland Ice Sheet reached the outer shelf during the LGM. Results from cosmogenic <sup>10</sup>Be and <sup>26</sup>Al exposure dating show that during the LGM, local cold-based ice-caps covered and preserved weathered interfjord plateaus in the Northeast Greenland fjord zone, whereas fjord troughs were filled up with dynamic ice draining the Greenland Ice Sheet. The dynamic ice reached at least 250 m a.s.l. at the mouth of Scoresby Sund at the southernmost end and probably ~600 m a.s.l. at the northernmost end of the fjord zone, indicating that there was a N-S gradient in glacial style presumably reflecting regional differences in topography of the coastal areas. The results presented in this thesis reveals a dynamic picture for the northeastern sector of the Greenland Ice Sheet suggesting that LGM ice margins were substantially more advanced than indicated by earlier reconstructions from the terrestrial record.</p>		
<b>Key words:</b> Cosmogenic, Greenland Ice Sheet, Glacial history, Ice dynamics, Scoresby Sund, Jameson Land, Store Koldewey		
<b>Classification system and/or index termes (if any):</b>		
<b>Supplementary bibliographical information:</b> 250 copies		<b>Language</b> English
<b>ISSN and key title:</b> 0281-3033 LUNDQUA Thesis		<b>ISBN</b> 978-91-87465-37-6
<b>Recipient's notes</b>	<b>Number of pages</b> 17 + 4 app.	<b>Price</b> 120 SEK
	<b>Security classification</b>	

**Distribution by (name and address)**

I, the undersigned, being the copyright owner of the abstract of the above-mentioned dissertation, hereby grant to all reference sources permission to publish and disseminate the abstract of the above-mentioned dissertation.

Signature  Date 2 March 2008

# Glacial history of Northeast Greenland: cosmogenic nuclide constraints on chronology and ice dynamics

Lena Håkansson

Quaternary Sciences, Department of Geology, GeoBiosphere Science Centre,  
Lund University, Sölvegatan 12, SE-223 62 Lund, Sweden

This thesis is based on four papers listed below (Appendices I-IV). All papers are published in or submitted to peer-reviewed international journals. Papers I and IV are reproduced with permission from Elsevier Ltd. and Blackwell publishing, respectively. Papers II and III have been submitted to the journals indicated. In the following, the papers are referred to by their Roman numeral.

## Appendix I

Håkansson, L., Briner, J., Alexanderson, H., Aldahan, A. & Possnert, G. 2007.  $^{10}\text{Be}$  ages from coastal east Greenland constrain the extent of the Greenland Ice Sheet during the Last Glacial Maximum. *Quaternary Science Reviews* 26, 2316-2321.

## Appendix II

Håkansson, L., Briner, J.P., Aldahan, A. & Possnert, G.  $^{10}\text{Be}$  and  $^{26}\text{Al}$  exposure ages of tors and meltwater channels on Jameson Land, east Greenland: implications for the Late Quaternary glaciation history. Manuscript submitted to *Quaternary Research*.

## Appendix III

Håkansson, L., Alexanderson, H., Hjort, C., Möller, P., Briner, J.P., Aldahan, A. & Possnert, G. The late Pleistocene glacial history of Jameson Land, central East Greenland derived from cosmogenic  $^{10}\text{Be}$  and  $^{26}\text{Al}$  exposure dating. Manuscript submitted to *Boreas*.

## Appendix IV

Håkansson, L., Graf, A., Strasky, S., Ivy-Ochs, S., Kubik, P.W., Hjort, C. & Schlüchter, C. 2007. Cosmogenic  $^{10}\text{Be}$ -ages from the Store Koldewey island, NE Greenland. *Geografiska Annaler* 89A (3), 195-202.



# Contents

<b>1.</b>	<b>Introduction</b> .....	1
1.1	<i>Background</i> .....	1
1.1.1	<i>The Canadian Arctic</i> .....	3
1.1.2	<i>Svalbard</i> .....	3
1.2	<i>Aims of the present study</i> .....	3
<b>2.</b>	<b>Study areas</b> .....	4
<b>3.</b>	<b>Cosmogenic nuclides</b> .....	6
3.1	<i>History</i> .....	6
3.2	<i>Theory</i> .....	6
3.3	<i>Cosmogenic exposure dating</i> .....	7
<b>4.</b>	<b>Results: summary of papers</b> .....	8
4.1	<i>Paper I</i> .....	9
4.2	<i>Paper II</i> .....	9
4.3	<i>Paper III</i> .....	10
4.4	<i>Paper IV</i> .....	10
<b>5.</b>	<b>Discussion</b> .....	11
5.1	<i>Rethinking the extent and dynamics of the Greenland Ice Sheet during the LGM</i> ....	11
5.2	<i>Methodological considerations</i> .....	12
<b>6.</b>	<b>Conclusions</b> .....	12
<b>7.</b>	<b>Ideas for future research</b> .....	13
<b>8.</b>	<b>Acknowledgements</b> .....	13
<b>9.</b>	<b>Swedish summary</b> .....	13
	<b>References</b> .....	15
	<b>Appendices</b>	



## 1. Introduction

### 1.1 Background

During periods of the last glacial cycle, ice sheets covered vast continental areas. At present, the Greenland Ice Sheet is the only larger remain from this time in the Northern Hemisphere. Nevertheless, this ice sheet still stores enormous volumes of freshwater and changes in this ice mass might have considerable consequences for the global climate and environment. Studying the history of the Greenland Ice Sheet is thus important for understanding the climate during glacial cycles, which in turn can shed light on what might happen to the ice sheet and the global climate in the nearest future.

Within formerly glaciated regions, the occurrence of highly weathered terrain has often been used as evidence either for the existence of ice free areas during the last glaciation (Ives, 1966; Nesje & Dahl, 1990; Ballantyne et al., 1998; Rae et al., 2004) or for the former distribution of cold-based ice allowing the preservation of pre-Quaternary landscapes (Sugden, 1978; Kleman, 1994; Sollid & Sørbel, 1994; Kleman & Hättestrand, 1999; Davis et al., 2006). Because highly weathered landscapes are often found on upland plateaus, the interpretation of these landscapes can constrain ice thickness and/or the thermal regime of Pleistocene ice sheets.

In the Northeast Greenland fjord zone, which comprises the presently ice-free continental margin between Scoresby Sund in the south and Germania Land in the north (Fig. 1A), interfjord plateaus and coastal lowlands are commonly strongly weathered, whereas fjords and major valleys are characterized by glacially eroded surfaces. The Late Pleistocene glacial history of this area has been reconstructed through decades of research, and based on intense bedrock weathering and the lack of deposits from the last glaciation many interfjord areas were thought to have been ice-free

throughout the last glacial cycle (e.g. Washburn, 1965; Lasca, 1969; Funder & Hjort, 1973; Hjort, 1979, 1981; Björck & Hjort, 1984; Funder & Hansen, 1996; Funder et al., 1994, 1998; Hansen et al., 1999). These studies thus described a last glacial maximum (LGM) scenario with outlet glaciers from the Greenland Ice Sheet restricted to the fjord troughs and terminating on the inner continental shelf. Similar reconstructions of limited LGM ice extent were also presented for Svalbard (Boulton 1979) and for the Canadian Arctic (Dyke & Prest, 1987), suggesting a minimalist glaciation scenario throughout the Arctic during the LGM.

The concept of restricted LGM glaciation in the Northeast Greenland fjord zone has, however, recently been challenged by marine data. Seismic profiling indicates the presence of a prominent moraine c. 50 km from the shelf break off the Kejsar Franz Joseph Fjord (Fig. 1A), interpreted to be a LGM terminal or recessional moraine (Evans et al., 2002). Furthermore, submarine channels, emanating from the lip of shelf troughs down the continental slope, have been interpreted as generated by a grounded ice sheet margin on the outer shelf or at the shelf break (Ó Cofaigh et al., 2004). Both these studies thus suggest grounded ice on the Northeast Greenland shelf during the LGM, but are not giving any further evidence of ice cover on land. However, Wilken & Minert (2006) suggested that channels on the shelf slope could rather have formed by outlet glaciers restricted to cross-shelf troughs and terminating some distance out on the shelf.

In recent years, cosmogenic exposure dating methods have provided new techniques to interpret differentially weathered landscapes (Stroeven et al., 2002; Fabel et al., 2002; Briner et al., 2003, 2005, 2006; Landvik et al., 2003; Marquette et al., 2004; Davis et al., 2006; Harbour et al., 2006) and in combination with new marine coring and imaging techniques this has led to a new understanding of the extent and dynamics of Late



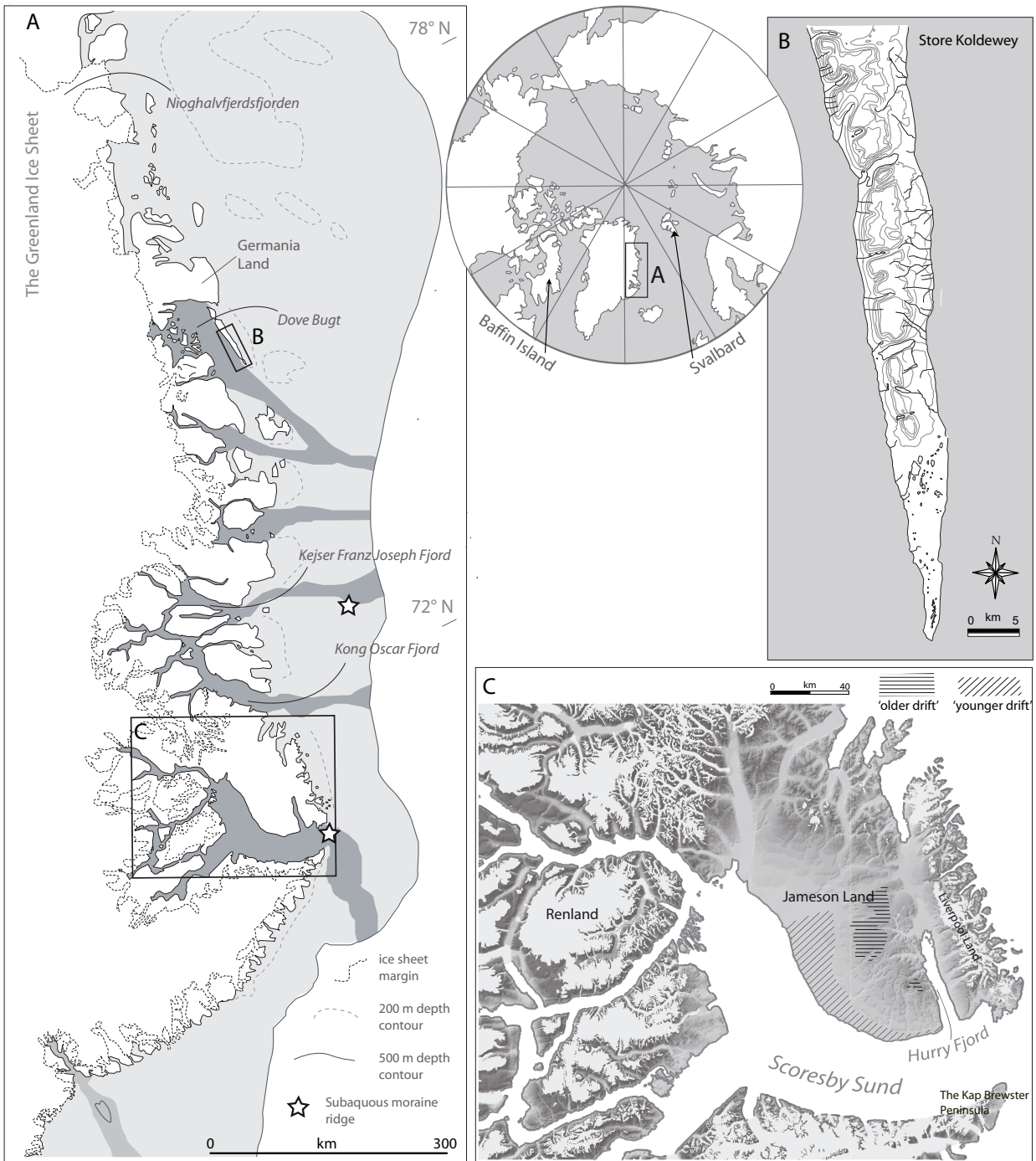


Figure 1. A. Map of Northeast Greenland. Study areas are marked with framed boxes and subaqueous moraine ridges are marked with stars at the mouth of Scoresby Sund (Dowdeswell et al., 1994) and on the shelf off the Kejser Franz Joseph Fjord (Evans et al., 2002). B. Map of the Store Koldewey island with 100 m contour lines. C. The Scoresby Sund area with distribution of 'older' and 'younger drift' after Ronnert & Nyborg (1994) and Möller et al. (1994)

Pleistocene ice sheets in differentially weathered fjord zones elsewhere in the Arctic.

### 1.1.1 The Canadian Arctic

Field investigations on eastern Baffin Island (Fig. 1A) identified areas with differences in the degree of weathering, so called weathering zones, which were used to suggest restricted glaciation in the eastern Canadian Arctic during the LGM (Pheasant & Andrews, 1973; Boyer & Pheasant, 1974). In the 1980s seismic stratigraphy (MacLean et al., 1986) and marine cores from the continental shelf off Baffin Island (Jennings et al., 1996) revealed evidence for grounded ice in these areas, challenging the minimalist concept presented by earlier studies. Recently, Baffin Island has been the focus of several studies applying cosmogenic exposure dating to weathering zone research. Bierman et al. (1999) obtained cosmogenic  $^{26}\text{Al}$  and  $^{10}\text{Be}$  data from tors in the southern part of the island, indicating that sampled surfaces had experienced multiple periods of exposure interrupted by shielding by non-erosive cold-based ice. Based on cosmogenic exposure dating and lake cores Miller et al. (2001) suggested that the southernmost part of Baffin Island was inundated by the LGM Laurentide Ice Sheet but that coastal interfjord uplands remained ice free. However, more recent work indicates that the LGM ice was even more extensive further to the north on Baffin Island. There, analyses of cosmogenic exposure dating suggests LGM ages for erratics perched on highly weathered inter-fjord plateaus and coastal lowlands, implying that cold-based ice dynamically connected to the Laurentide Ice Sheet covered these areas while ice streams filled the fjords (Briner et al., 2003, 2006).

### 1.1.2 Svalbard

During several decades it has been debated whether ice-free areas existed on Svalbard (Fig. 1A) during the LGM (e.g. Salvigsen, 1977; Forman,

1989; Mangerud et al., 1998). Based on cosmogenic  $^{10}\text{Be}$  exposure dating of erratics and bedrock, Landvik et al. (2003) presented evidence for the existence of nunataks on northwest Svalbard. Their results indicated that the last ice sheet that covered islands in the northwest retreated more than 80 ka ago and OSL dates of raised marine sediments close to the present-day sea level constrain the deglaciation after the last ice sheet advance to ~50 ka (Landvik et al., 2003). However, seismic stratigraphy and marine cores from further to the south on the continental shelf off western Svalbard have shown evidence for grounded LGM ice at the shelf-break (Landvik et al., 2005). Based on this they now suggest a topographically controlled LGM ice sheet configuration with ice streams filling the fjords and shelf troughs, with less dynamic ice over interfjord areas preserving delicate pre-LGM deposits. High resolution sea floor mapping on the shelf off northern and western Svalbard has revealed mega-scale lineations in cross shelf troughs suggesting that a topographically controlled ice sheet reached the shelf break around almost all of western and northern Svalbard (Ottensen et al., 2007).

### 1.2 Aims of the present study

In Northeast Greenland two conflicting hypotheses have been presented, from terrestrial and marine records, respectively: (i) extensive coastal areas were ice free whereas glacial ice filled the fjords as low gradient outlet glaciers terminating at the inner continental shelf or, (ii) the margin of the Greenland Ice Sheet reached all the way to the outer shelf or even to the shelf-break.

The aim of this thesis is to evaluate these two hypotheses, by applying cosmogenic exposure dating to erratics and bedrock in weathered interfjord areas in Northeast Greenland. A key objective is also to constrain the thermal regimes of the Late Pleistocene ice sheet advances, by investigating whether highly weathered landscapes along the Northeast Greenland coast have developed during prolonged



Figure 2. A. The summit plateau of the Store Koldewey island, looking north. B. Boulder on the summit plateau of Store Koldewey. C. Unconsolidated landforms of the 'older drift' on interior Jameson Land. D. Weathered sandstone bedrock. E. Tors on interior Jameson Land. F. Sampling of erratic boulder resting on regolith adjacent to tor-rich areas.

ice free conditions or have been preserved beneath cold-based ice.

## 2. Study areas

Fieldwork was conducted during four summer expeditions in 2003–2006 and samples for cosmogenic exposure dating presented in this thesis were collected from two areas in Northeast Greenland: the Store Koldewey island (76 °N) in the northernmost part and the Scoresby Sund area

(70–71 °N) in the southernmost part of the fjord zone (Fig. 1A).

The possibility arose to work on the Store Koldewey island in connection with the Greenland Sea cruise of the German research vessel “Polarstern” in the summer of 2003. This island is ~100 km long and situated at the outlet of the Dove Bugt Embayment blocks the outlet for major glacial advances from the Dove Bugt embayment (Fig. 1A). The landscape is dominated by mountain plateaus (~600–900 m a.s.l.) commonly cut by U-shaped

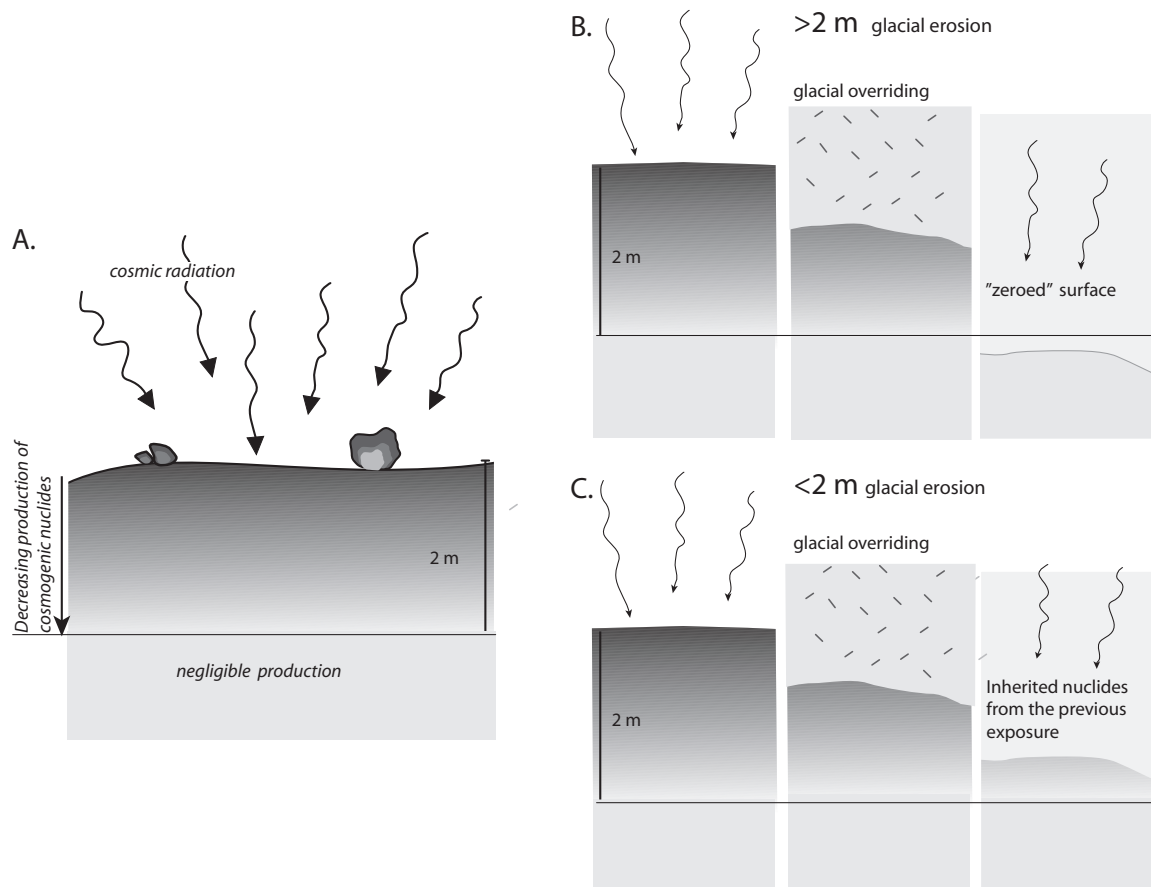


Figure 3. A. Cosmic radiation can produce cosmogenic nuclides in bedrock and boulders. The production takes place in the uppermost ~2 m of rock and decreases exponentially with depth. B. An example where a bedrock surface is overridden by glacial ice which erodes away >2 m of rock and thus all cosmogenic nuclides produced during the previous exposure are eroded away. When the bedrock surface again gets exposed following ice retreat, it is "zeroed" from old nuclides. C. In this example overriding ice erodes <2 m of rock resulting in that following deglaciation the exposed bedrock surface will still contain nuclides from the previous exposure

valleys trending from west to east (Figs 1B, 2A). Cosmogenic exposure dating results from boulders sampled on these plateaus (Fig. 2B) are presented in Paper IV.

The main fieldwork area during this project was the Jameson Land peninsula north of Scoresby Sund (Fig. 1C). Here three summer field seasons were spent in 2004–2006. In addition, a one-day helicopter trip took us to the Kap Brewster peninsula, on the southern side and at the very mouth of the fjord. Erratic boulders were sampled on the Kap Brewster Peninsula (Paper I) and samples from both erratics and bedrock were collected from interior Jameson Land (Fig. 2F; Papers II, III).

The Jameson Land Peninsula is composed of Mesozoic sedimentary rocks, mostly sandstone,

and has an asymmetric topographic profile. From the interior plateau areas the terrain gently slopes towards Scoresby Sund in the west and south whereas the eastern margin, facing Hurry Fjord, has a steeper gradient (Fig. 1C). On Jameson Land two areas covered with Late Pleistocene sediments have been identified: the 'older-drift' on the central plateaus (Fig. 2C) and the 'younger drift' on the lowlands along the Scoresby Sund coast (Fig. 1C; Möller et al., 1994; Ronnert & Nyborg, 1994). Between these two sediment covered regions the sandstone landscape is highly weathered, exhibiting blockfields and well-developed tors (Figs 2D, E).

### 3. Cosmogenic nuclides

#### 3.1 History

Already in the 1950's it was proposed by Davies & Schaffer (1955) that cosmogenic isotopes produced within minerals could be applied to geological problems. At that time all studies of the interactions between cosmic rays and minerals were restricted to meteorites because production rates in terrestrial rocks were much too low for the analytical instrumentation available. Until the early 1980's and the development of accelerator mass spectrometry (AMS) the studies of cosmogenic isotopes produced in terrestrial rocks stayed on a theoretical level (Lal & Peters, 1967). With AMS it finally became possible to measure even the extremely low concentrations of cosmic ray-derived isotopes within rocks from the surface of the Earth. Since the first studies demonstrating the usefulness of AMS for routine measurements of cosmogenic nuclides (Nishiizumi et al., 1986; Phillips et al., 1986), the use of cosmogenic nuclides to earth science related problems has increased significantly and this method is still continuously developing. One of the more common general applications to this technique has been to use the cosmogenic nuclide concentrations in a particular rock surface to estimate the time it has been exposed to cosmic radiation, so called cosmogenic exposure dating. If we can assume that a surface is related to a specific geologic event (e.g. a glaciation), then cosmogenic exposure dating provides means of directly dating this event.

#### 3.2 Theory

Cosmic ray particles entering the Earth's atmosphere produce a cascade of secondary radiation, which in turn can produce cosmogenic nuclides (e.g.  $^{10}\text{Be}$ ,  $^{14}\text{C}$ ,  $^{21}\text{Ne}$ ,  $^{26}\text{Al}$ ,  $^{36}\text{Cl}$ ) in the atmosphere but also within minerals in the uppermost ~2 m of the lithosphere, so called terrestrial cosmogenic nuclides

(Fig. 3A; Gosse & Phillips, 2001). The cosmic ray intensity is significantly reduced closer to the surface of the Earth which causes nuclide production rates to be much lower in rocks compared to the production rates in the atmosphere. Neutrons are those secondary cosmic ray particles responsible for the larger part of the production of terrestrial cosmogenic nuclides. A small fraction of the production is, however, caused by protons and muons.

For cosmogenic exposure dating purposes the most commonly used terrestrial cosmogenic nuclides are  $^{10}\text{Be}$  and  $^{26}\text{Al}$ , which are often measured in quartz separates. There are several reasons for choosing quartz; it has a simple structure, is widely distributed in rocks at the surface of the Earth and  $^{10}\text{Be}$  and  $^{26}\text{Al}$  production rates are high within quartz. It is also a relatively resistant mineral and thus easy to separate from other minerals using selective mineral dissolution with dilute acids (Kohl & Nishiizumi, 1992).

The rate at which cosmogenic isotopes are produced in the lithosphere is a function of altitude, latitude and time. The cosmic ray flux increases with higher altitude as air pressure and the shielding effect of the atmosphere decrease. At low latitudes the geomagnetic field will repel more incoming cosmic radiation, resulting in lower production rates compared to areas closer to the poles. In addition, changes in the geomagnetic field intensity will influence cosmic ray flux at low latitudes through time, but can be ignored for high latitudes. However, changes in air pressure over longer time periods might influence production rates on all latitudes. Such changes might be caused by the redistribution of high and low pressure systems due to climatic changes.

Cosmogenic exposure dating depends on correct determination of production rates. At any particular sampling site, two parameters are required to calculate the site specific production rate: (i) a scaling scheme describing the variation in production rates with time, elevation and latitude and, (ii) a reference production rate that is usually taken at present time,

sea level and high geomagnetic latitude. Several different scaling schemes have been suggested for the normalization of data to sea level exposure at high latitudes (Lal, 1991; Stone, 2000; Dunai, 2001; Lifton et al., 2005; Desilets et al., 2006). The most commonly used scaling scheme is the one first developed by Lal (1991) and later modified by Stone (2000), which is also used in this study.

### 3.3 Cosmogenic exposure dating

The calculation of nuclide exposure ages based on a single nuclide, e.g.  $^{10}\text{Be}$ , relies on the assumptions that the sampled surface has, (i) been constantly exposed and lacks inherited isotopes from previous exposures (requiring at least ~2 m of glacial erosion, Davis et al., 1999; Briner et al., 2006) and, (ii) experienced only minimal postdepositional erosion. These requirements will be fulfilled for most scoured bedrock surfaces and erratics in settings where substantial glacial erosion (>2 m) have taken place (Fig. 3B). Also, the texture of a surface (e.g. glacial striae) can provide strong evidence for negligible postdepositional erosion. Under these ideal circumstances a single nuclide may define the actual exposure age of a surface. However, in many cases the nuclide concentrations will reflect at least two variables; exposure and erosion. In terrain that has been covered by cold-based ice, or ice eroding <2m (Fig. 3C) nuclide concentrations might, in addition, reflect a third variable and that is shielding from cosmic radiation for substantial periods of time.

By measuring two radionuclides with different half-lives in the same sample, e.g.  $^{10}\text{Be}$  and  $^{26}\text{Al}$ , complex exposure/erosion/shielding histories can be constrained. Normally, the  $^{26}\text{Al}/^{10}\text{Be}$  ratio is plotted against the logarithm of measured  $^{10}\text{Be}$  concentration (Fig. 4; Lal, 1991; Bierman et al., 1999; Gosse & Phillips, 2001). The  $^{26}\text{Al}/^{10}\text{Be}$  ratio of a particular sample can plot in four areas in this diagram, all describing different sample histories which is shown graphically in Figure 4 and explained below.

I. Samples which have experienced constant

exposure with no erosion will plot on the “constant exposure curve”. In a continuously exposed surface  $^{10}\text{Be}$  and  $^{26}\text{Al}$  will be produced at a constant ratio ( $^{26}\text{Al}/^{10}\text{Be}=6.1$ ). If a surface is exposed for long enough (>100 ka), then the faster decay of  $^{26}\text{Al}$  (half-life of 700 ka) relative to  $^{10}\text{Be}$  (half-life of 1.3 Ma; Fink & Smith, 2007) will lead to a gradual decrease in the  $^{26}\text{Al}/^{10}\text{Be}$  ratio which is reflected in the ‘banana-shape’ of the constant exposure curve in Figure 4A. Examples are shown for where on the constant exposure curve a sample would plot if it has been exposed for 100, 400 or 800 ka, respectively (Fig. 4A). Saturation is reached at the endpoint of this curve, which means that the production of  $^{10}\text{Be}$  and  $^{26}\text{Al}$  equals the loss of radionuclides through decay.

II. Any constantly exposed eroding surface will plot within the so called “steady state erosion island” (Lal, 1991). If a sample has experienced constant, gradual and continuous erosion, then it would plot on the curve for the specific erosion rate. Figure 4A shows examples of erosion curves for three different erosion rates ( $e=1, 3$  and  $10 \text{ mm ka}^{-1}$ ). In an eroding surface, saturation will be reached at lower nuclide concentrations as shown by the end-points of erosion curves. The lower boundary of the erosion island, shown with a dashed line, represents the continuum of erosion end points resulting from a range of possible erosion rates.

III. Samples plotting below the “steady-state erosion island” indicate that exposure has been interrupted by one or several shielding events. If the surface gets partly or entirely shielded from cosmic radiation, e.g. by non-erosive ice, then this will lead to a decrease in the  $^{26}\text{Al}/^{10}\text{Be}$  ratio due to the faster decay of  $^{26}\text{Al}$  relative to  $^{10}\text{Be}$ . When a surface gets exposed again the  $^{26}\text{Al}/^{10}\text{Be}$  ratio will increase. The distance below the “steady-state erosion island” is proportional to the duration of shielding. Bierman et al. (1999) described three classes of complex exposure

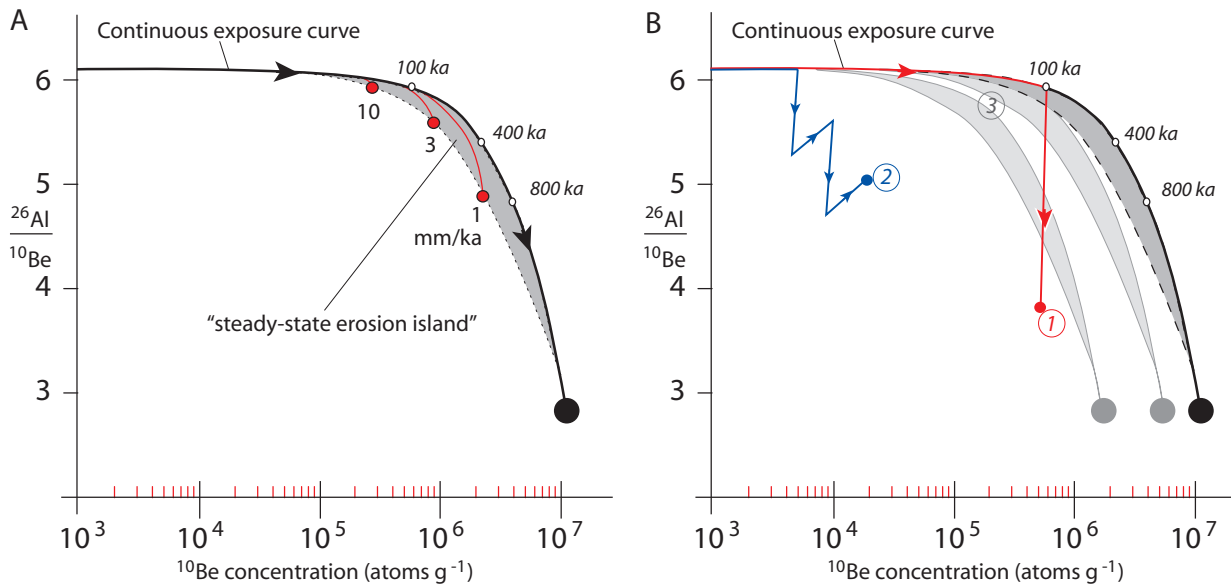


Figure 4. Two-isotope diagrams for interpreting  $^{10}\text{Be}$  and  $^{26}\text{Al}$  measurements.

histories and examples of these are shown in Figure 4B: The red line (1) shows continuous surface exposure without erosion for  $\sim 100$  ka, followed by  $\sim 400$  ka of burial by sufficiently thick ice or sediment. The blue zigzagged curve (2) shows how nuclide concentrations can evolve in a sample which had repeated periods of burial and exposure. The amplitude of this curve will be controlled by the duration of each exposure and burial period. The shaded area (3) shows exposure under cover, implying that a surface was only partly shielded from cosmic radiation by, e.g., sediment, snow or thin ice. The “steady-state erosion island” will be displaced to the left in the diagram as the shielding increases.

IV. Samples with  $^{26}\text{Al}/^{10}\text{Be}$  ratios higher than the production ratio of 6.1 will plot above the “constant exposure curve” and can not be explained by any combination of exposure, erosion and shielding. Such high ratios might be due to problems during preparation or AMS measurement. It seems to be more common for samples with young exposure ages to plot above the constant erosion curve. This might be because low nuclide concentrations will be

more sensitive to process blank correction. As an example, if the Be-blank was too high or the Al-blank too low, then this might have a disproportionate effect on the  $^{26}\text{Al}/^{10}\text{Be}$  ratios, driving them upward on the plot.

Where a rock or boulder surface has been shielded from cosmic radiation for long periods (a total of  $\sim 200$  ka or longer), the  $^{10}\text{Be}$  and  $^{26}\text{Al}$  concentrations can be used to calculate a minimum total exposure and total burial duration in accordance to the red line in Figure 4B. An important limitation with this approach is that the  $^{26}\text{Al}/^{10}\text{Be}$  ratios do not evolve significantly during shorter periods (tens of thousands of years) and thus shorter periods of cold-based ice cover can not be resolved by this approach.

#### 4. Results: summary of papers

Several researchers have contributed to this project. Those who have been involved in data contribution and preparation of the manuscripts appear as authors on Paper I-IV. Contributions are summarized in Table 1.

Task	Paper I	Paper II	Paper III	Paper IV
<b>Fieldwork</b>	Håkansson, L. Alexanderson, H.	Håkansson, L.	Håkansson, L. Alexanderson, H. Hjort, C.	Håkansson, L.
<b>Participating in fieldwork</b>		Elizabeth Thomas	Elizabeth Thomas	Ole Bennike, Holger Cremer Nadja Hultzsch Martin Klug Svenja Kobabe Berndt Wagner
<b>Sample preparation for cosmogenic exposure dating</b>	Håkansson, L.	Håkansson, L.	Håkansson, L.	Graf, A. Strasky, S.
<b>Providing cosmo lab facilities</b>	Briner, J.P. Dept. Geol., Buffalo, NY	Briner, J.P. Dept. Geol., Buffalo, NY	Briner, J.P. Dept. Geol., Buffalo, NY	Schlüchter, C. Inst. Geo. Sci., Bern
<b>AMS and target packing</b>	Possnert, G. Aldahan, A. Uppsala	Possnert, G. Aldahan, A. Uppsala	Possnert, G. Aldahan, A. Uppsala	Kubik, P. Ivy-Ochs, S. ETH Zürich
<b>Data interpretation</b>	Håkansson, L. Briner, J.P.	Håkansson, L. Briner, J.P.	Håkansson, L. Alexanderson, H. Hjort, C. Möller, P.	Håkansson, L.

Table 1. Contributors to the research results presented in Papers I-IV.

#### 4.1 Paper I

Håkansson, L., Briner, J., Alexanderson, H., Aldahan, A., Possnert, G. 2007. <sup>10</sup>Be ages from coastal east Greenland constrain the extent of the Greenland Ice Sheet during the Last Glacial Maximum. *Quaternary Science Reviews* 26, 2316-2321.

Paper I reports on <sup>10</sup>Be-ages from four erratic boulders perched at c. 250 m a.s.l. on the Kap Brewster peninsula at the mouth of Scoresby Sund. The average <sup>10</sup>Be-ages, calculated with an assumed maximum erosion rate of 1 cm ka<sup>-1</sup> and no erosion (respectively, 17.3 ± 2.3 ka and 15.1 ± 1.7 ka) overlap with a period of increased sediment input to the Scoresby Sund fan (19-15 ka). These results suggest that active ice channeled in the Scoresby Sund trough reached at least 250 m above the present sea level at the mouth of the fjord during the LGM. This implies that the LGM ice margin reached further out on the continental shelf than has hitherto been assumed. It is also suggested that active ice in the fjord during may have been buttressed to the north by cold-based ice, thus giving indirect evidence for

the presence of ice on the Jameson Land peninsula during the LGM.

#### 4.2 Paper II

Håkansson, L., Briner, J.P., Aldahan, A., Possnert, G. <sup>10</sup>Be and <sup>26</sup>Al exposure ages of tors and meltwater channels on Jameson Land, east Greenland: implications for the Late Quaternary glaciation history. Submitted to *Quaternary Research*.

Paper II presents <sup>10</sup>Be and <sup>26</sup>Al results from the weathered sandstone landscapes of interior Jameson Land and aims at testing for the preservation of tors and to investigate if the area was indeed covered by ice during the LGM as indirectly indicated in Paper I. Samples were collected from three different surface types; (i) the top surfaces of tors, (ii) the bottoms of meltwater channels and, (iii) fluvially eroded outcrops adjacent to channels. Isotope concentrations indicate that tors have been preserved through multiple glacial cycles beneath cold-based ice, whereas the average <sup>10</sup>Be exposure age of 16.9 ± 2.4 ka on meltwater channels suggests that these



were eroded after the LGM.

It is proposed that the sandstone landscapes on interior Jameson Land evolved by three main processes during at least the last two glacial cycles: (i) during interglacial and interstadial periods of exposure, sandstone surfaces weathered at a rate of  $\sim 10 \text{ mm ka}^{-1}$ , (ii) during periods of burial by cold-based ice, weathered rock slabs might have been decoupled from tors by entrainment of cold-based ice and, (iii) during deglaciations, meltwater followed existing fracture systems in the sandstone and eroded areas between tors by  $>2 \text{ m}$ . Paper II presents evidence for that Jameson Land was at least partly covered by cold-based ice during the LGM, but it does not conclude whether this ice was local or dynamically connected to the Greenland Ice Sheet.

#### 4.3 Paper III

*Håkansson, L., Alexanderson, H., Hjort, C., Möller, P., Briner, J., Aldahan, A., Possnert, G. The late Pleistocene glacial history of Jameson Land, central East Greenland, derived from cosmogenic  $^{10}\text{Be}$  and  $^{26}\text{Al}$  exposure dating Submitted to Boreas.*

The main objective of Paper III is to test whether or not the Greenland Ice Sheet covered Jameson land during the LGM, by using cosmogenic  $^{10}\text{Be}$  and  $^{26}\text{Al}$  exposure dating on erratics sampled from the central parts of the peninsula.  $^{10}\text{Be}$ -ages from a total of 44 erratics, resting both on weathered sandstone and sediment-covered surfaces, range between 10.7 and 262.1 ka. Eight erratics from weathered sandstone and till surfaces cluster around  $\sim 70 \text{ ka}$  whereas  $^{10}\text{Be}$ -ages from glaciofluvial landforms are substantially younger and range between 10.7 and 46.6 ka. Deflation is thought to be an important process on the sediment covered surfaces and the youngest exposure ages from such settings are suggested to result from exhumation. The older ( $>70 \text{ ka}$ ) samples have discordant  $^{26}\text{Al}$  and  $^{10}\text{Be}$  data and are interpreted to have been deposited by the Greenland Ice Sheet several glacial cycles ago. The

younger exposure ages ( $\leq 70 \text{ ka}$ ) are interpreted to represent deposition by a Late Saalian Greenland Ice Sheet advance but also by an early Weichselian advance from a local Liverpool Land-based ice-cap. The exposure ages younger than Saalian are explained by periods of shielding by cold-based ice during the Weichselian.

Paper III supports previous studies in that the Saalian ice sheet advance was the last to deposit thick sediment sequences and western erratics on interior Jameson Land. However, instead of Jameson Land being ice-free throughout the Weichselian it is documented that local cold-based ice covered and shielded large areas for substantial periods during the last glacial cycle.

#### 4.4 Paper IV

*Håkansson, L., Graf, A., Strasky, S., Ivy-Ochs, S., Kubik, P., Hjort, C., Schlüchter, C. 2007. Cosmogenic  $^{10}\text{Be}$ -ages from the Store Koldewey island, NE Greenland. *Geografiska Annaler* 89A (3), 195-202.*

The aim of Paper IV is to test whether or not the Store Koldewey island on the outer coast of Northeast Greenland was overridden by the Greenland Ice Sheet during the LGM. A total of seven samples for cosmogenic exposure dating were collected from weathered bedrock and boulders on the summit plateau of the island and from a moraine ridge on the glacially scoured lowland adjacent to the fjord. Among the samples from the summit plateaus, the two southernmost boulders give young exposure ages ( $11.5 \pm 0.7$  and  $14.6 \pm 0.8 \text{ ka}$ ), in contrast to the rest of the boulders ( $27.6 \pm 1.6$  and  $79.1 \pm 3.1 \text{ ka}$ ). Samples from weathered bedrock also give older ages ( $42.2 \pm 2.2 \text{ ka}$  and  $147.1 \pm 5.0 \text{ ka}$ ). A sampled boulder from the moraine ridge yields a  $^{10}\text{Be}$  exposure age of  $13.1 \pm 0.9 \text{ ka}$ .

Based on these exposure ages, Paper IV suggests that unscoured mountain plateaus at the outer coast in Northeast Greenland were covered, at least partly, by cold-based ice during the LGM. Because the dataset is small and all sampled boulders consist

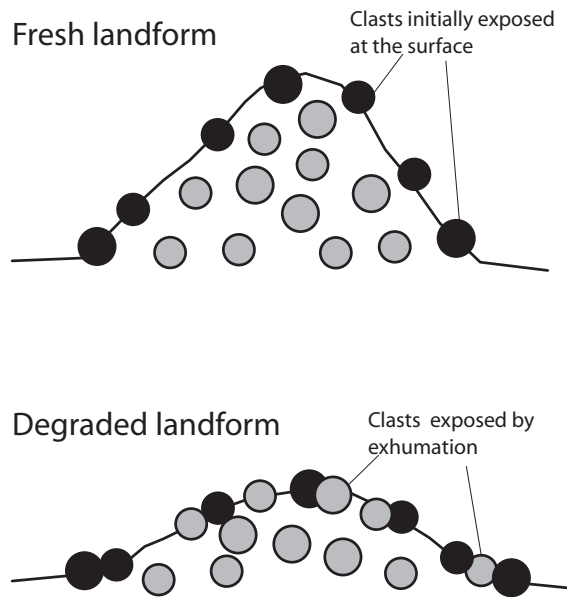


Figure 5. Degradation of unconsolidated landforms occurs as fine grained matrix is transported down slope by the action of wind, water and creep. Clasts initially exposed at the surface of the fresh landform are illustrated by black circles whereas clasts deposited within the landform are grey. As the landform degrades clasts are exhumed at the surface. Exhumed clasts will give anomalously young exposure ages.

of local bedrock, it is, however, left open whether the ice here was dynamically connected to the Greenland Ice Sheet or not. Regardless of the LGM ice sheet extent, this paper adds to a growing body of evidence suggesting considerable antiquity of crystalline unscoured terrain proximal to great ice sheets.

## 5. Discussion

### 5.1 Rethinking the extent and dynamics of the Greenland Ice Sheet during the LGM

In the Scoresby Sund area cosmogenic exposure dating results have contributed with three lines of evidence for testing the two contrasting hypotheses presented for the LGM extent of the ice sheet in the Northeast Greenland fjord zone (Papers I-III). The first piece in this jig-saw puzzle was presented in Paper I, which shows evidence for active ice at

the mouth of the Scoresby Sund trough reaching at least 250 m a.s.l., thus implying that the LGM ice margin reached further out on the continental shelf than has hitherto been assumed. It is also suggested that active ice in the fjord during the LGM may have been buttressed to the north by cold-based ice, thus giving indirect evidence for the presence of ice on the Jameson Land peninsula. Presented in Paper II, LGM exposure ages of meltwater channels on interior Jameson Land indeed show the presence of cold-based ice. In addition, Paper III presents exposure ages of erratics showing no indications of material transport by the Greenland Ice Sheet onto interior Jameson Land during the LGM. From these three lines of evidence a LGM scenario evolves for the Scoresby Sund area where local, mostly cold-based, ice-caps covered Jameson Land and coalesced with active ice in Scoresby Sund.

Paper IV presents exposure ages from the Store Koldewey island ~650 km further to the north, at the northernmost end of the fjord zone and tests for the regionality of the scenario presented for the Scoresby Sund area (Papers I-III). The exposure age results from Store Koldewey do indeed suggest that also interfjord plateaus in the northernmost part of the fjord zone were covered by cold-based ice. It is however, not concluded in Paper IV whether or not ice was dynamically connected to the Greenland Ice Sheet.

At Store Koldewey and further to the north the shelf is unusually broad and shallow and the modern ice sheet margin is commonly situated at sea level, whereas further to the south in the fjord zone the present ice sheet margin is fringed by high mountains (Fig. 1A). Based on a regional synthesis of the Greenland margin, Bennike & Björck (2002) suggested that these differences in the landscape might have allowed the LGM ice sheet to expand much further out on the shelf north of the fjord zone compared to in the fjord zone. This N-S gradient in glacial style would imply that ice at the outer coast was thicker around Store Koldewey and north thereof compared to Scoresby Sund, which opens up for the possibility that the Greenland Ice Sheet indeed expanded beyond Store Koldewey during

the LGM. On the southernmost summit plateau of Store Koldewey, closest to the outlet of the Dove Bugt embayment (Fig. 1A), two boulders show apparent exposure ages compatible with the LGM deglaciation, whereas boulders with older exposure ages are situated further to the north (Paper IV). If interpreting the southernmost boulders as deposited by the ice sheet, then a scenario could be suggested where active ice from the Greenland Ice Sheet filled up the Dove Bugt embayment and was buttressed by local cold-based ice on the Store Koldewey plateaus. However, at the outlet of the embayment where active ice was no longer channelized between high mountains, the ice flow would diverge and this could result in glacial transport of erratics onto the very southernmost part of the island. In line with this reasoning the position of boulders with apparent exposure ages compatible with the LGM deglaciation at ~600 m would indicate the thickness of active ice at the outlet of the Dove Bugt embayment.

The work presented in this thesis suggests a topographically controlled configuration of the northeastern sector of the Greenland Ice Sheet. Based on the cosmogenic exposure dating efforts alone, the exact ice marginal position on the continental shelf can not be constrained. However, I hypothesize that relatively fast-flowing ice draining the ice sheet was channelized in cross-shelf troughs and was thus capable of reaching further out on the shelf compared to the local cold-based ice-caps on interfjord areas which would have had steeper surface gradients.

## *5.2 Methodological considerations*

Recently, many studies have shown the importance of considering surface lowering of landforms for interpreting cosmogenic exposure age on drift, especially on old (pre-LGM) features. Putkonen & O'Neil (2006) proposed that degradation universally affects all sloping unconsolidated landforms and in a case study from southernmost South America,

Kaplan et al. (2007) show that apparent exposure ages from erratics are much younger than the landforms that they rest upon. Cobbles and boulders can be exhumed from the surface of unconsolidated landforms as fine grained matrix is transported down slope by the action of wind, water and creep (Putkonen & Swanson, 2003). These processes might lead to that cobbles and boulders will not get exposed at the sediment surface until long after their deposition, which in turn will lead to anomalously young exposure ages (Fig. 5; Putkonen & Swanson, 2003).

The above mentioned studies have major implications for the application of cosmogenic exposure dating to an area like interior Jameson Land, which is to a large extent covered by pre-Weichselian sediments. Paper III suggests that wind erosion is one of the most important surface lowering processes acting on unconsolidated landforms on Jameson Land. This is based on the existence of extensive deflation surfaces on sediment covered plateaus and the accumulation of sand dunes in sheltered positions (Adriellsson & Alexanderson, 2005). Stormy conditions during periods of the last glacial cycle are further indicated by dust in the Renland ice core (Fig. 1; Johnsen et al., 1992). Based on the cosmogenic exposure dating results from the 'older drift'-covered areas on interior Jameson Land (Paper III) it is stressed that deflation is an important process to consider when applying exposure dating to clasts on sandy unconsolidated landforms elsewhere in the Arctic.

## **6. Conclusions**

In this thesis I suggest that during the LGM, local cold-based ice-caps covered and preserved weathered interfjord plateaus in the Northeast Greenland fjord zone whereas fjord troughs were filled up with dynamic ice draining the Greenland Ice Sheet. In Scoresby Sund and probably also in the Dove Bugt embayment, the active ice was so thick

that it must have been buttressed by cold-based ice on interford plateaus. This scenario further implies ice streams thick enough to reach at least 250 m a.s.l. at the mouth of Scoresby Sund and ~600 m a.s.l. at the outlet of the Dove Bugt embayment.

The work presented here demonstrates that throughout the Northeast Greenland fjord zone the LGM ice limits were substantially more extensive than defined by earlier land-based work but that there was a N-S gradient in glacial style presumably reflecting regional differences in the topography of the coastal areas.

## 7. Ideas for future research

Taken together, my work applying cosmogenic exposure dating to differentially weathered landscapes in the Northeast Greenland fjord zone has provided insights into the dynamic behavior of the northeastern sector of the Greenland Ice Sheet during the LGM. The regionality of these results could be further investigated by applying this approach to other weathered interford plateaus in Northeast Greenland. This would be of particular importance for further constraining whether the Greenland Ice Sheet indeed overrode some coastal plateaus in the northernmost part of the fjord zone. Furthermore, an important focus would be to further investigate the LGM ice marginal position on the continental shelf.

## 8. Acknowledgements

First of all, I would like to thank my main PhD-advisor Christian Hjort for introducing me to the exiting field of polar research and for supporting me and sharing his extensive knowledge and experience from East Greenland. I also want to thank my co-advisors Per Möller, Svante Björck, Raimund Muscheler and Johan Kleman for their assistance and support.

I am deeply grateful for all the help and support that I have got from Jason Briner at the Geology Department in Buffalo, NY. Thank you for your never-ending enthusiasm and interest in my work and for introducing me to your amazing lab! I also want to acknowledge all the people in the Paleoclimate Lab in Buffalo and especially Elizabeth, Dale, Nic and Yarrow for being such a great team. I want to thank everybody at the Quaternary Department in Lund and especially Lena Adrielsson and Nicolaj Krog Larsen for many constructive and inspiring discussions.

I also want to thank Anders Schomacker, Helena Alexanderson, Maria Jensen, and Lena Adrielsson (again), not only for being such great colleagues but also for making my life during the last four years so much easier.

I had the pleasure of spending a great field season on Store Koldewey in 2003 with Ole Bennike, Holger Cremer, Nadja Hultsch, Martin Klug, Svenja Kobabe and Berndt Wagner. Thank you!

The research presented here was generously funded by the following grants: Helge Ax:son Johnsons Foundation, Swedish Society of Anthropology and Geography, Kungliga Fysiografiska Sällskapet, Kungliga Vetenskapsakademien, Kurt and Alice Wallenbergs Foundation, NorFa and the Japetus Steenstrup Foundation.

Special thanks go to my family and friends for their support, especially to Sanna and Anja for always being there for me and to Staffan for being so patient and for believing in me.

## 9. Swedish summary

*Senpleistocen nedisningshistoria på Nordöst-grönland: kosmogen exponeringsdatering, isutbredning och isdynamik*

Under den senaste istiden var periodvis stora delar av landmassorna på norra halvklotet istäckta. Idag är den Grönländska inlandsisen den enda

större återstoden av detta, men likväl binder den tillsammans med isen i Antarktis och jordens mindre glaciärer väldigt stora mängder vatten. Förändringar i dessa isars utbredning och volym kan få mycket stora konsekvenser för den globala miljön och för balansen i klimatet. Att undersöka spåren från den Grönländska Inlandsisens forntid är därför en viktig del i att skapa en ökad kunskap om istidscyklernas klimatförhållanden som i sin tur kan bidra till en bättre förståelse för vad som är på väg att hända med våra polarisar idag.

Dagens kunskap om Östgrönlands nedisningshistoria bygger på de omfattande studier som utförts framför allt under de senaste decennierna. Det råder dock fortfarande delade meningar om Inlandsisens utbredning och om förekomsten av isfria områden under det senaste globala nedisningsmaximat för ca 20 000 år sedan. Resultat från undersökningar på land tyder på att stora delar av de idag isfria landområdena också varit fria från is under hela den senaste istiden. Uppfattningen om en begränsad glaciation under denna tidsperiod står dock i kontrast till resultat från maringeologiska undersökningar vilka tolkats som att is nått hela vägen ut till kontinentalsockeln under det senaste nedisningsmaximat.

Inom mitt avhandlingsarbete har jag velat testa hypoteserna om den Grönländska inlandsisens utbredning genom en omfattande dateringssatsning baserad på analys av kosmogena isotoper ( $^{10}\text{Be}$  och  $^{26}\text{Al}$ ) i berggrund och flyttblock, s.k. kosmogen exponeringsdatering. Nedan följer en beskrivning av denna metodik.

Vår jord utsätts för en ständig dusch av kosmisk strålning, till största delen neutroner och protoner med tillräckligt stor energi för att orsaka kärnreaktioner då de kolliderar med andra partiklar. Vid dessa kärnreaktioner kan kosmogena isotoper bildas. Produktionen sker i huvudsak uppe i atmosfären men förekommer även i berggrundens översta två meter, orsakad av den kosmiska strålning som når jordens yta. Då en bergyta täcks av ett tillräckligt tjockt lager is, snö, sediment eller vatten upphör denna produktion. Dessutom medför

sönderfall av de radioaktiva isotoperna, samt erosion av berget, att koncentrationen av redan ackumulerade isotoper minskar. Om erosionen från en täckande is varit tillräcklig (mer än 2 meter) så kommer isens underlag att bli "nollställd" från gamla isotoper. Om isen däremot inte har eroderat fullt så mycket, eller kanske inte alls, så kommer den bergyta som exponeras efter isens tillbakadragande att innehålla "ärvda" isotoper från tidigare exponeringsperioder. När isen drar sig tillbaka och bergytan exponeras igen, fortsätter produktionen av kosmogena isotoper. Om man analyserar innehållet av kosmogena isotoper i en yta som isen "nollställt" får man en uppskattning av hur lång tid som gått sedan området blev isfritt och metoden fungerar som en absolut dateringsteknik. För en yta som inte blivit "nollställd" ger analysen av två olika radioaktiva isotoper med olika sönderfallshastigheter (oftast  $^{10}\text{Be}$  och  $^{26}\text{Al}$ ) inte någon absolut ålder, men kan däremot påvisa huruvida en bergyta under upprepade perioder har varit omväxlande exponerad och övertäckt av icke-eroderande glaciär-is.

Senare års utveckling av tekniken att analysera kosmogena isotoper som ackumulerats i litosfären har öppnat nya möjligheter för att testa de motsägelsefulla hypoteserna om den Grönländska inlandsisens utbredning i tid och rum samt förekomsten av isfria områden under den senaste nedisningen. Genom att provta och analysera både berggrund och flyttblock på de starkt förvittrade högplatåerna och de kustnära lågländerna i den Nordöstgrönländska fjordzonen är det alltså nu möjligt att utforska både Inlandsisens utbredning, och dess eroderande, alternativt landskapsbevarande karaktär. Analys av flyttblocken gör det möjligt att avgöra när en dynamisk och materialtransporterande is sist var så stor att den täckte dessa områden. Berggrundsproverna kan visa om de starkt förvittrade ytorna bevarats under upprepade perioder av övertäckning av kallbaserad, mer passiv is eller om vittringen är ett resultat av att dessa områden var isfria under senaste nedisningen.

Detta tillvägagångssätt har lett till en ny och mer dynamisk bild av den Grönländska inlandsisen

under det senaste nedisningsmaximat. I mitt avhandlingsarbete föreslår jag att lokala kallbaserade iskappor började tillväxa på de idag isfria kustnära platåerna längs den nordöstgrönländska kusten. Under nedisningsmaximat växte dessa samman med inlandsisens utlöparglaciärer som var kanaliserade i de många fjordarna. De kallbaserade iskapporna förblev förmodligen lokala, utan dynamisk koppling till inlandsisen. Det är dock möjligt att inlandsisen expanderade över även de högre kustområdena i den nordligaste delen av fjordzonen.

## References

- Adriellsson, L. & Alexanderson, H. 2005: Interactions between the Greenland Ice Sheet and the Liverpool Land coastal ice cap during the last two glacial cycles. *Journal of Quaternary Science* 20 (3), 269-283.
- Ballantyne, C. K., McCarroll, D., Nesje, A., Dahl, S. O. 1998: The last ice sheet in North-West Scotland: Reconstruction and implications. *Quaternary Science Reviews* 17, 1149-1184
- Bennike, O. & Björck, S. 2002: Chronology of the last recession of the Greenland Ice Sheet. *Journal of Quaternary Science* 17, 211-219.
- Bierman, P. R., Marsella, K. A., Patterson, C., Davis, P. T. & Caffee, M. 1999: Mid-Pleistocene cosmogenic minimum-age limits for pre-Wisconsin glacial surfaces in southwestern Minnesota and southern Baffin Island: a multiple nuclide approach. *Geomorphology* 27, 25-39.
- Björck, S. & Hjort, C. 1984: A re-evaluated glacial chronology for northern East Greenland. *Geologiska Föreningens i Stockholms Förhandlingar* 105, 235-243.
- Boulton, G.S. 1979: Glacial history of the Spitsbergen archipelago and the problem of a Barents Shelf ice sheet. *Boreas* 8, 31-57.
- Boyer, S.J. & Pheasant, D.R. 1974: Delimitation of weathering zones in the fiord area of Eastern Baffin Island, Canada. *Geological Society of America Bulletin* 85, 805-810.
- Briner, J. P., Miller, G., Davies, P. T., Bierman, P. R. & Caffee, M. 2003: Last Glacial Maximum ice sheet dynamics in the Canadian Arctic inferred from young erratics perched on ancient tors. *Quaternary Science Reviews* 22, 437-444.
- Briner, J. P., Miller, G. H., Davis, T. R. & Finkel, R. 2005: Cosmogenic exposure dating in arctic glacial landscapes: implications for the glacial history of northeastern Baffin Island, Arctic Canada. *Canadian Journal of Earth Sciences* 42, 67-84.
- Briner, J. P., Miller, G., Davies, P. T. & Finkel, R. 2006: Cosmogenic radionuclides from fiord landscapes support differential erosion by overriding ice sheets. *GSA Bulletin* 118, 406-430.
- Davies, R.T. & Schaffer, O. A. 1955: Chlorine-36 in nature. *Annals New York Academy of Science* 62, 105-122.
- Davis, P. T., Bierman, P. R., Marsella, K. A., Caffee, M. W. & Southon, J.R. 1999: Cosmogenic analysis of glacial terrains in the eastern Canadian Arctic: a test for inherited nuclides and the effectiveness of glacial erosion. *Annals of Glaciology* 28, 181-188.
- Davis, P. T., Briner, J. P., Coulthard, R. P., Finkel, R. W. & Miller, G. H. 2006: Preservation of Arctic landscapes overridden by cold-based ice sheets. *Quaternary Research* 65, 156-163.
- Desilets, D., Zreda, M. & Prabu, T. 2006: Extended scaling factors for in situ cosmogenic nuclides: new measurements at low latitude. *Earth and Planetary Science Letters* 246, 265-276.
- Dunai, T. 2001: Influence of secular variation of the magnetic field on production rates of in situ produced cosmogenic nuclides. *Earth and Planetary Science Letters*, 193, 197-212.
- Dyke, A.S. & Prest, V.K. 1987: Late Wisconsin and Holocene history of the Laurentide Ice Sheet. *Géographie physique et Quaternaire* 41, 237-263.
- Evans, J., Dowdeswell, J. A., Grobe, H., Niessen, F., Stein, R., Hubberten, H. W. & Whittington, R. J. 2002: Late Quaternary sedimentation in Kejsar Franz Joseph Fjord and the continental margin of East Greenland. In Dowdeswell, J. A., Ó Cofaigh, C. (eds.): *Glacier influenced sedimentation on high latitude continental margins*, 149-179. Geological Society of London: Special Publications 203, London, United Kingdom.
- Fink, D. & Smith, A. 2007: An inter-comparison of  $^{10}\text{Be}$  and  $^{26}\text{Al}$  AMS reference standards and the

- <sup>10</sup>Be half-life. *Nuclear Instruments and Methods in Physics Research B* 259, 600-609.
- Forman, S.L. 1989: Late Weichselian glaciation and deglaciation of the Forlandssundet area, western Spitzbergen, Svalbard. *Boreas* 18, 51-60.
- Funder, S. & Hansen, L. 1996: The Greenland Ice Sheet – a model for its culmination and decay during and after the last glacial maximum. *Bulletin of the Geological Society of Denmark* 42, 137-152.
- Funder, S. & Hjort C. 1973: Aspects of the Weichselian chronology in central East Greenland. *Boreas* 2, 69-84.
- Funder, S., Hjort, C. & Landvik, J. Y. 1994: The last glacial cycle in East Greenland, an overview. *Boreas* 23, 283-293.
- Funder, S., Hjort, C., Landvik, J. Y., Nam, S.-I., Reeh, N. & Stein, R. 1998: History of a stable ice margin – East Greenland during the middle and upper Pleistocene. *Quaternary Science Reviews* 17, 77-123.
- Gosse, J. C. & Phillips, F. M. 2001: Terrestrial in-situ cosmogenic nuclides; theory and application. *Quaternary Science Reviews* 20, 1275-1560.
- Hansen, L., Funder, S., Murray, A. S. & Mejdal, S. 1999: Luminiscence dating of the last Weichselian Glacier advance in East Greenland. *Quaternary Geochronology* 18, 179-190.
- Harbour, J., Stroeven, A. P., Fabel, D., Clarhäll, A., Kleman, J., Li, Y., Elmore, D. & Fink, D. 2006: Cosmogenic nuclide evidence for minimal erosion across two subglacial sliding boundaries of the late glacial Fennoscandian ice sheet. *Geomorphology* 75, 90-99.
- Hjort, C. 1979: Glaciation in northern East Greenland during the Late Weichselian and Early Flandrian. *Boreas* 8, 281-296.
- Hjort, C. 1981: A glacial chronology for northern East Greenland. *Boreas* 10, 259-274.
- Ives, J. D. 1966: Blockfields, associated weathering forms on mountain tops and the nunatak hypothesis. *Geografiska Annaler* 48A, 220-223
- Jennings, A.E., Tedesco, K.A., Andrews, J.T. & Kirby, M.E. 1996: Shelf erosion and glacial ice proximity in the Labrador Sea during and after Heinrich events (H-3 or 4 to H-0) as shown by foraminifera. In Andrews, J.T., Austin, W.E.N., Bergsten, H & Jennings, A.E. (eds.): *Late Quaternary Paleoceanography of the North Atlantic Margins*, 29-49. Geological Society Special Publications, London.
- Johnsen, S. J., Clausen, H. B., Dansgaard, W., Gundestrup, N. S., Hansson, M., Jonsson, P., Steffensen, J. P. & Sveinbjørnsdóttir, A. E. 1992: A “deep” ice core from East Greenland. *Meddelelser om Grønland, Geoscience* 29, 22 pp.
- Kaplan, M. R., Coranto, A., Hulton, N. R. J., Rabassa, J.O., Kubik, P. W. & Freeman, S. P. H. T. 2007: Cosmogenic nuclide measurements in southernmost South America and implications for landscape change. *Geomorphology* 87, 284-301.
- Kleman, J. 1994: Preservation of landforms under ice sheets and ice caps. *Geomorphology* 9, 19-32.
- Kleman, J. & Hätterstrand, C. 1999: Frozen-bed Fennoscandian and Laurentide ice sheets during the Late Glacial Maximum. *Nature* 402, 63-66.
- Kohl, C.P. & Nishiizumi, K. 1992: Chemical isolation of quartz for measurement of in-situ produced cosmogenic nuclides. *Geochimica et Cosmochimica Acta* 56, 3583-3587.
- Lal, D. 1991: Cosmic ray labeling of erosion surfaces: In-situ nuclide production rates and erosion models. *Earth and Planetary Science Letters* 104, 424-439.
- Lal, D. & Peters, B. 1967: Cosmic ray produced radioactivity on the earth. In Sitte, K. (ed): *Handbuch der Physik*. Springer, Berlin, pp. 551-612
- Landvik, J. Y., Brook, E. J., Gualtieri, L., Raisbeck, G., Salvigsen, O. & Yiou, F. 2003: Northwest Svalbard during the last glaciation: Ice-free areas existed. *Geology* 31, 905-908.
- Landvik, J.Y., Ingólfsson, Ó., Mienert, J., Lehman, S.J., Solheim, A., Elverhoi, A & Ottesen, D. 2005: Rethinking Late Weichselian ice dynamics in coastal NW Svalbard. *Boreas* 34, 7-24.
- Lasca, N. P. 1969. *The Surficial Geology of Skeldal, Mesters Vig, North East Greenland*. Meddelelser om Grønland 176:3, 56 pp
- Lifton, N., Bieber, J., Clem, J., Duldin, M., Evenson, P., Humble, J. & Pyle, R. 2005: Addressing solar modulation and long-term uncertainties in scaling secondary secondary cosmic rays for in situ cosmogenic nuclide applications. *Earth and Planetary Science Letters* 239, 140-161.
- MacLean, B., Williams, G.L., Jennings, A.E. &

- Blakeny, C. 1986: Bedrock and surficial geology of Cumberland Sound, N.W.T. Geological Survey of Canada, Ottawa.
- Mangerud, J., Dokken, T.M., Hebbeln, D., Heggen, B., Ingolfsson, O., Landvik, J.Y., Mejdahl, V., Svendsen, J.I. & Vorren, T.O. 1998: Fluctuations of the Svalbard-Barents Sea Ice Sheet during the last 150,000 years. *Quaternary Science Reviews* 17, 11-42.
- Marquette, G. C, Gray, J. T., Gosse, J. C., Courchesne, F., Stockli, L., Macpherson, G. & Finkel, R. 2004: Felsenmeer persistence under non-erosive ice in the Torngat Mountains and Kaumajet Mountains, Quebec and Labrador, as determined by soil weathering and cosmogenic nuclide exposure dating. *Canadian Journal of Earth Sciences* 41, 19-38.
- Miller, G.H., Wolfe, A.P., Steig, E.J., Sauer, P.E., Kaplan, M.R. & Briner, J.P. 2001: The Goldilocks dilemma: big ice, little ice, or “just-right” ice in the Eastern Canadian Arctic. *Quaternary Science Reviews* 21, 33-48.
- Möller, P., Hjort, C., Adrielsson, L. & Salvigsen, O. 1994: Glacial history of interior Jameson Land, East Greenland. *Boreas* 23, 320-348.
- Nesje, A. & Dahl, S. O. 1990: Autochthonous block fields in southern Norway – implications for the geometry, thickness and isostatic loading of the Late Weichselian Scandinavian ice sheet. *Journal of Quaternary Science* 5, 225-234.
- Nishiizumi, K., Lal, D., Klein, J., Middleton, R. & Arnold, J. R. 1986: Production of  $^{10}\text{Be}$  and  $^{26}\text{Al}$  by cosmic rays in terrestrial quartz in situ and implications for erosion rates. *Nature* 319, 134-135.
- Ó Cofaigh, C., Dowdeswell, J. A., Evans, J., Kenyon, N. H., Taylor, J., Mienert, J., & Wilken, M. 2004: Timing and significance of glacially influenced mass-wasting in the submarine channels of the Greenland Basin. *Marine Geology* 207, 39-54.
- Ottesen, D., Dowdeswell, J.A., Landvik, J.Y. & Mienert, J. 2007: Dynamics of the Late Weichselian ice sheet on Svalbard inferred from high-resolution sea-floor mapping morphology. *Boreas* 36, 286-306.
- Pheasant, D.R. & Andrews, J.T. 1973: Wisconsin glacial chronology and relative sea level movements, Narspaing Fiord Broughton Island, eastern Baffin Island, N.W.T. *Canadian Journal of Earth Sciences* 10, 1621-1642.
- Phillips, F. M., Leavy, B. D., Jannick, N. O., Elmore, D. & Kubik, P. W. 1986: The accumulation of cosmogenic chlorine-36 in rocks: a method for surface exposure dating. *Science* 231, 41-43.
- Putkonen, J. & O’Neil, M. A. 2006: Quaternary degradation of unconsolidated landforms in the western North America. *Geomorphology* 75, 408-419.
- Putkonen, J. & Swanson, T. 2003: Accuracy of cosmogenic ages for moraines. *Quaternary Research* 59, 255-261.
- Rae, A. C., Harrison, S., Mighall, T. & Dawson, A.G. 2004: Periglacial trimlines and nunataks of the last glacial maximum: the Gap of Dunloe, southwest Ireland. *Journal of Quaternary Science* 19, 87-97.
- Ronnert, L. & Nyborg, M. R. 1994: The distribution of different glacial landscapes on southern Jameson Land, East Greenland according to Landsat Thematic Mapper data. *Boreas* 23, 294-311.
- Salvigsen, O. 1977: Radiocarbon datings and the extension of the Weichselian ice sheet in Svalbard. *Norsk Polarinstitutt Årbok* 1976, 209-224.
- Stone, J. O. 2000: Air pressure and cosmogenic isotope production. *Journal of geophysical research* 105, 23753-23759.
- Stroeven, A. P., Fabel, D., Hättestrand, C. & Harbour, J. 2002: A relict landscape in the centre of the Fennoscandian glaciation: cosmogenic radionuclide evidence of tors preserved through multiple glacial cycles. *Geomorphology* 44, 145-154.
- Sollid, J. L. & Sørbel, L. 1994: Distribution of glacial landforms in Southern Norway in relation to the thermal regime of the last continental ice sheet. *Geografiska Annaler* 76, 25-36.
- Sugden, D. E. 1978: Glacial erosion by the Laurentide ice sheet. *Journal of Glaciology* 83, 367-391.
- Washburn, A.L. 1965: Geomorphic and vegetational studies in the Mesters Vig district. *Meddelelser om Grønland* 166, 60 pp.
- Wilken, M. & Mienert, W. 2006: Submarine glacial debris-flows, deep-sea channel and past ice stream behaviour of the east Greenland continental margin. *Quaternary Science Reviews* 25, 784-810.





# Appendix I





ELSEVIER

Quaternary Science Reviews 26 (2007) 2316–2321



Rapid communication

# $^{10}\text{Be}$ ages from central east Greenland constrain the extent of the Greenland ice sheet during the Last Glacial Maximum

Lena Håkansson<sup>a,b,\*</sup>, Jason Briner<sup>b</sup>, Helena Alexanderson<sup>c</sup>, Ala Aldahan<sup>d</sup>, Göran Possnert<sup>e</sup><sup>a</sup>Department of Geology, Quaternary Sciences, GeoBiosphere Centre, Sölvegatan 12, 223 62 Lund, Sweden<sup>b</sup>Department of Geology, University at Buffalo, 876 NSC, Buffalo, NY 14260, USA<sup>c</sup>Department of Physical Geography and Quaternary Geology, Stockholm University, SE-106 91 Stockholm, Sweden<sup>d</sup>Department of Earth Sciences, Villavägen 16, SE-752 36 Uppsala, Sweden<sup>e</sup>Tandem Laboratory, Uppsala University, SE-751 21 Uppsala, Sweden

Received 21 February 2007; received in revised form 27 July 2007; accepted 9 August 2007

## Abstract

Traditional ice sheet reconstructions have suggested two distinctly different ice sheet regimes along the East Greenland continental margin during the Last Glacial Maximum (LGM): ice to the shelf break south of Scoresby Sund and ice extending no further than to the inner shelf at and north of Scoresby Sund. We report new  $^{10}\text{Be}$  ages from erratic boulders perched at 250 m a.s.l. on the Kap Brewster peninsula at the mouth of Scoresby Sund. The average  $^{10}\text{Be}$  ages, calculated with an assumed maximum erosion rate of 1 cm/ka and no erosion (respectively,  $17.3 \pm 2.3$  ka and  $15.1 \pm 1.7$  ka) overlap with a period of increased sediment input to the Scoresby Sund fan (19–15 ka). The results presented here suggest that ice reached at least 250 m a.s.l. at the mouth of Scoresby Sund during the LGM and add to a growing body of evidence indicating that LGM ice extended onto the outer shelf in northeast Greenland.

© 2007 Elsevier Ltd. All rights reserved.

## 1. Introduction

The role that ice sheets play in the global climate system depends largely on their connection to adjacent ocean basins. Pleistocene ice sheets rimming the North Atlantic Ocean heavily influenced global oceanic circulation and abrupt climate change (Bond et al., 1993; Broecker, 1997; Clark et al., 1999; Jennings et al., 2006). Recent studies, many taking advantage of new marine coring and imaging techniques and dating methods (e.g., Zreda et al., 1999; Landvik et al., 2005; Ottesen et al., 2005), have led to a new understanding of the extent and dynamics of ice sheet margins during the Last Glacial Maximum (LGM). For example, recent cosmogenic exposure dating studies from Arctic Canada depict ice that terminated on the continental

shelf during the LGM (Briner et al., 2005), in some places overriding weathered, non-glacial landscapes (e.g., Briner et al., 2003; Davis et al., 2006).

Terrestrial-based studies in northeast Greenland depict LGM ice terminating at the mouth of fjords or on the inner shelf (e.g., Funder et al., 1998), whereas recent studies on the northeast Greenland continental shelf suggest that the Greenland Ice Sheet reached the shelf break during the LGM (e.g., O'Cofaigh et al., 2004). Here, we apply cosmogenic  $^{10}\text{Be}$  dating to erratics perched on a peninsula adjacent to the open ocean as an attempt to reconcile the marine studies with a terrestrial dataset.

## 2. Background and setting

The eastern margin of Greenland (spanning 60–81°N, Fig. 1) consists of two contrasting landscape types. South of Scoresby Sund (70°N), coastal areas consist of presently glaciated alpine topography, whereas north thereof a 100–200-km-wide unglaciated margin is composed of intensely weathered uplands dissected by deep fjords. Glacial troughs cross-cut the continental shelf outboard

\*Corresponding author. Department of Geology, Quaternary Sciences, GeoBiosphere Centre, Sölvegatan 12, 223 62 Lund, Sweden.

E-mail addresses: Lena.Hakansson@geol.lu.se (L. Håkansson), Jbriner@buffalo.edu (J. Briner), Helena.Alexanderson@natgeo.su.se (H. Alexanderson), Ala.Aldahan@geo.uu.se (A. Aldahan), Goran.Possnert@Angstrom.uu.se (G. Possnert).

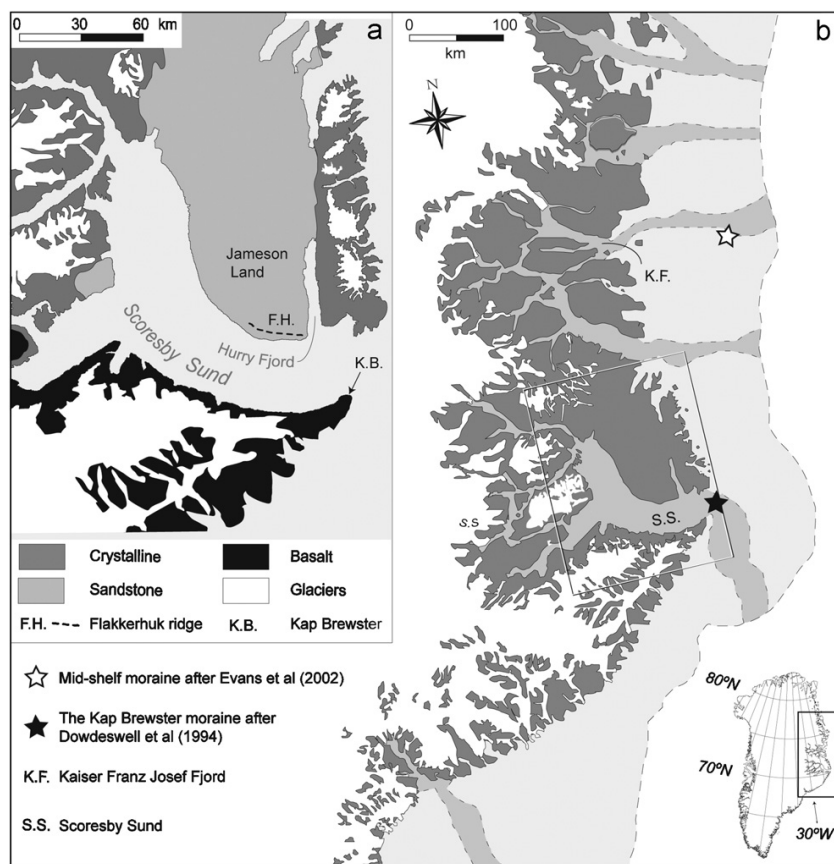


Fig. 1. (a) Bedrock map of the Scoresby Sund showing the source of sandstone erratics after Henriksen (1989). (b) Map of northeast Greenland. The dashed line marks the continental shelf break. Shaded areas bounded by dashed lines show cross-shelf troughs.

of major fjords both south and north of Scoresby Sund (Fig. 1).

Current reconstructions of the Greenland Ice Sheet south of Scoresby Sund, based on marine studies, depict an LGM margin at the edge of the continental shelf (Mienert et al., 1992; Andrews et al., 1996; Bennike and Björck, 2002). The glacial history of Scoresby Sund and northward is derived from both terrestrial and marine studies. Based on intense bedrock weathering and the lack of deposits from the last glaciation, interfjord uplands north of and at Scoresby Sund have long been thought to be ice-free throughout the LGM (Funder and Hjort, 1973; Hjort, 1981; Landvik, 1994). During recent decades, considerable effort has been put into both on- and offshore investigations of the Late Quaternary glacial history of this area. One large step was taken through the “Polar North Atlantic Margins” (PONAM) program, in which most investigations focused on the Scoresby Sund area (Fig. 1). This work led to the reconstruction of a large outlet glacier restricted to Scoresby Sund during the LGM, terminating at the Kap Brewster subaqueous moraine (Fig. 1; Dowdeswell et al., 1994) leaving Jameson Land and the

adjacent continental shelf free from ice (e.g., Möller et al. 1994; Funder et al., 1998). The northern margin of the Scoresby Sund outlet glacier during the LGM is thought to relate to the Flakkerhuk ridge on southern Jameson Land (Fig. 1), which is an erosional landform composed of pre-LGM sediments (Tveranger et al., 1994). This implies an ice elevation near Hurry Fjord (Fig. 1a) of <70 m a.s.l. (Fig. 1; Funder et al., 1998). Inland of the Flakkerhuk ridge the sandstone bedrock is exposed and intensely weathered.

Kap Brewster, a peninsula composed of Tertiary basalt bordering the southern mouth of Scoresby Sund, lies ~25 km down fjord from the eastern end of the Flakkerhuk ridge (Fig. 1). Sandstone erratics are perched above 230 m a.s.l. on Kap Brewster. The only sources for lithology of these erratics are either from Jameson Land or from the floor of Scoresby Sund (Fig. 1; Henriksen, 1989). Mangerud and Funder (1994) hypothesized that these erratics were deposited by Scoresby Sund ice during the LGM, because the erratics are near relatively fresh E–W oriented glacial striae, covered by a thin mantle of drift.

### 3. Methods and results

Samples for  $^{10}\text{Be}$  dating were collected from four erratic sandstone boulders, 40–70 cm high, from Kap Brewster (Fig. 2) during the summer of 2005. All samples were taken from flat upper boulder surfaces except for KB-4, which was taken from a sloping edge ~20 cm above ground (Table 1). The erratics are resting on a flat, well-drained ~5 cm thick drift unit draped over basaltic bedrock and are situated on elevations between 230 and 251 m a.s.l. Samples were processed for  $^{10}\text{Be}$  analysis at the University at Buffalo following procedures in Briner (2003).  $^{10}\text{Be}$  measurements were made at the Tandem Laboratory, Uppsala University and ages were calculated using a  $^{10}\text{Be}$  production rate of  $5.1 \pm 0.3 \text{ atoms g}^{-1} \text{ yr}^{-1}$  (Stone, 2000). Site-specific production rates were corrected for altitude (Lal, 1991; Stone, 2000) and  $^{10}\text{Be}$  concentrations were adjusted for sample thickness and shielding (Table 1). Because these samples are from high latitude (~70°N),

radionuclide production rates are not influenced by changes in the geomagnetic field (Gosse and Phillips, 2001). Bedrock weathering rates in arid arctic regions are relatively low (e.g.,  $1 \text{ mm ka}^{-1}$ ; Bierman et al., 1999). However, because the Kap Brewster erratics are composed of sandstone, we may expect higher erosion rates. The exact bedrock weathering rate is not known; therefore, we calculate  $^{10}\text{Be}$  ages for a range of values between 0 and  $10 \text{ mm ka}^{-1}$ .

The four different sandstone erratics have  $^{10}\text{Be}$  ages that range between  $9.1 \pm 1.6$  and  $16.6 \pm 3.2 \text{ ka}$  under  $0 \text{ mm ka}^{-1}$  erosion conditions (Fig. 2), and between  $9.8 \pm 1.7$  and  $19.3 \pm 3.8 \text{ ka}$  under  $10 \text{ mm ka}^{-1}$  erosion conditions (Table 1). The  $^{10}\text{Be}$  age of the youngest sample (KB-4) falls outside of the two-sigma range of the mean of the oldest three erratics. Since this sample was collected only 20 cm above the ground, compared to the other samples which were collected from 40- to 70-cm-high boulders, the anomalously younger age is likely due to shielding by

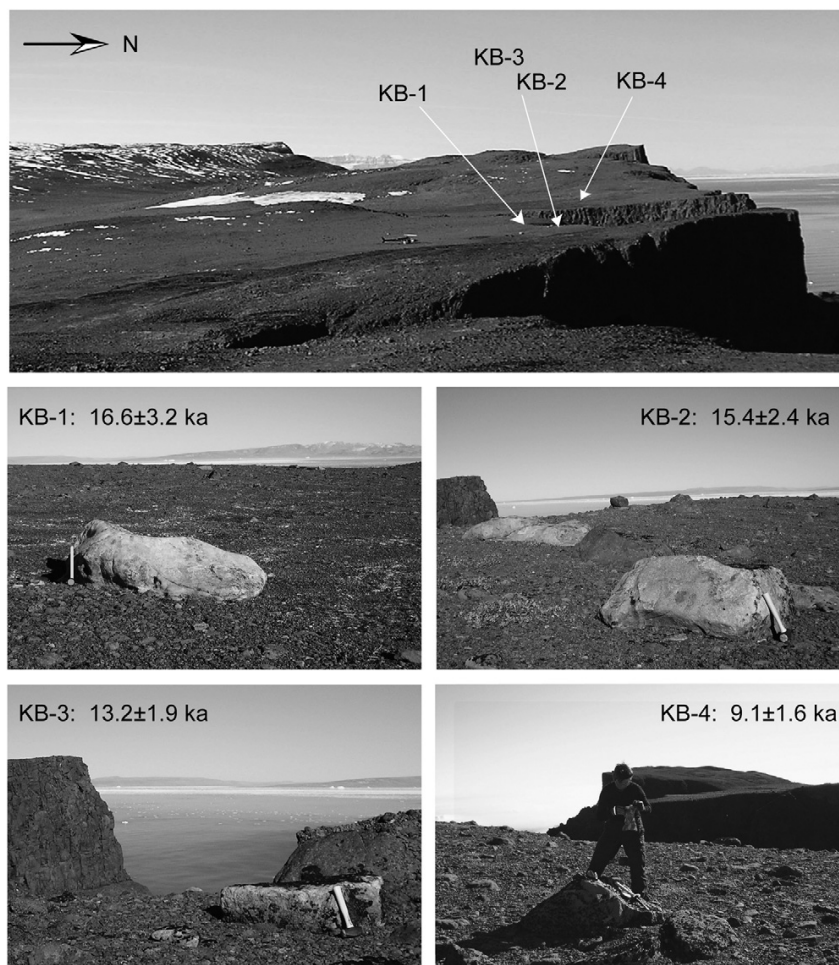


Fig. 2. Sampling area and sampled erratic boulders. The sledge hammer for scale is 30 cm long.  $^{10}\text{Be}$  ages shown in figure are calculated with no erosion and are corrected for shielding and sample thickness.

Table 1  
<sup>10</sup>Be results from Kap Brewster

Sample	Latitude (N)	Longitude (W)	Altitude (m)	Sample position <sup>a</sup>	Thickness correction <sup>b</sup>	Shielding correction <sup>c</sup>	Scaling factor <sup>d</sup>	<sup>10</sup> Be ( $\times 10^5$ atoms/g <sup>e</sup> )	<sup>10</sup> Be age (ka), no correction	<sup>10</sup> Be age (ka), $e = 0$ mm/ka	<sup>10</sup> Be age (ka), $e = 5$ mm/ka	<sup>10</sup> Be age (ka), $e = 1$ cm/ka
KB-1	70°09'03.4"	23°04'31.5"	230	Top surface, 70 cm	0.984	1	1.277	1.06 ± 0.17	16.6 ± 3.2	17.8 ± 3.5	19.3 ± 3.8	
KB-2	70°09'03.8"	23°04'33.7"	230	Top surface, 40 cm	0.984	1	1.277	0.99 ± 0.13	15.4 ± 2.4	16.5 ± 2.6	17.8 ± 2.8	
KB-3	70°09'03.2"	23°04'39.4"	251	Top surface, 40 cm	0.976	0.996	1.304	0.85 ± 0.10	13.2 ± 1.9	14.0 ± 2.0	14.9 ± 2.1	
KB-4	70°09'03.6"	23°04'49.8"	239	Sloping edge, 20 cm	0.976	0.884	1.288	0.51 ± 0.08	9.1 ± 1.6	9.4 ± 1.6	9.8 ± 1.7	

<sup>a</sup>Description of where on the boulder and from which height above ground the sample is taken.

<sup>b</sup>Thickness correction using exponential decrease in nuclide production and bulk density of 2.32 g/cm<sup>3</sup>.

<sup>c</sup>Correction for shielding by distant objects (and shielding by sample geometry for KB-4). Shielding < 5° is neglected.

<sup>d</sup>Scaling factor after Stone (2000).

<sup>e</sup>Correction for blank ( $3.0195 \pm 0.8235 \times 10^{-14}$ ).

<sup>f</sup>Ages calculated with erosion rates of 0 mm/ka, 5 mm/ka and 1 cm/ka.

either sediment or seasonal snow. Thus, we choose to discard the youngest age and base further discussions on the average age of the three oldest ages which ranges between  $15.1 \pm 2.5$  ka for minimum ( $0 \text{ mm ka}^{-1}$ ) and  $17.3 \pm 2.9$  ka for maximum erosion ( $10 \text{ mm ka}^{-1}$ ).

#### 4. Implications for the LGM ice configuration

Our <sup>10</sup>Be ages are consistent with exposure of Kap Brewster soon after the LGM, thus suggesting that the peninsula was covered by ice during the LGM as has been hypothesized by Mangerud and Funder (1994). The elevation of the erratics indicates a minimum thickness of c. 250 m a.s.l. for this ice. To reconcile ice being >250 m thick on Kap Brewster, yet <70 m thick on the opposite side of Scoresby Sund, earlier reconstructions (Mangerud and Funder, 1994) have suggested that the southern side of the Scoresby Sund glacier was higher because it was fed by local tributary glaciers from the south (Fig. 3a). This ice configuration implies that ice-flow over Kap Brewster was directed from the basalt plateaus south of Scoresby Sund, where there is no source for the sandstone erratics (Fig. 1a). Thus, it would require that erratics were deposited by an earlier extensive advance of the Greenland Ice Sheet and later re-deposited on Kap Brewster by a local ice merging with the outlet glacier in Scoresby Sund during the LGM. In this scenario we would expect to have inherited <sup>10</sup>Be in the samples, since they would have been exposed before the LGM and we would expect our samples to be older (have higher <sup>10</sup>Be concentrations). Rather we suggest that the young erratics on Kap Brewster require LGM ice with flow lines parallel to the fjord trough, reaching at least 250 m a.s.l. at the mouth of Scoresby Sund.

If the glacial striae on Kap Brewster indeed are from the LGM as suggested by Mangerud and Funder (1994) this indicates that the ice was sliding at its bed at 250 m a.s.l. during this time. However, at the same elevation on the north side of Scoresby Sund the terrain is intensely weathered. It is possible that active ice within the previously depicted LGM limit on Jameson Land was buttressed by cold-based ice preserving the old landscapes beyond this limit (Fig. 3b). In other settings it has been found that cold-based ice can override and preserve weathered non-glacial landscapes (Kleman, 1994; Fabel et al., 2002; Briner et al., 2003, 2006; Sugden et al., 2005; Davis et al., 2006). The Scoresby Sund trough is deepest in the southern part, whereas the northern side gently rises towards Jameson Land (Fig. 3; Dowdeswell et al., 1993). Ice filling Scoresby Sund would be channelized in the southern part bounded by the southern steep slope of the trough, thus facilitating fast ice flow in this part of the trough. Thus, the asymmetric trough morphology could explain why ice was eroding its bed on Kap Brewster, yet was cold-based at the same elevation on Jameson Land.

Sediment cores from the northern part of the Scoresby Sund fan document an increased sediment flux to this part of the fan between 19 and 15 ka, interpreted as ice rafted

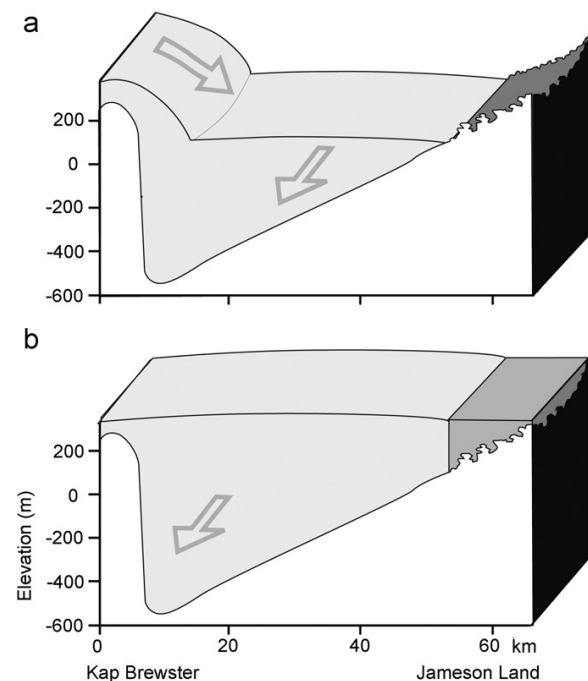


Fig. 3. Simplified illustration of two alternative LGM ice configurations in Scoresby Sund: (a) as suggested by Mangerud and Funder (1994) and (b) as suggested by this study. The bathymetric information is after Dowdeswell et al. (1993).

debris from ice situated at the Kap Brewster moraine more than 100 km away (Stein et al., 1993; Nam et al., 1995). Further south, at the mouth of the cross-shelf trough, Dowdeswell et al. (1997) show debris flow activity during the LGM. In line with traditional LGM ice reconstructions (e.g., Funder et al., 1998), they suggest that the debris flow lobes might derive either from strong cross-shelf transport from an ice front located at the mouth of Scoresby Sund during the LGM or from direct sediment delivery from extensive ice earlier during the last glacial cycle. Other studies of similar glacier-fed subaqueous fans have shown that the large number of debris flows making up these fan systems is a result of ice at the continental shelf break (King et al., 1996; Vorren and Laberg, 1997; Vorren et al., 1998; Dowdeswell and Elverhøi, 2002; Sejrup et al., 2004).

Based on a regional synthesis of the Greenland margin, Bennike and Björck (2002) suggested that LGM ice covered at least parts of the broad and shallow northeast Greenland shelf. Seismic data off Kaiser Franz Josef Fjord show a prominent moraine ca 50 km from the shelf break interpreted to be a LGM terminal or recessional moraine (Fig. 1b; Evans et al., 2002). Furthermore, O’Cofaigh et al. (2004) suggest that submarine channels on the continental shelf slope emanating from the lip of shelf troughs are generated by glacier ice on the outer shelf or at the shelf break. Radiocarbon dates show that mass wasting in these

channels ceased around 13 ka, indicating that the last time these channels were active was during the LGM.

The traditional LGM reconstructions have suggested two distinctly different ice sheet regimes along the coast of East Greenland; ice to the shelf break south of Scoresby Sund and ice extending no further than to the inner shelf north thereof. The present study challenges these reconstructions by adding to a growing body of evidence indicating LGM ice extending onto the outer shelf also at and north of Scoresby Sund.

## 5. Conclusion

Previous LGM reconstructions of the northeastern sector of the Greenland Ice Sheet are based mainly on terrestrial studies and depict ice terminating at the mouth of fjords and sounds. In contrast, recent marine data from the northeast Greenland continental shelf suggest that the ice extended onto the outer shelf or even as far as the continental shelf break during the this time. Our average  $^{10}\text{Be}$  ages, calculated with an assumed maximum erosion rate of 1 cm/ka and no erosion (respectively  $17.3 \pm 2.9$  and  $15.1 \pm 2.5$  ka) overlap with a period of increased sediment input on the northern part of the Scoresby Sund fan (19–15 ka), indicating the timing of the LGM ice sheet advance in East Greenland. The results presented here suggest that ice reached at least 250 m a.s.l. at the mouth of Scoresby Sund during the LGM, implying that ice reached the outer shelf at this time and that sliding ice in the fjord trough may have been buttressed by cold-based ice on Jameson Land.

## Acknowledgments

The fieldwork was funded by the Helge Axson Johnson Foundation and the Swedish Association for Anthropology and Geography (SSAG). The Danish Polar Centre and the Swedish Polar Research Secretariat provided logistic support. Christian Hjort is acknowledged for valuable discussions. We also wish to thank Jon Landvik and an anonymous reviewer for helpful comments and suggestions on the manuscript.

## References

- Andrews, J.T., Jennings, A.E., Cooper, T., Williams, K.M., Mienert, J., 1996. Late Quaternary sedimentation along fjord to shelf (trough) transect, East Greenland (ca. 68°N). In: Andrews, J.T., Austin, W.E.N., Bergsten, H., Jennings, A.E. (Eds.), Late Quaternary Paleogeography of the North Atlantic Margins, vol. 111. Geological Society Special Publication, pp. 153–167.
- Bennike, O., Björck, S., 2002. Chronology of the last recession of the Greenland Ice Sheet. *Journal of Quaternary Science* 17, 211–219.
- Bierman, P.R., Marsella, K.A., Patterson, C., Davis, P.T., Caffee, M., 1999. Mid-Pleistocene cosmogenic minimum-age limits for pre-Wisconsinan glacial surfaces in southwestern Minnesota and southern Baffin Island: a multiple nuclide approach. *Geomorphology* 27, 25–39.



- Bond, G., Broecker, W., Johnsen, S., McManus, J., Labeyrie, L., Jouzel, J., Bonani, G., 1993. Correlations between climate records from North Atlantic sediment and Greenland ice. *Nature* 365, 143–147.
- Briner, J.P., 2003. The last glaciation of the Clyde Region, Northeastern Baffin Island, Arctic Canada. Boulder. Ph.D. Thesis, University of Colorado, Boulder, USA, 282pp.
- Briner, J.P., Miller, G.H., Davies, P.T., Bierman, P.R., Caffee, M., 2003. Last Glacial Maximum ice sheet dynamics in the Canadian Arctic inferred from young erratics perched on ancient tors. *Quaternary Science Reviews* 22, 437–444.
- Briner, J.P., Miller, G.H., Davies, P.T., Finkel, R., 2005. Cosmogenic exposure dating in arctic glacial landscapes: implications for the glacial history of northeastern Baffin Island, Arctic Canada. *Canadian Journal of Earth Sciences* 42, 67–84.
- Briner, J.P., Miller, G.H., Davies, P.T., Finkel, R., 2006. Cosmogenic radionuclides from fiord landscapes support differential erosion by overriding ice sheets. *GSA Bulletin* 118, 406–430.
- Broecker, W.S., 1997. Thermohaline circulation, the Achilles heel of our climate system: will man-made CO<sub>2</sub> upset the current balance? *Science* 278, 1582–1588.
- Clark, P.U., Alley, R.B., Pollard, D., 1999. Northern hemisphere ice-sheet influences on global climate change. *Science* 286, 1104–1111.
- Davis, P.T., Briner, J.P., Coulthard, R.P., Finkel, R.W., Miller, G.H., 2006. Preservation of Arctic landscapes overridden by cold-based ice sheets. *Quaternary Research* 65, 156–163.
- Dowdeswell, J.A., Elverhøi, A., 2002. The timing of initiation of fast-flowing ice streams during a glacial cycle inferred from glaciomarine sedimentation. *Marine Geology* 188, 3–14.
- Dowdeswell, J.A., Villinger, H., Whittington, R.J., Marienfeld, P., 1993. Iceberg scouring in the Scoresby Sund and on the East Greenland continental shelf. *Marine Geology* 111, 37–53.
- Dowdeswell, J.A., Uenzelmann-Neben, G., Whittington, R.J., Marienfeld, P., 1994. The Late Quaternary sedimentary record in Scoresby Sund, East Greenland. *Boreas* 23, 294–310.
- Dowdeswell, J.A., Kenyon, N.H., Laberg, J.S., 1997. The glacier-influenced Scoresby Sund Fan: evidence from GLORIA and 3.5 kHz records. *Marine Geology* 143, 207–221.
- Evans, J., Dowdeswell, J.A., Grobe, H., Niessen, F., Stein, R., Hubberten, H.W., Whittington, R.J., 2002. Late Quaternary sedimentation in Kejsars Franz Joseph Fjord and the continental margin of East Greenland. In: Dowdeswell, J.A., O’Cofaigh, C. (Eds.), *Glacier Influenced Sedimentation on High Latitude Continental Margins*. Geological Society, London, UK, Special Publications, vol. 203, London, pp. 149–179.
- Fabel, D., Stroeven, A.P., Harbour, J., Kleman, J., Elmore, D., Fink, D., 2002. Landscape preservation under Fennoscandian ice sheets determined from in situ produced <sup>10</sup>Be and <sup>26</sup>Al. *Earth and Planetary Science Letters* 201, 397–406.
- Funder, S., Hjort, C., 1973. Aspects of the Weichselian chronology in central East Greenland. *Boreas* 2, 69–84.
- Funder, S., Hjort, C., Landvik, J.Y., Nam, S.-I., Reeh, N., Stein, R., 1998. History of a stable ice margin—East Greenland during the middle and upper Pleistocene. *Quaternary Science Reviews* 17, 77–123.
- Gosse, J.C., Phillips, F.M., 2001. Terrestrial in-situ cosmogenic nuclides: theory and application. *Quaternary Science Reviews* 20, 1275–1560.
- Henriksen, N., 1989. Scoresby Sund omradets geologi. *Geologisk beskrivelse og kort 1:500,000, map sheet 12, Scoresby Sund, Danmarks og Grønlands Geologiske Undersøgelse, Copenhagen, Denmark*.
- Hjort, C., 1981. A glacial chronology for northern East Greenland. *Boreas* 10, 259–274.
- Jennings, A.E., Hald, M., Smith, M., Andrews, J.T., 2006. Freshwater forcing from the Greenland Ice Sheet during the Younger Dryas: evidence from southeastern Greenland shelf cores. *Quaternary Science Reviews* 25, 282–298.
- King, E.L., Sejrup, H.P., Hafliðason, H., Elverhøi, A., Aarseth, I., 1996. Quaternary seismic stratigraphy of the North Sea Fan: glacially-fed gravity flow aprons, hemipelagic sediments and large submarine slides. *Marine Geology* 130, 293–316.
- Kleman, J., 1994. Preservation of landforms under ice sheets and ice caps. *Geomorphology* 9, 19–32.
- Lal, D., 1991. Cosmic ray labeling of erosion surfaces: in-situ nuclide production rates and erosion models. *Earth and Planetary Science Letters* 104, 424–439.
- Landvik, J.Y., 1994. The last glaciation of Germania Land and adjacent areas, northeast Greenland. *Journal of Quaternary Science* 9, 81–92.
- Landvik, J.Y., Ingólfsson, O., Mienert, J., Lehman, S.J., Solheim, A., Elverhøi, A., Otesen, D., 2005. Rethinking Late Weichselian ice sheet dynamics in coastal NW Svalbard. *Boreas* 34, 7–24.
- Mangerud, J., Funder, S., 1994. The interglacial-glacial record at the mouth of Scoresby Sund, East Greenland. *Boreas* 23, 349–358.
- Mienert, J., Andrews, J.T., Milliman, J.D., 1992. The East Greenland continental margin (65°N) since the last deglaciation: changes in sea floor properties and ocean circulation. *Marine Geology* 106, 217–238.
- Möller, P., Hjort, C., Adrielsson, L., Salvigsen, O., 1994. Glacial history of interior Jameson Land, East Greenland. *Boreas* 23, 320–348.
- Nam, S.I., Stein, R., Grobe, H., Hubberten, H., 1995. Late Quaternary glacial-interglacial changes in sediment composition at the East Greenland continental margin and their paleoceanographic implications. *Marine Geology* 122, 243–262.
- O’Cofaigh, C., Dowdeswell, J.A., Evans, J., Kenyon, N.H., Taylor, J., Mienert, J., Wilken, M., 2004. Timing and significance of glacially influenced mass-wasting in the submarine channels of the Greenland Basin. *Marine Geology* 207, 39–54.
- Ottesen, D., Rise, L., Knies, J., Olsen, L., Henriksen, S., 2005. The Vestfjorden-Trænadjupe paleo-ice stream drainage system, mid Norwegian continental shelf. *Marine Geology* 218, 175–189.
- Sejrup, H.P., Hafliðason, H., Hjelstuen, B.O., Nygård, A., Bryn, P., Lien, R., 2004. Pleistocene development of the SE Nordic Seas margin. *Marine Geology* 213, 169–200.
- Stein, R., Grobe, H., Hubberten, H., Marienfeld, P., Nam, S., 1993. Latest Pleistocene to Holocene changes in glaciomarine sedimentation in Scoresby Sund and along the adjacent East Greenland continental margin: preliminary results. *Geo-Marine Letters* 13, 9–16.
- Stone, J.O., 2000. Air pressure and cosmogenic isotope production. *Journal of Geophysical Research* 105, 23753–23759.
- Sugden, D.E., Balco, G., Cowdery, S.G., Stone, J.O., Sass, III, 2005. Selective glacial erosion and weathering zones in the coastal mountains of Mary Bird Land, Antarctica. *Geomorphology* 67, 317–334.
- Tveranger, T., Houmark-Nielsen, M., Løvberg, K., Mangerud, J., 1994. Eemian-Weichselian stratigraphy of the Flakkerhuk ridge, southern Jameson land, East Greenland. *Boreas* 23, 359–384.
- Vorren, T.O., Laberg, J.S., 1997. Trough mouth fans—paleoclimate and ice-sheet monitors. *Quaternary Science Reviews* 16, 865–881.
- Vorren, T.O., Laberg, J.S., Blaume, F., Dowdeswell, J.A., Kenyon, N.H., Mienert, J., Rumohr, F., 1998. The Norwegian-Greenland continental margins: morphology and late Quaternary sedimentary processes and environment. *Quaternary Science Reviews* 17, 273–302.
- Zreda, M., England, J., Phillips, F., Elmore, D., Sharma, P., 1999. Unblocking of the Nares Strait by Greenland and Ellesmere ice-sheet retreat 10,000 years ago. *Nature* 398, 139–142.

## Appendix II



Short paper

# $^{10}\text{Be}$ and $^{26}\text{Al}$ exposure ages of tors and meltwater channels on Jameson Land, east Greenland: implications for the Late Quaternary glaciation history

Lena Håkansson <sup>a\*</sup>, Jason P. Briner <sup>b</sup>, Ala Aldahan <sup>c</sup>, Göran Possnert <sup>d</sup>

<sup>a</sup> *GeoBiosphere Science Centre, Department of Geology Quaternary Sciences, Sölvegatan 12, 223 62 Lund, Sweden*

<sup>b</sup> *Department of Geology, University at Buffalo, Buffalo, NY 14260, USA*

<sup>c</sup> *Department of Earth Sciences, Villavägen 16, SE-752 36 Uppsala, Sweden*

<sup>d</sup> *Tandem Laboratory, Uppsala University, SE-751 21 Uppsala, Sweden*

---

## Abstract

We measured  $^{10}\text{Be}$  and  $^{26}\text{Al}$  in samples from sandstone tors and meltwater channels on the Jameson Land peninsula, east Greenland to test for the preservation of tors and to investigate whether or not the area was covered by ice during the last glacial maximum (LGM). Isotope concentrations indicate that tors have been preserved through multiple glacial cycles beneath cold-based ice. The average  $^{10}\text{Be}$  exposure age of  $16.9 \pm 2.4$  ka on meltwater channels indicates that these eroded during the LGM deglaciation, suggesting that Jameson Land was covered by cold-based ice during the LGM.

*Keywords:* Cosmogenic; Jameson Land; Tor formation; Greenland Ice Sheet; Meltwater channels; Glaciation; Exposure age

---

## Introduction

Tors are weathering remnants of bare bedrock rising above a surrounding platform of regolith (Selby, 1982). Within formerly glaciated regions, the occurrence of tors has often been used as evidence either for the existence of ice free areas within or near glaciated terrain (Ives, 1966; Nesje and Dahl, 1990; Ballantyne et al., 1998; Rae et al., 2004) or for the former distribution of cold-based ice allowing the preservation of pre-Quaternary landscapes (Sugden, 1978; Kleman, 1994; Sollid and Sørbel, 1994; Kleman and Hätterstrand, 1999). Because highly weathered landscapes and tors are often found on upland plateaus, the interpretation of these landscapes can constrain ice thickness and/or the thermal regime of Pleistocene ice sheets. Although tors have been studied for decades, constraining the rates of tor formation has proven difficult, limiting their usefulness to provide chronological information on glaciation. However, since the application of cosmogenic radionuclides to weathered landscapes, rates of tor formation and the relationship between tors and glaciation have become

better understood (Bierman et al., 1999; Marsella et al., 2000; Stroeven et al., 2002; Marquette et al., 2004; Briner et al., 2003, 2005, 2006; Sugden et al., 2005; Davis et al., 2006; Phillips et al., 2006; Darmody et al., 2008).

Along the east Greenland continental margin (Fig. 1), from Scoresby Sund and northwards, interfjord plateaus are highly weathered whereas fjord troughs are characterized by smooth surfaces of glacial erosion. Previous work suggested that the last advance of the Greenland Ice Sheet that covered interfjord plateaus occurred during Marine Isotope Stage (MIS) 6 and that the different degree of weathering from plateau to fjord exists because interfjord plateaus remained ice free throughout the last glacial cycle (Funder and Hjort, 1973; Hjort, 1979, 1981; Funder and Hansen, 1996; Funder et al., 1994, 1998). It was also suggested that meltwater channels and tor landscapes on the Jameson Land peninsula were formed during and following MIS 6 deglaciation, respectively (Möller et al., 1994). However, reconstructions advocating only limited glaciation of the northeast Greenland continental margin throughout the last glacial cycle have recently been challenged by marine studies suggesting that the

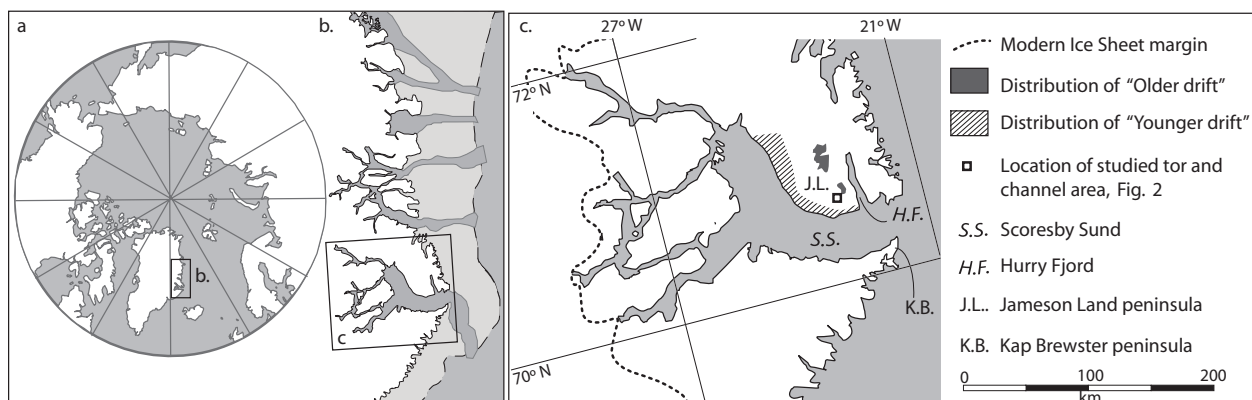


Fig. 1. Maps showing: A. the Arctic and the location of Greenland, B. central East Greenland ~68-74°N. The continental shelf is marked as a light grey area and cross-shelf troughs are shown in darker grey. C. The Scoresby Sund area and Jameson land. Detailed site maps (Figs. 4, 5 and 6) are marked with framed boxes. The dashed frame shows the transect in Figure 8.

Greenland Ice Sheet reached the outer shelf or even the shelf break during the Last Glacial Maximum (LGM; Evans et al., 2002; O’Cofaigh et al., 2004).

In the present study we present cosmogenic  $^{10}\text{Be}$  and  $^{26}\text{Al}$  exposure ages from tors and meltwater channels on Jameson Land. Our main objectives are to (i) investigate whether tors indeed developed after MIS 6 or if these features are older than previously thought and (ii) test whether or not Jameson land remained ice free during the last glacial cycle.

## Setting

The Jameson Land peninsula (70°-71° N) is situated ~200 km from the present margin of the Greenland Ice Sheet at the northern side of Scoresby Sund, a major fjord system in east Greenland (Fig. 1). The peninsula has an asymmetric topographic profile; from the plateau areas of interior Jameson Land the terrain gently slopes towards Scoresby Sund in the west and south, whereas the eastern margin, facing Hurry Fjord (Fig. 1c), has a steeper gradient. The plateaus form the watershed between east-draining rivers towards Hurry Fjord and the many, and often large, river valleys draining west and south towards Scoresby Sund. On Jameson Land two areas covered by Late Quaternary glacial sediments have been described; the plateaus in the interior of the peninsula where these sediments are referred to as the ‘older drift’ and the low elevation area bordering Scoresby Sund where the sediment cover is referred to as the ‘younger drift’ (Fig. 1c; Ronnert and Nyborg, 1994; Möller et al., 1994). Between these two drift-covered areas is an area largely without sediment cover, referred to as the ‘drift-less’ area where weathered Jurassic sandstone bedrock is exposed

(Ronnert and Nyborg, 1994).

### *Tors in the ‘drift-less’ area, Jameson Land*

Extensive areas with exposed weathered sandstone bedrock are found in the southern part of the “drift-less area” where tor-rich interfluvial areas are abundant along the middle Fynselv River and its tributaries (Fig. 1; Schunke, 1986; Hjort and Salvigsen, 1991; Möller et al., 1994). The tors are formed in Jurassic sandstone and lie between c. 230-550 m a.s.l. Well developed tors are most abundant at the higher elevations.

This study is focused on an interfluvial plateau surface at 400-550 m a.s.l. (~70°38N, 23°07W) surrounded by >100-m-deep v-shaped canyons (Figs. 2a). The interior of the interfluvial area is covered by regolith and in places by thin patches of ground moraine, whereas tor areas are concentrated along the edges of the interfluvial area (Figs. 1 and 3).

Tors have weathered into rounded forms (Fig. 2b), the dimensions and architecture of which are controlled by a rhombic fracture system. Weathered, detached tor-blocks are observed adjacent to tors (Fig. 2c). Many tors are surrounded by bare bedrock surfaces modified by fluvial erosion forming fracture-controlled channel systems (Fig. 3). Only tors far away from the channels are surrounded by regolith. The formation of channels on the interfluvial surface requires a significant amount of flowing water more than 100 m above the modern day drainage, which is the depth of the surrounding canyons. Thus, the observed channel systems are difficult to explain by modern fluvial erosion; we interpret them as having formed by glacier-derived meltwater.

The investigated area exhibits a range of meltwater



Figure 1. (a) The deep canyon of the Fynselv River. (b) Rounded tors. (c) Detached tor blocks c. 2 m in diameter. (d) Wide channel c. 30 m across. (e) Narrow channel. (d) Weathering pit on the top surface of tor. (e) Channels dissect undulating smooth outcrops.

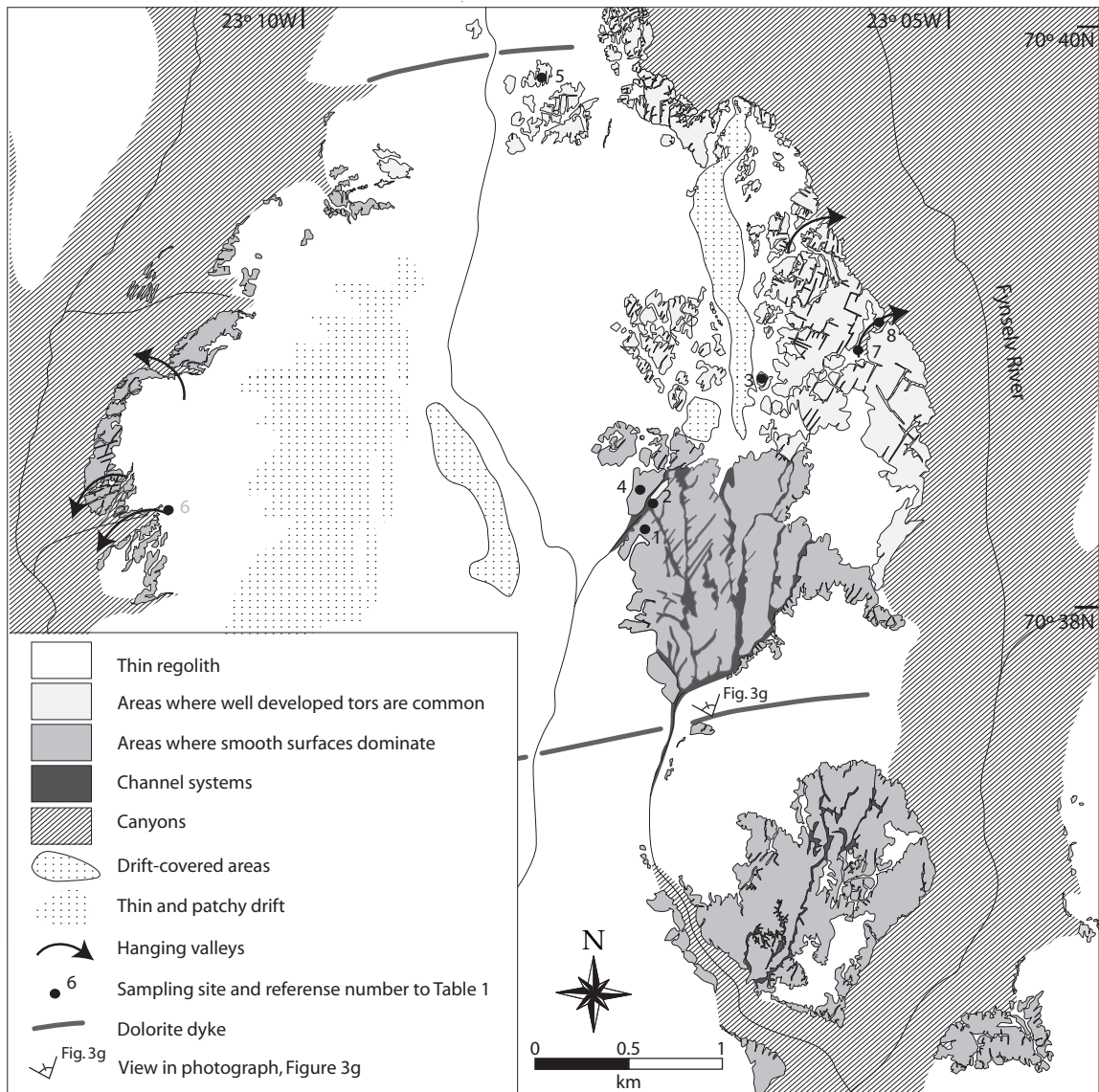


Figure 3. The investigated tor and channel area showing sample positions with reference number to Table 1. The map illustrates the distribution of channels and tor-rich areas and is based on aerial photographs and field mapping.

channel sizes; wide channels up to 30 m across (Fig. 2d), narrower channels 2-5 m wide (Fig. 2e) and abundant open fissures up to 1 m wide. Two types of fracture controlled channels systems are represented: dendritic channel systems draining across the interfluvial plateau and wide channels that terminate above cliffs along major canyons (hanging valleys; Fig. 3). The fluvial modification of sandstone decreases away from the bottoms of the dendritic channels. We classify bedrock surfaces in three groups: (i) tors, (ii) smooth outcrops and (iii) meltwater channel beds (Fig. 3). Tors are at higher

elevations than other surfaces (Fig. 2f). Some of these tor surfaces exhibit circular weathering pits up to 20 cm deep. Smooth surfaces are found on undulating outcrops adjacent to channels where weathering pits are <15 cm deep (Fig. 2g), with rare exceptions in the coarser parts of the sandstone where pedestals <0.5 m tall and >0.5 m in diameter have formed. The bedrock-floored meltwater channels rarely show a weathered relief >5 cm.

## **<sup>26</sup>Al and <sup>10</sup>Be cosmogenic exposure dating**

To constrain the exposure time of the tors and the timing of meltwater incision of the interfluvial plateau, bedrock surfaces showing different degree of weathering were sampled for cosmogenic exposure dating. Samples were collected from bedrock surfaces using hammer and chisel and the position and elevation was obtained using a hand-held GPS receiver. Shielding from the surrounding horizon was measured with a compass. Samples were processed for <sup>10</sup>Be and <sup>26</sup>Al analysis at the University at Buffalo following procedures modified after Kohl and Nishiizumi (1992) and Briner (2003). About 40 g of clean quartz from each sample was dissolved in batches of 11 and one process blank (Table 1). Known amounts SPEX brand Be and Al carrier was added to all samples including the blank. <sup>10</sup>Be/<sup>9</sup>Be ratios were measured at the Tandem Laboratory at Uppsala University and <sup>26</sup>Al/<sup>27</sup>Al ratios were measured at PRIME lab, Purdue University.

Ages were calculated with the CRONUS-Earth exposure age calculator (version 2.1; <http://hess.ess.washington.edu/math/>; Balco et al., 2008) using constant production rates and the scaling scheme for spallation by Lal (1991) and Stone (2000). This program uses a reference <sup>10</sup>Be production rate of 4.96±0.43 atoms/g/yr ( $\sigma_2$ , sea level, high latitude and standard atmosphere). The program calculates <sup>26</sup>Al ages with a production rate based on the production ratio of <sup>26</sup>Al/<sup>10</sup>Be=6.1. Correction was made for shielding by the surrounding horizon and for sample thickness using exponential decrease in nuclide production and a bulk density of 2.38 g cm<sup>-3</sup> for sandstone <sup>10</sup>Be and <sup>26</sup>Al ages are reported in Table 1.

The calculation of single cosmogenic exposure ages relies on the assumptions that a sampled surface has firstly been constantly exposed and lacks inherited isotopes from previous exposures, requiring at least c. 2 m of glacial erosion (Davis et al., 1999; Briner et al., 2006) and secondly, experienced only minimal post-glacial surface erosion. This will be the case for most striated bedrock surfaces in settings where substantial glacial erosion took place. However, for weathered bedrock surfaces in areas covered by non-erosive ice, isotope concentration is the combination of the isotopes produced during exposure since deglaciation and inherited isotopes from previous exposures, minus isotopes lost by post-glacial erosion. Where bedrock is shielded from cosmic radiation for long periods (~200 ka or longer; e.g. via burial by non-erosive ice), the burial duration can be constrained using the disequilibrium of <sup>10</sup>Be and <sup>26</sup>Al concentrations (Lal 1991; Bierman et al., 1999; Fabel et al., 2002; Briner et

al., 2006; Harbour, et al., 2006). Thus, paired <sup>10</sup>Be and <sup>26</sup>Al data can be used to identify and constrain complex exposure/shielding histories.

## **Apparent cosmogenic exposure ages**

Fifteen <sup>10</sup>Be and seven <sup>26</sup>Al measurements show that apparent exposure ages and the degree of bedrock weathering is closely correlated; the top surfaces of tors are the oldest and meltwater channels the youngest (Table 1; Figs. 4 and 5). Five of the Al-samples have <sup>26</sup>Al/<sup>10</sup>Be ratios above or equivalent to the <sup>26</sup>Al/<sup>10</sup>Be production ratio of 6.1, whereas one sample from a highly weathered tor (06-FE-56; Fig. 2f) has a ratio of 4.8±0.8. We have calculated <sup>10</sup>Be ages under 0 and 10 mm ky<sup>-1</sup> erosion conditions (Table 1)

Three samples from tors have apparent <sup>10</sup>Be ages ranging between 32.8±4.0 and 48.0±5.9 ka under 0 mm ky<sup>-1</sup> and 44.2±7.7 and 80.1±8.8 under 10 mm ky<sup>-1</sup> conditions. <sup>10</sup>Be ages from eight samples from smooth surfaces range between 17.7±2.6 and 34.4±4.4 and 34.4 ka under 0 mm ky<sup>-1</sup> and 20.4±3.5 and 47.1±8.8 under 10 mm ka<sup>-1</sup> conditions. Four samples were taken from the bottom of channels; three of these (06-FE-19, -24 and -25) are from wide channels at least 30 m across whereas the fourth (06-FE-52) is from the bottom of a c. 5-m-wide channel in the dendritic system.

<sup>10</sup>Be ages range between 15.7±2.1 and 12.5±1.6 ka under 0 mm ka<sup>-1</sup> conditions and between 17.7±2.7 and 13.6±1.9 ka under 10 mm ka<sup>-1</sup> conditions. The <sup>10</sup>Be age of the youngest sample (from the smallest channel; 06-FE-52) falls outside of the two-sigma range of the mean of the oldest three samples.

## **Discussion**

### *Formation of the tor and channel area*

Sandstone weathering rates of >5 mm ka<sup>-1</sup> have been estimated from arctic settings (Linge et al., 2006) and rates between 7-18 mm ka<sup>-1</sup> have been described from low-latitude desert areas (Paradise, 1995). Because the specific weathering rates of sandstone in Jameson Land is unknown, we have chosen to calculate <sup>10</sup>Be ages under 0 and 10 mm ky<sup>-1</sup> erosion conditions (Table 1), but think that ages calculated with the higher value may be the most realistic. Therefore we use the <sup>10</sup>Be-ages calculated with 10 mm ky<sup>-1</sup> in the following discussion.

Of all samples from the Fynselv interfluvial plateau surface, only tors have <sup>26</sup>Al/<sup>10</sup>Be ratios lower than the



Table 1.  $^{10}\text{Be}$  and  $^{26}\text{Al}$  ages are calculated using the Cronus-Earth exposure age calculator (<http://hess.ess.washington.edu/math/>); Balco et al 2008)

Sample	Site no. on Fig 3	Latitude (°N)	Longitude (°W)	Elevation (m asl)	Shielding correction	Dissolved quartz (g)	$^{10}\text{Be}$ ( $10^5$ atoms $\text{g}^{-1}$ )	$^{26}\text{Al}$ ( $10^5$ atoms $\text{g}^{-1}$ )	$^{10}\text{Be}$ age (ka) e=0mm $\text{ka}^{-1}$ ab	$^{10}\text{Be}$ age (ka) e=10mm $\text{ka}^{-1}$ ab	$^{26}\text{Al}$ age (ka) <sup>a</sup>	$^{26}\text{Al}/^{10}\text{Be}$ ratio
<b>Tors</b>												
06-FE-5	1	70 38.080	23 08.176	495	1	40.0	3.15 ± 0.15	n/a	36.2 ± 4.7	50.7 ± 9.7	n/a	n/a
06-FE-56	2	70 38.309	23 07.748	462	1	40.8	4.04 ± 0.11	19.22 ± 2.80	48.0 ± 5.9	80.1 ± 18.8	37.4 ± 6.5	4.8 ± 0.8
06-FE-65	3	70 38.704	23 06.548	456	1	41.3	2.76 ± 0.07	15.90 ± 1.93	32.8 ± 4.0	44.2 ± 7.6	31.1 ± 4.7	5.8 ± 0.9
<b>Smooth outcrops</b>												
06-FE-55	2	70 38.054	23 07.893	443	1	40.0	2.40 ± 0.13	14.86 ± 1.44	28.9 ± 3.8	37.2 ± 6.5	29.4 ± 3.9	6.2 ± 0.9
06-FE-48	4	70 38.318	23 08.129	470	1	39.2	1.88 ± 0.15	13.12 ± 1.65	22.1 ± 3.2	26.4 ± 4.7	25.2 ± 3.9	7.0 ± 1.2
06-FE-46	4	70 38.353	23 08.077	524	1	40.9	3.08 ± 0.15	n/a	34.4 ± 4.4	47.1 ± 8.8	n/a	n/a
06-FE-50	4	70 38.318	23 08.129	470	1	40.0	2.29 ± 0.12	n/a	26.9 ± 3.5	33.8 ± 5.7	n/a	n/a
06-FE-57	2	70 38.194	23 07.959	449	1	40.2	1.74 ± 0.10	n/a	20.8 ± 2.7	24.6 ± 3.9	n/a	n/a
06-FE-67	5	70 39.968	23 07.120	490	1	41.1	2.27 ± 0.05	n/a	26.1 ± 3.2	32.6 ± 5.1	n/a	n/a
06-FE-53	2	70 37.999	23 08.041	430	1	40.7	1.68 ± 0.10	11.66 ± 1.39	20.4 ± 2.7	24.1 ± 3.8	23.3 ± 3.5	7.0 ± 1.1
06-FE-51	2	70 38.152	23 08.047	444	1	40.1	1.48 ± 0.13	n/a	17.7 ± 2.6	20.4 ± 3.4	n/a	n/a
<b>Meltwater channels</b>												
06-FE-19	6	70 38.404	23 12.700	377	1	40.0	1.13 ± 0.05	n/a	14.5 ± 1.9	16.2 ± 2.3	n/a	n/a
06-FE-25	7	70 38.589	23 05.868	500	0.989	40.9	1.36 ± 0.08	n/a	15.7 ± 2.1	17.7 ± 2.7	n/a	n/a
06-FE-24	8	70 39.148	23 05.898	510	0.968	40.0	1.30 ± 0.03	8.57 ± 0.94	15.1 ± 1.8	17.0 ± 2.3	16.3 ± 2.3	6.6 ± 0.9
06-FE-52	2	70 37.999	23 08.041	425	0.206	40.1	0.23 ± 0.01	2.20 ± 0.39	12.5 ± 1.6	13.6 ± 1.9	18.7 ± 3.8	9.4 ± 1.9

Note: n/a: not analyzed or not applicable

a:  $^{10}\text{Be}$  production rate of  $4.96 \pm 0.43$  atoms  $\text{g}^{-1} \text{yr}^{-1}$ . The  $^{26}\text{Al}$  production rate is based on the production ratio  $^{26}\text{Al}/^{10}\text{Be}$  of 6.1

b: Ages are calculated for erosion conditions of 0 mm and 10 mm  $\text{ka}^{-1}$ . e refers to erosion rate

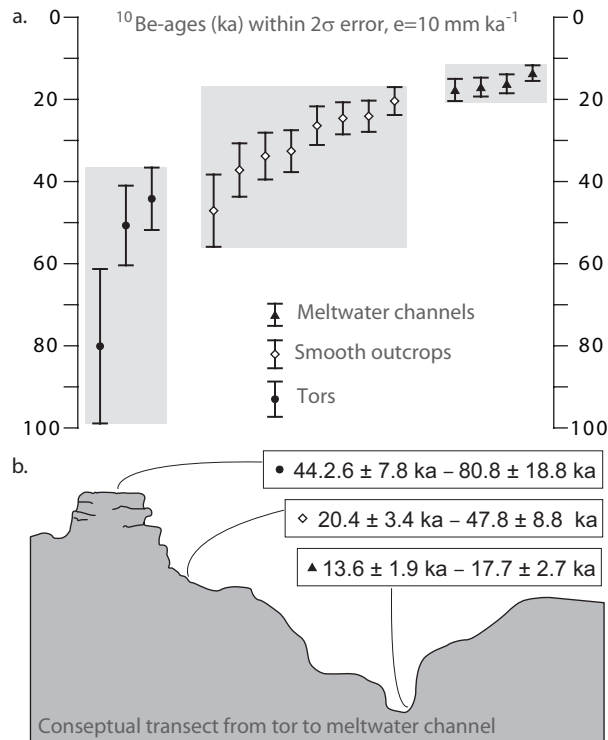


Figure 4. (a) Distribution of  $^{10}\text{Be}$ -ages from all samples (Table 1) calculated with an erosion rate of  $10 \text{ mm ka}^{-1}$  within 2 sigma error. (b) Profile showing a conceptual transect from tor via smooth outcrops to meltwater channels beds. The range of  $^{10}\text{Be}$ -ages (erosion rate of  $10 \text{ mm ka}^{-1}$ ) is shown for each surface type.

production ratio (Table. 1), indicating a complex exposure history. Bierman et al. (1999) described three scenarios of complex exposure histories, all of which require burial: (i) continuous surface exposure with or without erosion, followed by burial of sufficiently-thick ice or sediment, (ii) repeated buried and exposed periods, or (iii) a surface was recently exposed and the isotopes were produced beneath a continuous cover of sediment, snow or ice. From paired isotope data alone there is no way to determine which of these scenarios best fits the Fynselv tors; however, the minimum exposure and minimum burial duration can be constrained.

The  $^{26}\text{Al}/^{10}\text{Be}$  ratio of 4.8 from the oldest tor sample (O6-FE-56; Tab. 1) corresponds to a minimum total exposure and burial history of  $\sim 450 \text{ ka}$ , with  $\sim 370 \text{ ka}$  of total burial and  $\sim 80 \text{ ka}$  of total exposure (assuming an erosion rate of  $10 \text{ mm ka}^{-1}$ ). Similar isotope concentrations and ratios for samples from Baffin Island have been interpreted in line with the second scenario of Bierman et al., 1999, by brief intervals ( $\sim 10 \text{ ka}$ ) of exposure during peak interglacials alternating with long periods ( $\sim 100 \text{ ka}$ ) of shielding by cold-based ice during

glacial periods (Miller et al., 2006). Recent cosmogenic exposure dating results from erratics on interior Jameson Land suggest that the area may have indeed covered by cold-based ice late in the last glacial cycle (Håkansson 2008). The data reported in Håkansson et al. (2008) also indicate that the area has been exposed for  $\sim 70 \text{ ka}$  since the MIS 6 deglaciation, which would imply that during this period most of the total exposure for the oldest tor sample occurred. However, this scenario does not easily explain the long duration of burial recorded in the tor sample. It has been documented that cold-based ice is capable of modifying tors by entrainment of blocks (André, 2004; Phillips et al., 2006). This process would cause episodic erosion in which slabs of rock (e.g.,  $>2\text{-m}$ -thick) is removed rapidly, and results in discordant paired isotope data (Gosse and Phillips, 2001). Detached tor blocks are present adjacent to tors on the Fynselv interfluv surface, thus, this erosion model may apply to these tors. Regardless of the exact exposure history of the investigated tors, our dataset indicates that these surfaces were preserved through multiple glacial cycles beneath cold-based ice and thus, we are able to exclude the scenario whereby tors formed only by post-glacial weathering following the MIS 6 deglaciation.

Samples from smooth outcrops and meltwater channels have  $^{26}\text{Al}/^{10}\text{Be}$  ratios consistent with single periods of exposure. The average  $^{10}\text{Be}$  exposure age of  $16.9 \pm 2.4$  from the channel bottoms suggests that these were most recently eroded during deglaciation of ice covering Jameson Land during the LGM. If both smooth surfaces and channel bottoms experienced  $>2 \text{ m}$  of erosion during the LGM deglaciation, then both surface types should yield similar exposure ages. Because the ages on smooth surfaces are slightly older than the channel bottoms, we suggest that these surfaces contain inheritance due to insignificant erosion ( $<2 \text{ m}$ ) during the LGM. Alternatively, the smooth surfaces may have eroded significantly ( $>2 \text{ m}$ ) at some point within the last  $\sim 200 \text{ ka}$  (i.e. the minimum time for  $^{10}\text{Be}$  and  $^{26}\text{Al}$  data to resolve complex exposure histories). A potential earlier meltwater erosion event most likely occurred during the deglaciation following the MIS 6 advance of the Greenland Ice Sheet  $\sim 130 \text{ ka}$  (Funder et al., 1994, 1998).

#### *Implications for the glaciation history*

Previous reconstructions for the Greenland Ice Sheet have advocated limited glaciation of the northeast Greenland continental margin throughout the last glacial cycle (Funder and Hjort, 1973; Hjort, 1979, 1981; Funder

and Hansen, 1996; Funder et al., 1994, 1998). Limited LGM glaciation scenarios have been challenged by recent work on the continental shelf suggesting that the Greenland Ice Sheet reached the outer shelf or even the shelf break during this time (Evans et al., 2002; O’Cofaigh et al., 2004).

In addition, recent cosmogenic exposure dating results from distal land areas have similarly challenged the restricted ice reconstructions for the LGM.  $^{10}\text{Be}$ -ages of  $17.3\pm 2.3$ - $15.1\pm 1.7$  ka from sandstone erratics perched at 250 m a.s.l. on the Kap Brewster peninsula at the mouth of Scoresby Sund indicate that ice was much thicker and more extensive during the LGM than previously reconstructed by terrestrial studies (Håkansson et al., 2007). Furthermore, the reconstruction suggests that active ice in Scoresby Sund was buttressed by cold-ice on interior Jameson Land during the LGM.

This work supports the presence of cold-based ice on the Jameson Land peninsula during the LGM. Based on findings from stratigraphic investigations (Möller et al., 1994, Funder et al., 1998) and from cosmogenic exposure dating on erratics (Håkansson 2008) it is suggested that no material transport occurred onto the peninsula during the LGM. Thus, we suggest that our average  $^{10}\text{Be}$  exposure age of  $16.9\pm 2.4$  ka on meltwater channels records the timing of disintegration of local ice over Jameson Land. This age overlaps the exposure ages from the fjord mouth ( $17.3\pm 2.3$ - $15.1\pm 1.7$  ka) and post dates a period of rapid sedimentation and meltwater discharge events between 19-15  $^{14}\text{C}$  ka (Nam et al., 1995; Stein et al., 1996).

## Conclusions

Our  $^{10}\text{Be}$  and  $^{26}\text{Al}$  results indicate that tors have been preserved through multiple glacial cycles beneath cold-based ice and thus, these features are much older than previously thought. We proposed that bedrock landscapes in the ‘drift-less’ area of Jameson Land evolved via three main processes during at least the last two glacial cycles: (i) during interglacial and interstadial periods of exposure, sandstone surfaces were weathered at  $\sim 10$  mm  $\text{ky}^{-1}$ , (ii) during periods of burial by cold-based ice, weathered rock slabs might be decoupled from tors by modification by flowing local ice (iii) and during deglaciation, meltwater follows the fracture system in the sandstone and erodes areas between tors by  $> 2$  m. The average  $^{10}\text{Be}$  exposure age of  $16.9\pm 2.4$  ka on meltwater channels indicates that channels eroded during the LGM deglaciation which in turn suggests that Jameson Land was covered by cold-based ice during the LGM.

## Acknowledgements

This research was funded by Helge Ax:son Johnson Foundation and Kungliga Fysiografiska Sällskapet i Lund. The Danish Polar Centre and POLOG provided logistic support. Elizabeth Thomas is acknowledged for enthusiastic help and great company in the field. Nicolaj Krog Larsen, Lena Adrielsson and Christian Hjort are thanked for valuable discussions and constructive comments on this manuscript.

## References

- Andre, M.F., 2004. The geomorphic impact of glaciers as indicated by tors in North Sweden (Aurivaara, 68°N). *Geomorphology* 57, 403-421.
- Balco, G., Stone, J.O., Lifton, N.A., Dunai, T.J., A complete and easily accessible means of calculating surface exposure ages or erosion rates from  $^{10}\text{Be}$  and  $^{26}\text{Al}$  measurements. *Quaternary Geochronology* (2008)
- Ballantyne, C.K., McCarroll, D., Nesje, A., Dahl, S.O., 1998. The last ice sheet in North-West Scotland: Reconstruction and implications. *Quaternary Science Reviews* 17, 1149-1184
- Bierman, P.R., Marsella, K.A., Patterson, C., Davis, P.T., Caffee, M., 1999. Mid-Pleistocene cosmogenic minimum-age limits for pre-Wisconsin glacial surfaces in southwestern Minnesota and southern Baffin Island: a multiple nuclide approach. *Geomorphology* 27, 25-39.
- Briner, J. P., 2003. The last glaciation of the Clyde region, north-eastern Baffin Island, arctic Canada: Cosmogenic isotopes constraints on Laurentide Ice Sheet dynamics and chronology. PhD thesis, University of Colorado, Boulder Colorado, pp. 300.
- Briner, J.P., Miller, G., Davies, P.T., Bierman, P.R., Caffee, M., 2003. Last Glacial Maximum ice sheet dynamics in the Canadian Arctic inferred from young erratics perched on ancient tors. *f. 22*, 437-444.
- Briner, J.P., Miller, G.H., Davis, T.R., Finkel, R., 2005. Cosmogenic exposure dating in arctic glacial landscapes: implications for the glacial history of northeastern Baffin Island, Arctic Canada. *Canadian Journal of Earth Sciences* 42, 67-84.
- Briner, J.P., Miller, G.H., Davis, T.R., Finkel, R., 2006. Cosmogenic radionuclides from fiord landscapes support differential erosion by overriding by ice sheet. *GSA Bulletin* 118, 406-420.
- Davis, P.T., Bierman, P.R., Marsella, K.A., Caffee,

- M.W., Southon, J.R., 1999. Cosmogenic analysis of glacial terrains in the eastern Canadian Arctic: a test for inherited nuclides and the effectiveness of glacial erosion. *Annals of Glaciology* 28, 181-188.
- Davis, P.T., Briner, J.P., Coulthard, R.P., Finkel, R.W., Miller, G.H., 2006. Preservation of Arctic landscapes overridden by cold-based ice sheets. *Quaternary Research* 65, 156-163.
- Darmody, R.G., Thorn, C.E., Seppälä, M., Campbell, S.W., Li, Y.K., Harbour, J., 2008. Age and weathering status of granite tors in Arctic Finland (~68N°). *Geomorphology* 94, 10-23.
- Evans, J., Dowdeswell, J.A., Grobe, H., Niessen, F., Stein, R., Hubberten, H.W., Whittington, R.J., 2002. Late Quaternary sedimentation in Kajsers Franz Joseph Fjord and the continental margin of East Greenland. In: Dowdeswell, J. A., Ó Cofaigh, C. (eds.), *Glacier influenced sedimentation on high latitude continental margins*, Geological Society of London: Special Publications 203, London, United Kingdom, pp.149-179.
- Fabel, D., Stroeven, A.P., Harbour, J., Kleman, J., Elmore, D., Fink, D., 2002. Landscape preservation under Fennoscandian ice sheets determined from in situ produced Be-10 and Al-26. *Earth and Planetary Science Letters* 201, 397-406.
- Funder, S., Hansen, L., 1996. The Greenland Ice Sheet – a model for its culmination and decay during and after the last glacial maximum. *Bulletin of the Geological Society of Denmark* 42, 137-152.
- Funder, S., Hjort C., 1973. Aspects of the Weichselian chronology in central East Greenland. *Boreas* 2, 69-84.
- Funder, S., Hjort, C., Landvik, J.Y., 1994. The last glacial cycle in East Greenland, an overview. *Boreas* 23, 283-293.
- Funder, S., Hjort, C., Landvik, J.Y., Nam, S.-I., Reeh, N., Stein, R., 1998. History of a stable ice margin – East Greenland during the middle and upper Pleistocene. *Quaternary Science Reviews* 17, 77-123.
- Gosse, J.C., Phillips, F.M., 2001. Terrestrial in-situ cosmogenic nuclides; theory and application. *Quaternary Science Reviews* 20, 1275-1560.
- Harbour, J., Stroeven, A.P., Fabel, D., Clarhäll, A., Kleman, J., Li, Y., Elmore, D., Fink, D., 2006. Cosmogenic nuclide evidence for minimal erosion across two subglacial sliding boundaries of the late glacial Fennoscandian ice sheet. *Geomorphology* 75, 90-99.
- Hjort, C., 1979. Glaciation in northern East Greenland during the Late Weichselian and Early Flandrian. *Boreas* 8, 281-296.
- Hjort, C., 1981. A glacial chronology for northern East Greenland. *Boreas* 10, 259-274.
- Hjort, C., Salvigsen, O., 1991. The channel and tor landscape in southeastern Jameson Land, East Greenland. *LUNDQUA Report* 33, 23-26.
- Håkansson, L. The Late Quaternary Glacial History of Northeast Greenland; cosmogenic isotope constraints on chronology and ice dynamics. *LUNQUA thesis* (2008)
- Håkansson, L., Briner, J., Alexanderson, H., Aldahan, A. & Possnert, G. 2007: <sup>10</sup>Be ages from coastal northeast Greenland constrain the extent of the Greenland Ice Sheet during the Last Glacial Maximum. *Quaternary Science Reviews* 26, 2316-2321.
- Ives, J.D., 1966. Blockfields, associated weathering forms on mountain tops and the nunatak hypothesis. *Geografiska Annaler* 48A, 220-223
- Kleman, J., 1994. Preservation of landforms under ice sheets and ice caps. *Geomorphology* 9, 19-32.
- Kleman, J., Hätterstrand, C., 1999. Frozen-bed Fennoscandian and Laurentide ice sheets during the Late Glacial Maximum. *Nature* 402, 63-66.
- Kohl, C.P., Nishiizumi, K., 1992. Chemical isolation of quartz for measurement of in situ-produced cosmogenic nuclides. *Geochimica et Cosmochimica Acta* 56, 3583-3587.
- Lal, D., 1991. Cosmic-ray labeling of erosion surfaces – in situ nuclide production-rates and erosion models. *Earth and Planetary Science Letters* 104, 124-129.
- Linge, H., Larsen, E., Kjaer, K.H., Demidov, I.N., Brook, E.J., Raisbeck, G.M., Yiu, F., 2006. Cosmogenic <sup>10</sup>Be exposure age dating across Early to Late weichselian ice-marginal zones in northwestern Russia. *Boreas* 35, 576-586.
- Marcella, K.A., Bierman, P.R., Davies, P.T., Caffee, M.W., 2000. Cosmogenic <sup>10</sup>Be and <sup>26</sup>Al ages for the last glacial maximum, eastern Baffin Island, arctic Canada. *Geological Society of America Bulletin* 112, 1296-1312.
- Marquette, G.C., Gray, J.T., Gosse, J.C., Courchesne, F., Stockli, L., Macpherson, G., Finkel, R., 2004. Felsenmeer persistence under non-erosive ice in the Torngat and Kaumajet Mountains, Quebec and Labrador, as determined by soil weathering and cosmogenic nuclide exposure dating. *Canadian Journal of Earth Sciences* 41, 19-38.
- Miller, G.H., Briner, J.P., Lifton, N.A., Finkel, R.C., 2006. Limited ice-sheet erosion and complex exposure histories derived from in situ cosmogenic <sup>10</sup>Be, <sup>26</sup>Al and <sup>14</sup>C on Baffin Island, Arctic Canada. *Quaternary*

- Geochronology 1, 74-85.
- Möller, P., Hjort, C., Adrielsson, L., Salvigsen, O., 1994. Glacial history of interior Jameson Land, East Greenland. *Boreas* 23, 320-348.
- Nam, S.I., Stein, R., Grobe, H., Hubberten, H. 1995. Late Quaternary glacial-interglacial changes in sediment composition at the East Greenland continental margin and their paleoceanographic implications. *Marine Geology* 122, 243-262.
- Nesje, A., Dahl, S.O., 1990. Autochthonous block fields in southern Norway – implications for the geometry, thickness and isostatic loading of the Late Weichselian Scandinavian ice sheet. *Journal of Quaternary Science* 5, 225-234.
- Ó Cofaigh, C., Dowdeswell, J.A., Evans, J., Kenyon, N.H., Taylor, J., Mienert, J., Wilken, M. 2004. Timing and significance of glacially influenced mass-wasting in the submarine channels of the Greenland Basin. *Marine Geology* 207, 39-54.
- Phillips, W.M., Hall, A.M., Mottram, R., Fifield, L.K., Sugden, D.E., 2006. Cosmogenic <sup>10</sup>Be and <sup>26</sup>Al exposure ages of tors and erratics, Cairngorm Mountains, Scotland: Timescales for the development of a classic landscape of selective linear glacial erosion. *Geomorphology* 73, 222-245.
- Rae, A.C., Harrison, S., Mighall, T., Dawson, A.G., 2004. Periglacial trimlines and nunataks of the last glacial maximum: the Gap of Dunloe, southwest Ireland. *Journal of Quaternary Science* 19, 87-97.
- Ronnert, L., Nyborg, M.R., 1994. The distribution of different glacial landscapes on southern Jameson Land, East Greenland, according to Landsat Thematic Mapper Data. *Boreas* 23, 311-319.
- Schunke, E., 1986. Periglazialformen und Morphodynamik im südlichen Jameson Land, Ost-Grönland. *Abhandlungen der Akademie der Wissenschaften in Göttingen*. Vandenhoeck & Ruprecht, Göttingen, 142 pp.
- Stein, R., Nam, S.-I., Grobe, H., Hubberten, H., 1996. Late Quaternary glacial history and short-term ice rafted debris fluctuations along the east Greenland continental margin. In: Andrews et al. (eds), *Late Quaternary Paleoclimatology of the North Atlantic Margins*, Geological Society Special Publication 111, pp. 135-151.
- Selby, M.J., 1982. *Hillslope Materials and Processes*. Oxford University Press, Oxford, UK, pp. 186-187.
- Sollid, J.L., Sørbel, L., 1994. Distribution of glacial landforms I Southern Norway in relation to the thermal regime of the last continental ice sheet. *Geografiska Annaler* 76, 25-36.
- Stone, J.O., 2000. Air pressure and cosmogenic isotope production. *Journal of Geophysical Research* 105, 23753-23759.
- Stroeven, A.P., Fabel, D., Hättestrand, C., Harbour, J., 2002. A relict landscape in the centre of the Fennoscandian glaciation: cosmogenic radionuclide evidence of tors preserved through multiple glacial cycles. *Geomorphology* 44, 145-154.
- Sugden, D.E., 1978. Glacial erosion by the Laurentide ice sheet. *Journal of Glaciology* 83, 367-391.
- Sugden, D.E., Balco, G., Cowdery, S.G., Stone, J.O., Sass, III L.C., 2005. Selective glacial erosion and weathering zones in the coastal mountains of Mary Bird Land, Antarctica. *Geomorphology* 67, 317-334.

## Appendix III



# The late Pleistocene glacial history of Jameson Land, central East Greenland derived from cosmogenic $^{10}\text{Be}$ and $^{26}\text{Al}$ exposure dating

LENA HÅKANSSON, HELENA ALEXANDERSON, CHRISTIAN HJORT, PER MÖLLER, JASON P. BRINER, ALA ALDAHAN, GÖRAN POSSNERT

Håkansson, L., Alexanderson, H., Hjort, C., Möller, C., Briner, J.P., Aldahan, A. & Possnert, G.: The late Pleistocene glacial history of Jameson Land, central east Greenland derived from cosmogenic  $^{10}\text{Be}$  and  $^{26}\text{Al}$  exposure dating. *Submitted to Boreas*.

Previous work has presented contrasting views of the last glaciation on Jameson Land, central East Greenland and there is still a debate about whether the area was (i) ice free, (ii) covered with a local cold-based ice cap(s) or (iii) overridden by the Greenland Ice Sheet during the last glacial maximum (LGM). Here we use cosmogenic exposure ages from erratics to reconcile these contrasting views. A total of 44 erratics resting both on weathered sandstone and on sediment-covered surfaces have been sampled from four areas on interior Jameson Land and give  $^{10}\text{Be}$ -ages between 10.7 and 262.1 kyr. Eight erratics from weathered sandstone and till covered surfaces cluster around ~70 kyr whereas  $^{10}\text{Be}$ -ages from glaciofluvial landforms are substantially younger and range between 10.7 and 46.6 kyr. Deflation is thought to be an important process on the sediment covered surfaces and the youngest exposure ages are suggested to result from exhumation. The older (>70 kyr) samples have discordant  $^{26}\text{Al}$  and  $^{10}\text{Be}$  data and are interpreted to have been deposited by the Greenland Ice Sheet several glacial cycles ago. The younger dates ( $\leq 70$  kyr) are interpreted to represent deposition both by the ice sheet during the Late Saalian and an advance from the local Liverpool Land ice-cap in the early Weichselian. The exposure ages younger than Saalian are explained by periods of shielding by cold-based ice during the Weichselian. Our work supports previous studies in that the Saalian ice sheet advance was the last to deposit thick sediment sequences and western erratics on interior Jameson Land. However, instead of Jameson Land being ice-free throughout the Weichselian we document that local cold-based ice covered and shielded large areas for substantial periods of the last glacial cycle.

Lena Håkansson ([lenna.hakansson@geol.lu.se](mailto:lenna.hakansson@geol.lu.se)), Christian Hjort and Per Möller, GeoBiosphere Science Centre, Department of Geology, Quaternary Sciences, Lund University, Sölvegatan 12, S-223 62 Lund, Sweden; Helena Alexanderson, Norwegian University of Life Sciences, Department of Plant and Environmental Sciences, PO Box 5003, NO-1432 Ås, Norway; Jason P. Briner, Department of Geology, University at Buffalo, Buffalo, NY 14260, USA; Ala Aldahan, Department of Earth Sciences, Villavägen 16, SE-752 36 Uppsala, Sweden; Göran Possnert, Tandem Laboratory, Uppsala University, SE-751 21 Uppsala, Sweden.

The Late Pleistocene glacial history of the Northeast Greenland continental margin has been reconstructed from decades of research (e.g. Washburn, 1965; Lasca, 1969; Funder, 1972; Funder & Hjort 1973; Hjort 1979, 1981; Björck & Hjort 1984; Funder & Hansen 1996; Funder *et al.* 1998; Nam *et al.* 1995; Stein *et al.* 1996; Hansen *et al.* 1999; Funder 2004). Much of the focus has been on the fjord area of Scoresby Sund and the Jameson Land Peninsula (Fig. 1), an area with an extensive Quaternary sediment record in a presently ice-free part of central East Greenland. Sugden (1974) described Jameson Land as an area with little or no signs of glacial erosion, mainly based on the highly weathered landscapes in the interior of the peninsula and he proposed that the area had been covered by cold-based ice during the last glacial maximum (LGM). Funder (1989) suggested that lack of evidence of glacial erosion could rather be a result of long periods with ice free conditions. The view of a restricted Greenland Ice Sheet advance during the LGM was supported by results of the Polar North Atlantic Margins (PONAM) project in the early 1990's. Then stratigraphic evidence

was presented for deposition by the Greenland Ice Sheet on interior Jameson Land during the Late Saalian in Marine Isotope Stage (MIS) 6 (Möller *et al.* 1994; Funder *et al.* 1994, 1998).

There is still a debate, however, about whether the Greenland Ice Sheet only reached the inner continental shelf leaving extensive coastal areas free from ice (e.g. Funder 2004; Wilken & Mienert 2006), or if it reached all the way onto the outer shelf or even to the shelf-break during the LGM (Evans *et al.* 2002; O'Coiffaigh *et al.* 2004).

In recent years, cosmogenic exposure dating methods have provided new techniques to interpret differentially weathered landscapes and this has led to a new understanding of the extent and dynamics of Pleistocene ice sheets elsewhere in the Arctic (Stroeven *et al.* 2002; Fabel *et al.* 2002; Briner *et al.* 2003, 2005, 2006; Landvik *et al.* 2003; Marquette *et al.* 2004; Davis *et al.* 2006; Harbour *et al.* 2006).

In the present study we use cosmogenic  $^{10}\text{Be}$ - and  $^{26}\text{Al}$ -ages from 44 erratics to test whether the interior of Jameson Land was (i) ice free, (ii) covered with a



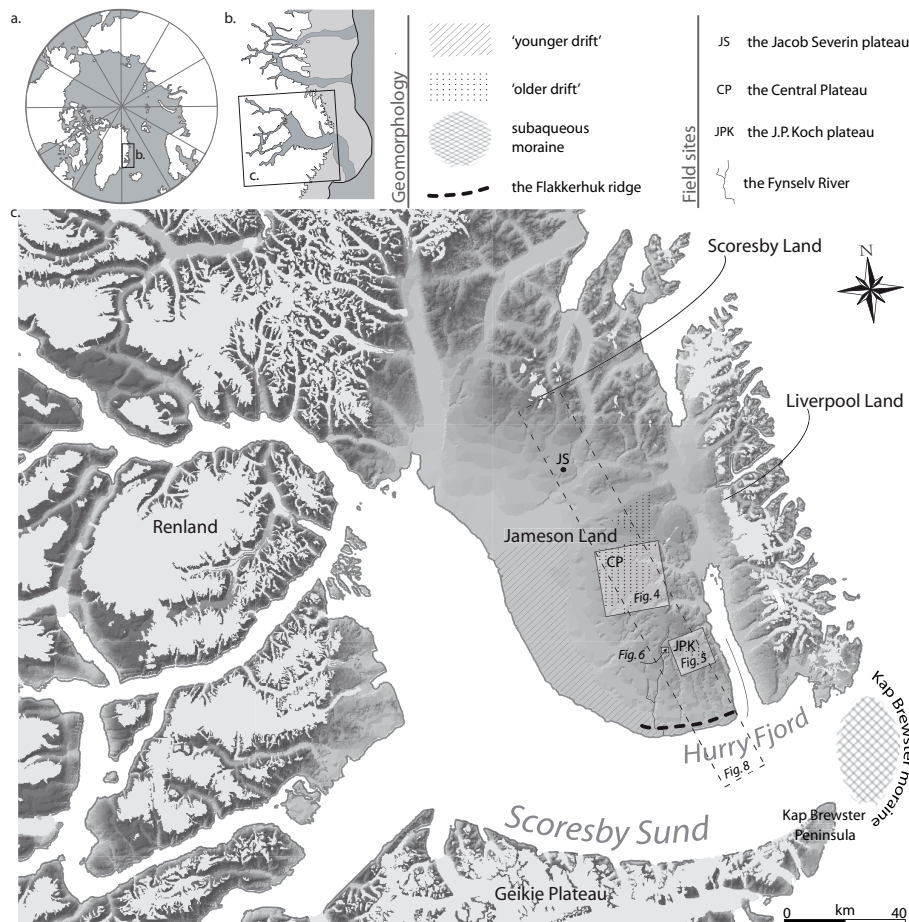


Fig. 1. Maps showing: A. the Arctic and the location of Greenland, B. central East Greenland  $\sim 68\text{--}74^\circ\text{N}$ . The continental shelf is marked as a light grey area and cross-shelf troughs are shown in darker grey. C. The Scoresby Sund area and Jameson land. Detailed site maps (Figs 4, 5 and 6) are marked with framed boxes. The dashed frame shows the transect in Figure 8.

local cold-based ice cap(s) or (iii) overridden by the Greenland Ice Sheet during the LGM.

## Geologic setting

Scoresby Sund ( $70\text{--}71^\circ\text{N}$ ,  $22\text{--}28^\circ\text{W}$ ) is one of the major fjord systems in East Greenland (Fig. 1). The coastal areas beyond the present margin of the Greenland Ice Sheet in the Scoresby Sund region are dominated by three landscape types: (i) closest to the ice-sheet margin, deep fjords are cut into ice-covered high mountain plateaus of Caledonian crystalline bedrock, (ii) north of Scoresby Sund, on the Jameson Land Peninsula, Mesozoic sandstones and shales make up low-relief ice-free terrain and, (iii) south of Scoresby Sund, on the basaltic Geikie plateau, and east of Jameson Land, on the Caledonian crystalline terrain of Liverpool Land, the landscape has an alpine relief from local glaciation (Fig. 1).

The Jameson Land Peninsula has an asymmetric topographic profile. From the plateau areas of interior Jameson Land the terrain gently slopes towards

Scoresby Sund in the west and south whereas the eastern margin, facing Hurry Fjord, has a steeper gradient (Fig. 1). The plateaus form the watershed between east-draining rivers towards Hurry Fjord and the many, and commonly large, river valleys draining west and south towards Scoresby Sund.

## Previous investigations

Two areas covered by Late Quaternary glacial sediments have been described on Jameson Land; the 'older drift' and the 'younger drift' (Ronnert & Nyborg 1994). The former has been mapped on the upland plateaus on the interior of the peninsula (Möller *et al.* 1994), the latter on low elevation areas bordering Scoresby Sund (Ronnert & Nyborg 1994; Fig. 1). Between these two regions is the so-called 'driftless area' where weathered sandstone is exposed and glacial deposits only occur as scattered erratics and more rarely as thin patches of till (Hjort & Salvigsen 1991; Ronnert & Nyborg 1994).

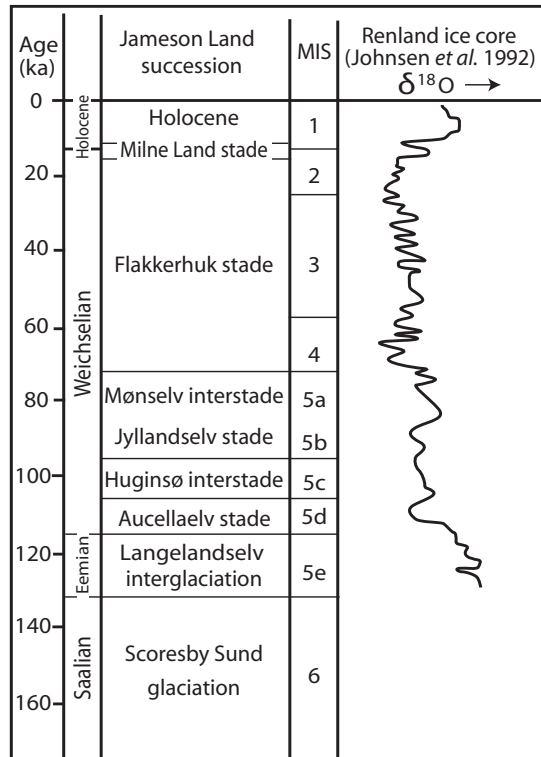


Fig. 2. The Late Quaternary succession of Jameson Land and its proposed correlation with the European chronostratigraphy and the marine oxygen isotope stratigraphy according to Funder *et al.* (1994). Also the correlation with the  $\delta^{18}O$ -record from the Renland ice core is shown (Johnsen *et al.* 1992)

### The 'older drift'

Already in the early parts of the 20th century, glacial and fluvial deposits were described on interior Jameson Land by Otto Nordenskjöld and referred to as the 'Jameson Land Drift' (Nordenskjöld 1907). It was suggested that these sediments were deposited during an extensive glaciation, first named the Kap Mackenzie stadial (Funder & Hjort 1973), later the Scoresby Sund glaciation and it was regarded to be early Weichselian or older in age (Funder 1984, 1989). The 'Jameson Land Drift', later referred to as the 'older drift' (Ronnert & Nyborg 1994) is found as a continuous sheet both on the Central Plateau at 450-500 m a.s.l. and on the J.P. Koch plateau at altitudes >750 m a.s.l. (Fig.1). Erratics on weathered mountain plateaus on northern Jameson Land (e.g. Jacob Severin Bjerg, Fig. 1) and discontinuous patches of till in the 'drift-less' area (e.g. the Fynselv area) have also been correlated with the 'older drift' (Möller *et al.* 1994).

Within the PONAM project, the stratigraphy of interior Jameson Land was investigated in river valleys at the edges of the Central Plateau (Möller *et al.* 1994). Successions of proglacial sediments and subglacial till were described and interpreted as having been deposited during two glacial advances in lakes dammed between

the western edge of the Central Plateau and the margin of an advancing outlet glacier in Scoresby Sund. It was also suggested that till was deposited by the ice sheet successively overriding the plateau during the later of the two advances. Five thermo luminescence (TL) ages constrain the deposition of till on the plateau to between 222 and 167 kyr, which indicate that the ice sheet advance took place during the Late Saalian (Möller *et al.* 1994). Investigations at the eastern margin of the Central Plateau (Fig. 1) have shown that lakes were also dammed by a glacier advancing onto the plateau from Liverpool Land in the east during the Saalian (Möller *et al.* 1994; Adrielsson & Alexanderson, 2005). The stratigraphy also reveals an ice advance from Liverpool Land during the Weichselian constrained by optically stimulated luminescence (OSL) ages from aeolian sediment giving it a maximum age of 109 kyr (Adrielsson & Alexanderson 2005).

### The 'younger drift'

Along the Scoresby Sund coast, the 'younger drift' extends up to ~200 m a.s.l. (Fig. 1). Previous work has identified lacustrine and marine sediments and three thin and discontinuous till layers interpreted as three different advances of outlet glaciers in the Scoresby Sund during the Weichselian, reaching no further than the upper boundary of the 'younger drift'. It was suggested that the two oldest of advances of outlet glaciers occurred in the early Weichselian, during the Aucella- and the Jyllandselv stades (Fig. 2; Landvik *et al.* 1994; Lyså & Landvik 1994; Tveranger *et al.* 1994; Funder *et al.* 1998). Hansen *et al.* (1999) interpreted part of the lacustrine sediments of the 'younger drift' as having been deposited in ice-dammed lakes adjacent to an outlet glacier advancing and retreating in Scoresby Sund during the last glaciation. OSL ages of the glaciolacustrine sediments constrain this last ice advance in the Scoresby Sund to between 60 and 10 kyr (Flakkerhuk stadi). During the Late Weichselian, the northern margin of the outlet glacier was thought to be related to the Flakkerhuk ridge on southern Jameson Land (Fig. 1), which is an erosional landform composed of pre-LGM sediments (Tveranger *et al.* 1994). This implies an ice elevation near Hurry Fjord of <70 m a.s.l. during the LGM (Funder *et al.* 1998). The limited ice thickness near the fjord mouth was used to argue that the LGM ice terminated at the Kap Brewster subaqueous moraine (Fig. 1; Dowdeswell *et al.* 1994) leaving Jameson Land above the 'younger drift' limit ice free and the adjacent continental shelf free from grounded ice (e.g. Möller *et al.* 1994; Funder *et al.* 1998).



Fig. 3. A. The Jacob Severin plateau at ~450 m a.s.l. with Scoresby Sund in the background. B. Windpolished quartzite erratic boulder on the Jacob Severin plateau (sample CF-17). C. The Central Plateau with the mountains of Liverpool Land in the background. Picture is taken from the plateau north of the Ugleelv valley. D. Section in glaciofluvial ridge on the eastern Central Plateau, south of the Ugleelv valley. The ridge is dominated by sandy sediments and on the surface there is a concentration of pebbles and cobbles. E. Esker on the J.P. Kochs Fjeld plateau. Site JPK1. F. Sandstone tors in the Fynselv area. G. Crystalline erratic boulder on ground moraine in the Fynselv area (sample 06-FE-60)

## Methods

Samples for cosmogenic  $^{10}\text{Be}$  and  $^{26}\text{Al}$  exposure dating were collected manually from boulders using hammer and chisel. Cobbles and pebbles were collected from flat, well-drained surfaces, and samples consist of either a single cobble or an amalgamated sample of

~15 clasts of about the same size (Table 1). Sample location and elevation was obtained using a GPS receiver. Shielding from surrounding objects was measured with a compass.

Samples were processed at the University at Buffalo for  $^{10}\text{Be}$  and  $^{26}\text{Al}$  analysis following procedures modified after Kohl & Nishiizumi (1992) and Briner

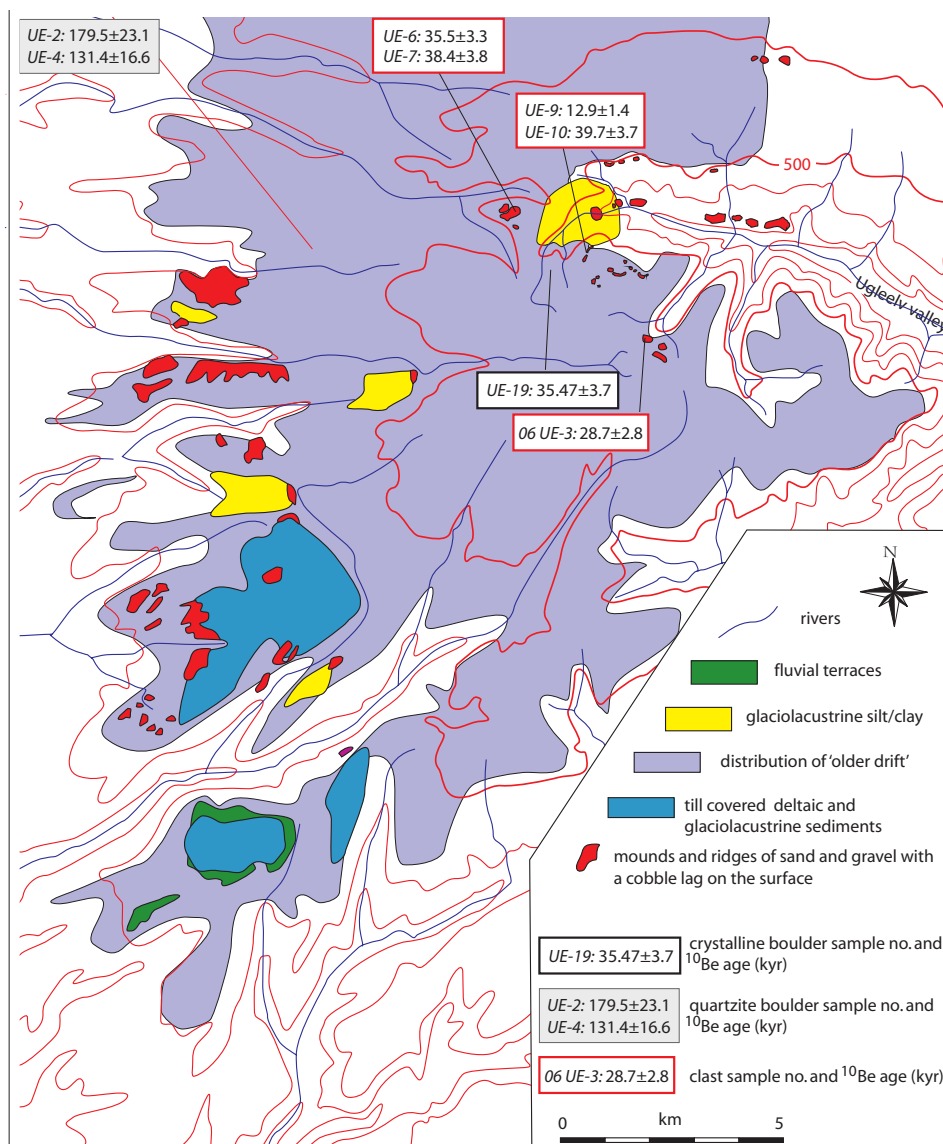


Fig. 4. Map of the Central Plateau based on Möller et al (1994) and Adrielsson & Alexanderson (2005), combined with field mapping in 2006. Location of sampling sites and  $^{10}\text{Be}$  ages are shown in inserted boxes.

(2003). First, samples were crushed and sieved. Then the 425–850  $\mu\text{m}$  fraction of each sample was treated in acid solutions to dissolve clay minerals and organic material. Quartz was purified through selective mineral dissolution in heated sonication baths with dilute  $\text{HF-HNO}_3$ . About 40 g of clean quartz from each sample was dissolved in batches of 11 and one process blank. Known amounts SPEX brand Be- and Al-carrier was added to all samples including the blank. Once dissolved and evaporated, samples were treated with perchloric acid to remove fluoride and run through an anion column to remove Fe, Ti and Mn. Finally Be and Al were separated in a cation column and Be and Al hydroxides were precipitated, dried, heated and packed in targets for AMS measurements.  $^{10}\text{Be}/^9\text{Be}$  ratios were measured at the Tandem Laboratory at Uppsala University and  $^{26}\text{Al}/^{27}\text{Al}$  ratios were measured at PRIME lab, Purdue University. Ages were calculated

with the CRONUS-Earth exposure age calculator (version 2.1; <http://hess.ess.washington.edu/math/>, Balco et al., 2008) using constant production rates and the scaling scheme for spallation by Lal (1991) and Stone (2000). This program uses a reference  $^{10}\text{Be}$  production rate of  $4.96 \pm 0.43$  atoms/g/yr ( $\sigma_2$ , sea level, high latitude and standard atmosphere). The program calculates  $^{26}\text{Al}$  ages with a production rate based on the production ratio  $^{26}\text{Al}/^{10}\text{Be}$  of 6.1. Correction was made for sample thickness using exponential decrease in nuclide production and a bulk density of  $2.68 \text{ g cm}^{-3}$ . The diameter of each cobble is used as its sample thickness, whereas the average diameter is used for amalgamated clast samples. The topographic shielding for all samples was less than  $5^\circ$  and was thus considered negligible. All  $^{10}\text{Be}$  and  $^{26}\text{Al}$  data are presented in Table 1.

The calculation of single cosmogenic exposure ages

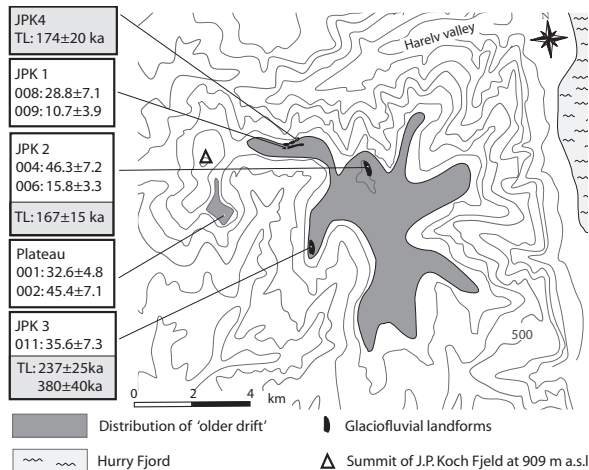


Fig. 5. Map of J.P. Kochs Fjeld after Möller et al. (1994) showing drift distribution and location of glaciofluvial landforms. Our  $^{10}\text{Be}$  results are shown together with TL ages from Möller et al. (1994).

relies on several assumptions, including that a sampled surface has been constantly exposed, lacks inherited isotopes from previous exposures (requiring at least ~2 m of glacial erosion; Davis *et al.* 1999, Briner *et al.* 2006), and has experienced only minimal post-glacial surface erosion. This will likely be the case for most samples from erratics and bedrock surfaces from settings where substantial erosion took place. There are, however, at least two scenarios where these assumptions will be violated. First, exhumation of clasts from unconsolidated sediments will lead to anomalously young exposure ages (Putkonen & Swanson 2003). Second, cold-based ice has the potential to preserve both old bedrock surfaces and erratics deposited during earlier glaciations and thus samples from such surfaces might contain inherited isotopes from previous exposure, resulting in exposure ages much older than the last deglaciation (Briner *et al.* 2005).

Where bedrock and erratics are shielded from cosmic radiation for long periods (~200 ka or longer; e.g. via burial by non-erosive ice), the burial duration can be constrained using the disequilibrium of  $^{10}\text{Be}$  and  $^{26}\text{Al}$  concentrations (Lal 1991; Bierman *et al.* 1999; Gosse & Phillips 2001; Fabel *et al.* 2002; Briner *et al.* 2006; Harbour *et al.* 2006). In a continuously exposed surface  $^{10}\text{Be}$  and  $^{26}\text{Al}$  will be produced at a constant ratio ( $^{26}\text{Al}/^{10}\text{Be}=6.1$ ). If a surface gets shielded from cosmic radiation by non-erosive ice, then the faster decay of  $^{26}\text{Al}$  (half-life of 700 kyr) relative to  $^{10}\text{Be}$  (half-life of 1.3 Myr, Fink & Smith, 2007) will lead to a decrease in the  $^{26}\text{Al}/^{10}\text{Be}$  ratio. Paired isotope data can thus constrain exposure and burial durations.

## Results

### Jakob Severin plateau – the ‘drift-less area’

The Jakob Severin plateau (71°12N, 23°29W; Fig. 3A) is a sandstone plateau at ~450 m a.s.l. situated less than 30 km to the south from the mountainous Scoresby Land with present cirque glaciation at ~1000 m a.s.l. (Fig. 1). This plateau is covered by thin regolith composed of sand and flat, sandstone cobbles. Along the plateau edges weathered sandstone is exposed in small outcrops. Quartzite erratics occur scattered across the plateau and are suggested to be part of the ‘older drift’ (Möller *et al.* 1994).

Samples were taken from three wind polished, 0.4–0.6 m high quartzite boulders resting on regolith (Fig. 3B) and two rounded quartzite cobbles perched on weathered bedrock outcrops (Tab. 1).  $^{10}\text{Be}$  ages from boulders range between 64.7±8.8 and 68.8±9.0 kyr. Two of these samples (CF-17, 23) have  $^{26}\text{Al}/^{10}\text{Be}$  ratios (within one sigma error) equivalent to the production ratio of 6.10±0.08. The two cobbles gave  $^{10}\text{Be}$  ages of 53.4±9.5 and 71.2±7.4 kyr (Table 1). The  $^{10}\text{Be}$  age of the youngest sample (CF-20) falls outside of the two sigma range of the average age for the oldest four erratics. The average exposure age of the oldest four is 68.2±8.5 kyr.

### The Central Plateau – the ‘older drift’

The Central Plateau (~70°N, 22°W; Figs 1, 3C, 4) is situated ~40 km southeast of Jakob Severin Bjerg and constitutes an extensive flat area at 400–550 m a.s.l. This plateau is covered by thin sandy till (Möller *et al.* 1994) with a high abundance of wide-based erratic boulders, most of which reach less than 0.2 m above the till surface, and cobble-sized material (mostly quartzite) which has a western provenance and Caledonian crystalline rocks which have source areas both to the west and on Liverpool Land to the east. At around 400 m a.s.l. the western and southern parts of the plateau are incised by rivers discharging into Scoresby Sund. Below this elevation the ‘older drift’ sediments become discontinuous with increased relief of the landscape (Fig. 4).

Along the margin of the Central Plateau there are several mounds and plateaus (up to 50 m high) and ridges (up to 10 m high) composed of unconsolidated sediments (Fig. 4). Large mounds and plateaus are found mostly along the western plateau margin and are interpreted as erosional remnants of the glaciolacustrine sediments deposited during the Saalian glaciation (Möller *et al.* 1994). Most of the considerably lower ridges are concentrated to the eastern plateau around the Ugleelv valley (Fig. 4). These landforms are composed of sand

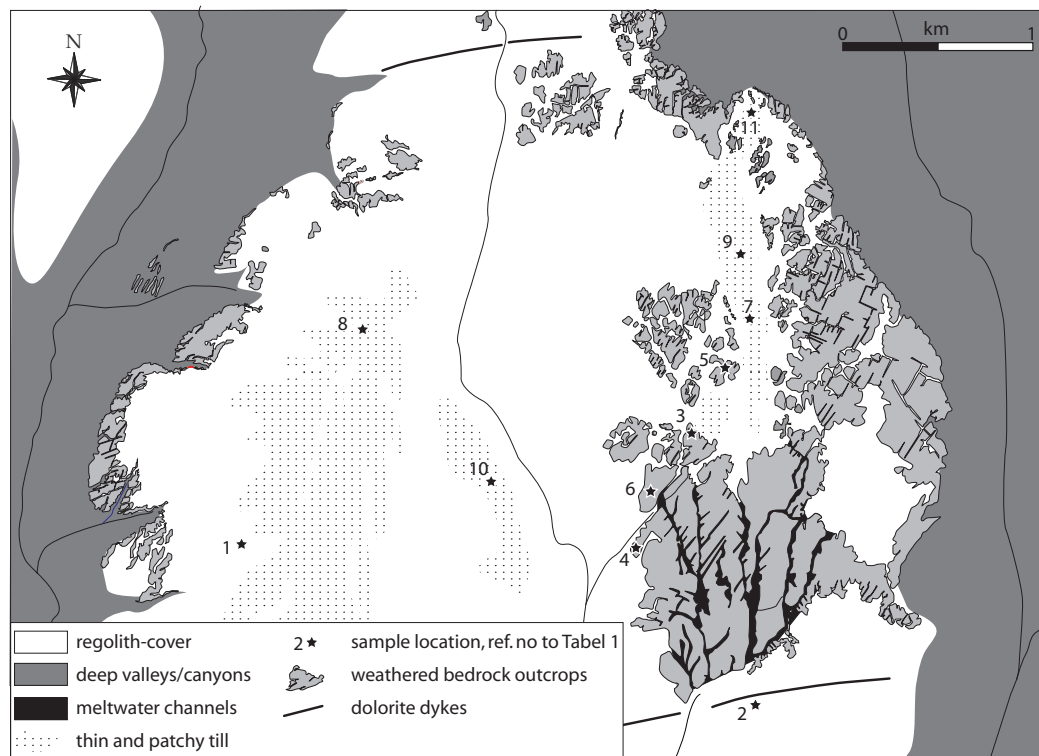


Fig. 6. Map of the sampled tor area at the upper reaches of the Fynselv showing distribution of drift-cover and tor-rich areas. Sampling sites (for 06-samples, see Table 1) are shown with stars.

and gravel with some cobble-sized clasts and have been interpreted as glaciofluvial ridges deposited by an early Weichselian advance from the Liverpool Land ice cap into the valley (Adrielson & Alexanderson 2005). On the surfaces of these landforms there is a concentration of cobble-sized crystalline erratic material (Fig. 3D). A total of eight samples were collected from boulders on the till plain and from clasts on the surfaces of glaciofluvial ridges around the Ugleelv valley (Fig. 4; Table 1). Two samples (UE-2, 4) were taken from 0.3–0.5 m high quartzite boulders on the western part of the plateau and these give  $^{10}\text{Be}$  ages of  $131.4 \pm 16.6$  and  $179.5 \pm 23.1$  kyr (Table 1). One sample was collected from a 0.6 m high crystalline boulder on the eastern plateau margin adjacent to the Ugleelv valley (UE-19) has a  $^{10}\text{Be}$  age is  $35.4 \pm 3.7$  kyr. One cobble and four amalgamated clast samples were collected from the surfaces of three ridges along the Ugleelv valley (Fig. 4). The cobble sample gives a  $^{10}\text{Be}$  age of  $13.5 \pm 1.5$  kyr and clast samples range between  $29.4 \pm 2.8$  and  $40.3 \pm 3.7$  kyr.

#### *The J.P. Koch plateau – the ‘older drift’*

J.P. Koch Fjeld is a basalt-capped mountain, reaching 909 m a.s.l. South and east of the mountain Jurassic sandstone forms a flat plateau at 750–850 m a.s.l. (Fig. 5), covered by a thin till sheet and with weathered

sandstone outcrops exposed along the plateau edges. Ridges and mounds are found near the plateau margin at sites JPK1, 2 and 3 (Fig. 3E) and terrace systems occur along the edges and on the upper slopes of the Hareelv valley at site JPK4 (Fig. 5). The landforms are composed of sand and coarse-grained sediments with a maximum particle size of  $\sim 0.4$  m and clasts are predominantly quartzite and crystalline erratics (Möller *et al.* 1994). There is a concentration of cobbles on the surface of these landforms and more rarely erratic boulders  $< 0.6$  m. Boulder-sized erratics are common on the thin drift sheet covering the plateau. These landforms were interpreted as eskers and kames (Möller *et al.* 1994). Three TL ages from sites JPK1–3 range between 167 and 380 kyr (Fig. 5) and based on these ages and the content of western quartzite boulders it has been suggested that they were deposited by the Greenland Ice Sheet during the Saalian glaciation (Möller *et al.* 1994).

A total of seven samples were collected from boulders on the J.P. Koch plateau (Table 1; Fig. 5). Two samples are from quartzite boulders on the surface of the glaciofluvial ridge at site JPK1, one of them from a 0.4 m high boulder resting on the flat crest far away from the slopes (sample 009), the other a 0.6 m high boulder resting on a gently sloping surface slightly below the crest (sample 008). Two quartzite boulders were taken from the crest of the glaciofluvial ridge at site JPK 2

Table 1. Exposure ages are calculated using the online Chronus age calculator version 2.1 (<http://hess.ess.washington.edu/math/>; Balco et al 2008)

Sample <sup>a</sup>	Surface type <sup>b</sup>	Sample height (m)	Latitude (°N)	Longitude (°W)	Elevation (m a.s.l.)	Thickness corr. <sup>c</sup>	<sup>10</sup> Be (10 <sup>5</sup> atoms/g)	<sup>26</sup> Al (10 <sup>5</sup> atoms/g)	<sup>10</sup> Be age (kyr BP) <sup>d</sup>	<sup>26</sup> Al age (kyr BP)	<sup>26</sup> Al/ <sup>10</sup> Be ratio
<b>Jacob Severin Bjerg</b>											
<b>Quartzite boulders</b>											
CF-17	1a	0.4	71°12.266	23°29.010	444	0.983	5.66 ± 0.29	33.27 ± 3.52	68.8 ± 9.0	71.1 ± 7.5	5.9 ± 0.5
CF-23	1a	0.6	71°12.257	23°28.576	445	0.983	5.34 ± 0.33	29.70 ± 3.25	64.7 ± 8.8	63.8 ± 7.0	5.6 ± 0.5
CF-14	1a	0.4	71°12.270	23°28.526	446	0.983	5.62 ± 0.30	n/a	68.1 ± 9.0	n/a	n/a
<b>Cobbles</b>											
CF-19	1b	n/a	71°12.257	23°28.576	445	0.944	5.63 ± 0.39	n/a	71.2 ± 7.4	n/a	n/a
CF-20	1b	n/a	71°12.257	23°28.576	445	0.921	4.32 ± 0.56	n/a	53.4 ± 9.5	n/a	n/a
<b>The Central Plateau</b>											
<b>Quartzite boulders</b>											
UE-2	2a	0.3	70°54.261	23°15.457	446	0.983	14.42 ± 0.51	n/a	179.5 ± 23.1	n/a	n/a
UE-4	2a	0.5	70°54.347	23°21.538	410	0.983	10.31 ± 0.31	n/a	131.4 ± 16.6	n/a	n/a
<b>Crystalline boulders</b>											
UE-19	2a	0.6	70°54.589	23°06.515	496	0.983	3.08 ± 0.17	n/a	35.4 ± 3.7	n/a	n/a
<b>Amalgamated clast samples</b>											
06-UE-3	2b	n/a	70°53.808	23°04.449	507	0.959	2.51 ± 0.10	n/a	29.4 ± 2.8	n/a	n/a
UE-6	2b	n/a	70°55.208	23°09.266	513	0.959	3.14 ± 0.10	n/a	36.4 ± 3.4	n/a	n/a
UE-7	2b	n/a	70°55.208	23°09.266	513	0.967	3.40 ± 0.16	n/a	39.1 ± 3.9	n/a	n/a
UE-10	2b	n/a	70°54.328	23°06.358	533	0.967	3.57 ± 0.11	n/a	40.3 ± 3.7	n/a	n/a
<b>Cobbles</b>											
UE-9	2b	n/a	70°54.328	23°06.358	533	0.944	1.17 ± 0.08	n/a	13.5 ± 1.5	n/a	n/a
<b>J.P. Koch Fjeld</b>											
<b>Quartzite boulders</b>											
001	2b	0.4	70°39	22°46	782	0.983	3.67 ± 0.31	n/a	32.6 ± 4.8	n/a	n/a
004	2b	0.2	70°39	22°46	792	0.983	5.25 ± 0.51	n/a	46.3 ± 7.2	n/a	n/a
006	2b	0.3	70°39	22°46	782	0.983	1.79 ± 0.30	n/a	15.8 ± 3.3	n/a	n/a
008	2b	0.6	70°39	22°46	769	0.983	3.22 ± 0.69	n/a	28.8 ± 7.1	n/a	n/a
009	2b	0.4	70°39	22°46	770	0.983	1.20 ± 0.41	n/a	10.7 ± 3.9	n/a	n/a

Table 1. (continued)

Sample <sup>a</sup>	Surface type <sup>b</sup>	Sample height (m)	Latitude (°N)	Longitude (°W)	Elevation (m a.s.l.)	Thickness corr. <sup>c</sup>	<sup>10</sup> Be (10 <sup>5</sup> atoms/g)	<sup>26</sup> Al (10 <sup>5</sup> atoms/g)	<sup>10</sup> Be age (kyr BP) <sup>d</sup>	<sup>26</sup> Al age (kyr BP)	<sup>26</sup> Al/ <sup>10</sup> Be ratio
<b>Crystalline boulders</b>											
002	2a	0.1-0.3	70°39	22°46	775	0.983	5.08 ± 0.51	n/a	45.4 ± 7.1	n/a	n/a
011	2b	0.1-0.5	70°39	22°46	768	0.983	3.97 ± 0.65	n/a	35.6 ± 7.3	n/a	n/a
<b>Fynselv</b>											
<b>Quartzite boulders</b>											
FE-12	1a	0.3	70°36.348	23°15.192	338	0.983	12.00 ± 0.62	61.03 ± 6.36	165.1 ± 22.2	151.4 ± 15.8	5.1 ± 0.4
FE-13	1a	0.6	70°36.130	23°16.300	318	0.983	9.07 ± 0.56	49.09 ± 5.44	126.2 ± 13.9	123.2 ± 13.6	5.4 ± 0.5
FE-3	1a	0.1	70°34.554	23°17.592	257	0.983	12.94 ± 0.43	n/a	194.2 ± 18.8	n/a	n/a
FE-5	1a	0.15	70°34.549	23°16.433	257	0.983	11.94 ± 0.57	n/a	178.5 ± 18.4	n/a	n/a
FE-10	1a	0.6	70°36.418	23°14.462	353	0.983	18.90 ± 0.88	n/a	262.1 ± 27.4	n/a	n/a
FE-16	1a	0.4	70°32.225	23°16.367	235	0.983	6.53 ± 0.33	n/a	97.9 ± 10.0	n/a	n/a
FE-14	1a	0.4	70°35.234	23°16.288	323	0.983	7.90 ± 0.50	43.41 ± 4.67	108.9 ± 12.0	108.8 ± 11.7	5.5 ± 0.5
06-FE-28 (1)	1b	0.7	70°39.286	23°10.513	487	0.983	9.03 ± 0.24	n/a	106.4 ± 9.9	n/a	n/a
06-FE-63 (2)	1a	0.35	70°37.360	23°07.606	442	0.983	19.48 ± 0.46	n/a	247.4 ± 23.5	n/a	n/a
06-FE-64 (2)	1a	0.3	70°37.360	23°07.606	442	0.983	17.70 ± 0.46	n/a	223.6 ± 21.3	n/a	n/a
06-FE-2 (3)	1b	0.3	70°38.392	23°08.075	493	0.983	12.89 ± 0.38	n/a	152.8 ± 14.5	n/a	n/a
06-FE-4 (4)	1b	0.2	70°38.080	23°08.176	495	0.983	16.90 ± 1.22	n/a	202.1 ± 23.9	n/a	n/a
06-FE-12 (5)	1b	0.25	70°38.591	23°07.140	531	0.983	11.97 ± 0.29	n/a	136.3 ± 12.7	n/a	n/a
06-FE-45 (6)	1b	0.3	70°38.353	23°08.077	525	0.983	6.87 ± 0.22	n/a	77.6 ± 7.3	n/a	n/a
06-FE-30 (7)	2a	0.5	70°38.647	23°06.893	485	0.983	5.82 ± 0.18	n/a	68.1 ± 6.4	n/a	n/a
06-FE-40 (8)	2a	0.4	70°36.746	23°07.184	486	0.983	9.24 ± 0.26	n/a	109.1 ± 10.2	n/a	n/a
<b>Crystalline boulders</b>											
06-FE-59 (9)	2a	1.5	70°38.862	23°06.842	506	0.983	6.05 ± 0.20	n/a	69.5 ± 6.3	n/a	n/a
06-FE-60 (9)	2a	1.9	70°38.862	23°06.842	506	0.983	7.68 ± 0.18	n/a	88.6 ± 8.1	n/a	n/a
06-FE-69 (9)	2a	0.8	70°38.862	23°06.842	506	0.983	2.00 ± 0.18	n/a	22.8 ± 2.9	n/a	n/a
06-FE-62 (10)	2a	0.5	70°38.190	23°09.656	467	0.983	2.76 ± 0.25	n/a	32.6 ± 4.1	n/a	n/a
<b>Amalgamated clast samps</b>											
06FE-31 (7)	1b	n/a	70°38.647	23°06.893	485	0.967	5.81 ± 0.19	n/a	69.2 ± 6.5	n/a	n/a
06FE-32 (7)	2a	n/a	70°38.647	23°06.893	485	0.967	5.23 ± 0.16	n/a	62.1 ± 5.8	n/a	n/a
06-FE-61 (11)	2a	n/a	70°39.401	23°06.345	528	0.967	5.96 ± 0.16	n/a	68.1 ± 6.2	n/a	n/a

<sup>a</sup> Sample ID. For samples from the Fynselv area numbers in brackets refer to site number in Figure 6.

<sup>b</sup> surface type that the sample is resting on; (1a) regolith, (1b) weathered bedrock outcrops, (2a) ground moraine and (2b) glaciofluvial landforms

<sup>c</sup> thickness correction calculated for a density of 2.68 g/cm<sup>3</sup>

<sup>d</sup> <sup>10</sup>Be-ages are calculated using the cronus calculator version 2.1 (Balco et al. 2008)



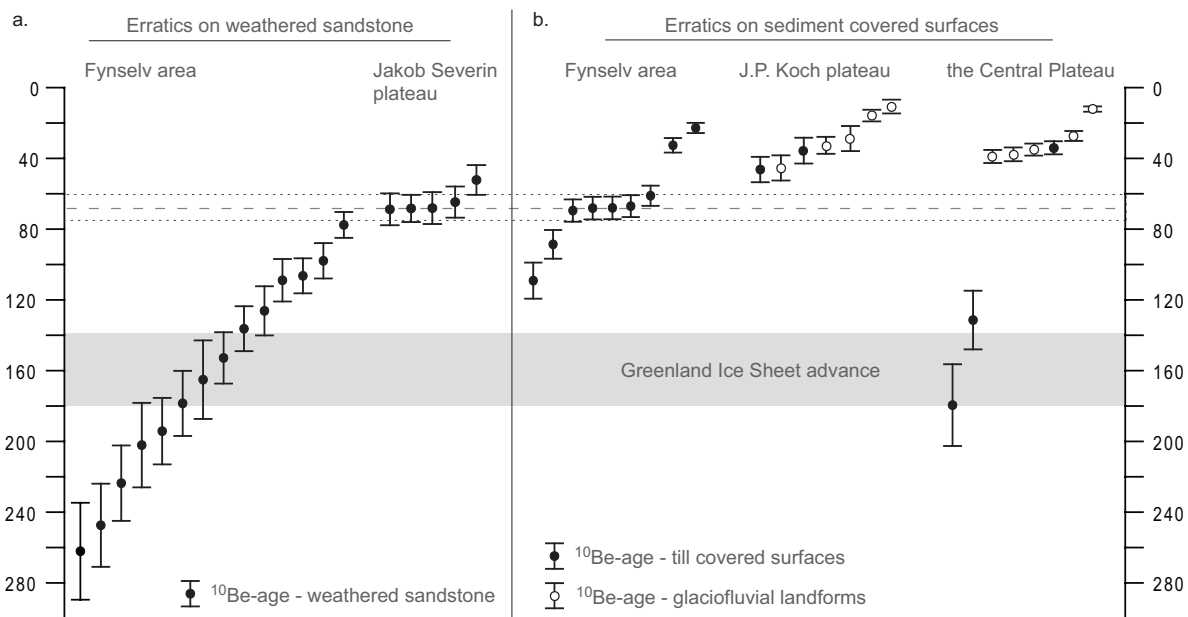


Fig. 7. All  $^{10}\text{Be}$ -ages on erratics from interior Jameson Land presented within two sigma error (Table 1). A. The distribution of  $^{10}\text{Be}$ -ages from erratics resting on weathered sandstone- and B. sediment-covered surfaces. Shading indicates the timing of the Saalian advance of the Greenland Ice Sheet (Funder et al. 1994). The dashed lines show the average exposure age within two sigma error of eight erratics on weathered sandstone on the Jakob Severin plateau and till covered surfaces in the Fynselv area.

(samples 004 and 006) and one crystalline boulder was sampled from the crest of the glaciofluvial ridge at site JPK3 (sample 011). Samples were also collected from the till covered plateau south of the summit of J.P Koch Fjeld, from one quartzite (sample 001) and one crystalline boulder (sample 002).

The ages form two groups, one slightly younger than the other, but both groups are substantially younger than TL ages from sediment samples in this area (Fig. 5; Möller et al. 1994). Samples 006 and 009 give  $^{10}\text{Be}$  ages of  $15.8 \pm 3.3$  and  $10.7 \pm 3.9$  kyr, whereas the remaining five samples range between  $28.8 \pm 7.1$  and  $46.3 \pm 7.2$  kyr (Table 1).

#### The Fynselv area—the 'drift-less area'

The Fynselv River has its source northwest of the J.P. Koch plateau and discharges to the south into Scoresby Sund (Fig. 1). The upper and middle reaches of this river flows through the 'drift-less' area and it has formed deep canyons surrounded by extensive interfluves of exposed weathered sandstone between ~550-250 m a.s.l. The centre of interfluves is covered by regolith. Along the edges of the canyon tor-rich areas are common (Fig. 3F) and in some areas systems of meltwater channels follow fracture systems within the sandstone (Fig. 6; Schunke 1986; Hjort & Salvigsen 1991; Håkansson 2008).

In the Fynselv area drift cover is rare and occurs only as patches of sandy till, and single erratics, usually

on regolith-covered centres of interfluves but also on weathered sandstone outcrops within tor areas. The drift cover is dominated by rounded quartzite cobbles and wind-polished quartzite boulders less than 0.6 m high. Large (up to 2 m high) and angular crystalline erratics occur scattered on till covered surfaces (Fig. 3G).

Twenty three samples were collected from boulders and clasts resting on both till and weathered bedrock (Table 1). Most samples (sample ID starting with 06-) were taken from one area at the upper reaches of the river (~70°38 N, 23°07 W; Figs 1, 6). The remaining samples were collected from areas further to the south, down-stream along the Fynselv River and all of these are from regolith covered surfaces on the centre of interfluves.

In total 14 samples from wind-polished quartzite erratics, 0.1-0.6 m high and one clast sample (06FE-31) were collected from weathered bedrock surfaces or surfaces covered by regolith. The clast sample gives a  $^{10}\text{Be}$  age of  $69.2 \pm 6.5$  kyr. Acquired  $^{10}\text{Be}$  ages for boulders are scattered between  $77.6 \pm 7.3$  and  $262.1 \pm 27.4$  kyr and  $^{26}\text{Al}/^{10}\text{Be}$  ratio (within one sigma error) for one of these samples (FE-14) is equivalent to the production ratio whereas for two samples (FE-12, 13) the paired isotope data are discordant (Table 1). Samples were also collected from the thin patches of till along the upper reaches of the river (Fig. 6); two clast samples (06FE-32, 61) give  $^{10}\text{Be}$  ages of  $62.1 \pm 5.8$  and  $68.1 \pm 6.2$  kyr, four samples from crystalline boulders

0.4-1.9 m high range between  $22.8 \pm 2.9$  and  $88.6 \pm 8.1$  kyr and two quartzite boulders (06FE-30, 40) 0.4 and 0.5 m give  $^{10}\text{Be}$  ages of  $68.1 \pm 6.4$  and  $109.1 \pm 10.2$  kyr. The larger part of the dataset from the Fynselv area shows a scattered distribution of  $^{10}\text{Be}$  ages that range from  $22.8 \pm 2.9$  to  $262.1 \pm 27.4$  kyr, but five samples (06FE-30, 31, 32, 59, 61) form a cluster with an average age (within two sigma error) of  $67.4 \pm 6.2$  kyr.

### Summary of exposure ages

$^{10}\text{Be}$  exposure ages of erratics from interior Jameson land have been divided into two groups based on whether sampled erratics were resting on weathered sandstone (Fig. 7A) or on sediment (Fig. 7B). Erratics on weathered sandstone surfaces in the Fynselv area have “old” exposure ages with a scattered distribution between  $\sim 78$  and 262 kyr. However, there are also a few “old” samples from sediment covered surfaces; two are from the Fynselv area and two from the till plain on the western Central Plateau (Fig. 7). The youngest erratics on weathered sandstone surfaces are from the Jacob Severin plateau and cluster around  $\sim 70$  kyr, which is very similar to ages of erratics from till in the Fynselv area. The exposure ages from the J.P. Koch- and the eastern Central Plateau are younger compared to the rest of the data set (Fig. 7), but also considerably younger than the age proposed by earlier work for glaciofluvial landforms on these plateaus (Fig. 5; Möller *et al.* 1994; Adrielsson & Alexanderson 2005). On these two sediment-covered plateaus samples cluster around the oldest ages (Fig. 7). A similar distribution of ages is also seen for sediment-covered surfaces in the Fynselv area.

### Discussion

In the Fynselv area, all “old” erratics ( $^{10}\text{Be}$  exposure ages between  $\sim 78$  and 262 kyr; Fig. 7; Table 1) are situated on or adjacent to well-developed tors indicating that both erratics and tors may have been preserved by cold-based non-erosive ice. This is indeed suggested by discordant paired isotope data from two of these erratics (samples FE-12, 13) indicating a complex exposure/burial history longer than  $\sim 200$  kyr, probably due to periods of shielding by cold-based ice. Based on measured  $^{26}\text{Al}$  and  $^{10}\text{Be}$  concentrations in these two samples (Table 1), a minimum duration can be estimated for their total exposure and burial. The results indicate that the boulders were originally eroded from their source areas between ca 250 and 430 kyr ago and then exposed for ca 126-165 kyr. Either these erratics were originally deposited on Jameson Land or they were entrained by a later advance of the ice sheet and

successively brought to their present locations.

Results from previous work has indicated the presence of cold based ice on interior Jameson Land during the LGM but it has not been able to conclude whether this ice was dynamically connected to the Greenland Ice Sheet or not (Håkansson *et al.* 2007; Håkansson 2008). The only samples in the present study with LGM/Late Glacial  $^{10}\text{Be}$  ages from interior Jameson Land are taken from the surfaces of glaciofluvial ridges on the J.P. Koch- and the Central Plateau. The ages of these landforms have been independently constrained indicating that they were deposited during the Saalian and early Weichselian, respectively (Möller *et al.* 1994; Adrielsson & Alexanderson 2005). Recent investigations have suggested that when using cosmogenic exposure dating on old (pre-LGM) landforms surface lowering processes causing exhumation need to be considered (Putkonen & O’Neil 2006; Briner 2007; Kaplan *et al.* 2007). Cobbles and boulders on sampled glaciofluvial landforms have similar maximum particle size and clast lithologies as the sediment within these features. The clast concentrations on landform surfaces are thus interpreted as a result of exhumation, mainly through deflation. This process will be more efficient in lowering surfaces of the glaciofluvial landforms composed of sediment with a sandy matrix and only few clasts compared to on the sandy till, which contains more clasts and less matrix. This is supported by the fact that the oldest samples from the glaciofluvial landforms fall within the same range as samples on the till plain (Fig. 7). Stormy periods, when surface lowering and thus exhumation of material might be more active, are indicated by high dust concentrations in the Renland ice core during the Weichselian in general, and during the coldest periods in particular (Johnsen *et al.* 1992). Strong winds are also indicated by the numerous wind polished boulders found all over interior Jameson Land. Following this reasoning we suggest the LGM/Late Glacial  $^{10}\text{Be}$  ages on glaciofluvial landforms to be a result of exhumation rather than to represent a LGM advance of the Greenland Ice Sheet. Because we consider that exhumation has been an important process especially on glaciofluvial landforms, the oldest  $^{10}\text{Be}$  exposure ages,  $\sim 46$  and  $\sim 40$  kyr are used to put minimum constraints on the total exposure of the J.P. Koch- and the eastern Central plateau respectively. The clustering of exposure ages around  $\sim 70$  kyr from erratics on both sediment and sandstone could be interpreted as representing an early Flakkerhuk stade (MIS 4) advance of the Greenland Ice Sheet. There is indeed evidence in the stratigraphy of the ‘younger drift’ for an advance of an outlet glacier in Scoresby Sund starting around  $\sim 70$  kyr (Hansen *et al.* 1999). However, there are no indications, neither in the stratigraphy nor on the continental shelf that this glacial advance was extensive enough to reach onto interior Jameson Land.

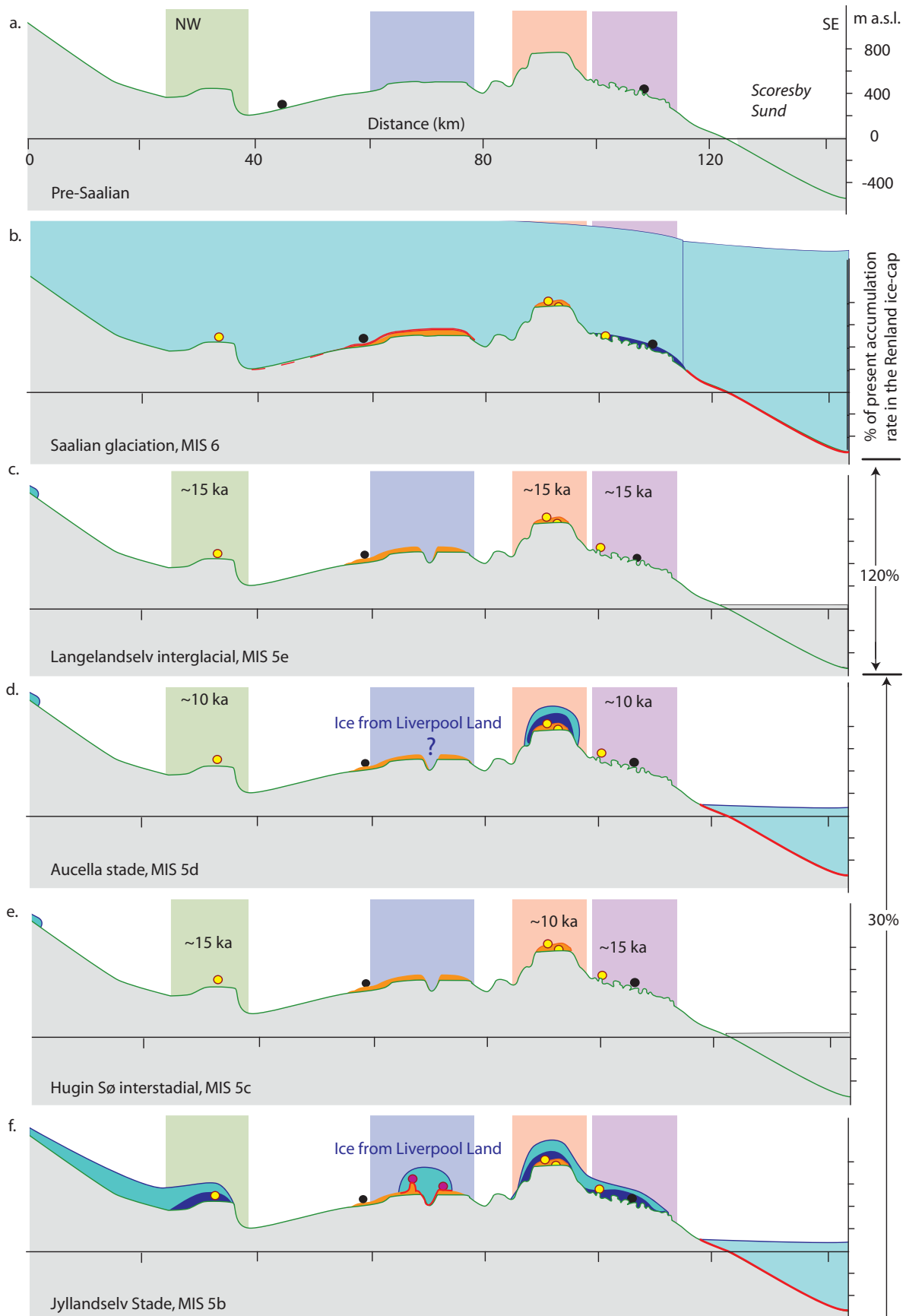
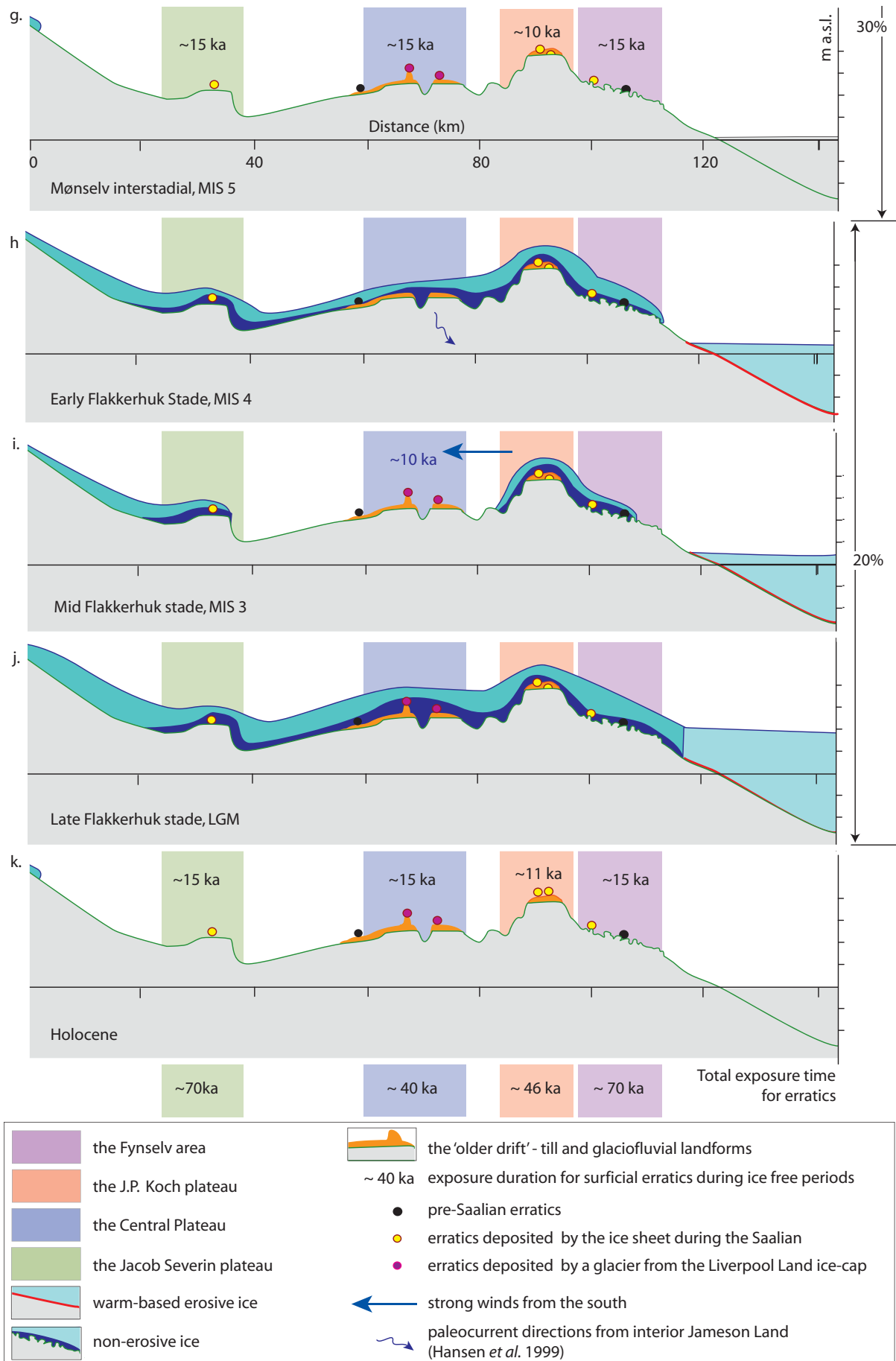


Fig. 8. Simplified model showing one possible scenario for the Late Quaternary glacial geological development of interior Jameson Land. Accumulation rate in the Renland ice-cap after Johnsen et al. (1992)



Marine cores from the shelf-break outside Scoresby Sund show lower sedimentation during MIS 4 compared to all other periods during the last glacial cycle (Nam *et al.* 1995). Thus, an extensive advance of the ice sheet during this time is considered less likely. Instead we suggest that erratics were deposited during the Saalian glaciation, which is the last time when material transport onto interior Jameson Land is recorded in the stratigraphy. Our exposure ages are, however, much younger than the Saalian deglaciation (the transition between MIS 6 and 5e  $\sim$ 130 kyr, Funder *et al.* 1994). We suggest that the exposure ages younger than Saalian are the result of periods of shielding by cold-based ice during the Weichselian. This implies that during the last  $\sim$ 130 kyr the Jacob Severin plateau and the Fynselv area were exposed for a total of  $\sim$ 70 kyr and covered by ice for  $\sim$ 60 kyr. The J.P. Koch plateau, situated on elevations  $\sim$ 300 m higher compared to the other areas, would have been exposed for at least 46 kyr according to the oldest exposure ages and therefore covered for 85 kyr. These periods of shielding are too short to be resolved by paired  $^{10}\text{Be}$  and  $^{26}\text{Al}$  data and accordingly samples from the Jacob Severin plateau (CF-17, 23) give  $^{26}\text{Al}/^{10}\text{Be}$  ratios indicating “constant exposure”. On the Central Plateau the oldest samples suggest a minimum exposure period of  $\sim$ 40 kyr. The duration of shielding will, however, depend on the timing of the Weichselian advance from the Liverpool Land ice-cap. This advance is only constrained in time with three OSL ages on aeolian sediment, a maximum of 109 kyr and two minimum ages of 27 and 10 kyr. Adrielsson & Alexanderson (2005) argued that the greatest dynamic response of the Liverpool Land ice-cap most likely took place in the early Weichselian (during MIS 5b or MIS 5d) because of high precipitation indicated by the Renland ice core (Johnsen *et al.* 1992; Adrielsson & Alexanderson 2005).

### A glaciation model of the Late Pleistocene on Jameson Land

The Renland ice core indicates that there was a 20 % higher accumulation in the Renland ice cap (Fig. 1) during the MIS 5e, compared to the present (Johnsen *et al.* 1992; Fig. 2). Such high accumulation during the transition from interglacial to glacial climate would favour growth of local ice caps on high-elevation regions such as the two presently glaciated areas to the north and east of Jameson Land (Fig. 1); the Scoresby Land mountains ( $\sim$ 1000 m a.s.l.) and Liverpool Land (highest peak is  $\sim$ 1400 m a.s.l.) but also on the J.P. Koch plateau ( $\sim$ 800 m a.s.l.). The Scoresby Land and Liverpool Land mountains were most likely glaciated throughout the last glacial cycle. Out of the three accumulation centres mentioned above, Liverpool

Land is the most heavily glaciated at present and due to its coastal location it would probably have received more precipitation compared to the other areas all through the last glacial cycle. The J.P. Koch plateau is situated on lower elevations compared to the other two areas and in addition its location further away from the coast will also result in less precipitation.

Based on the  $^{10}\text{Be}$  and  $^{26}\text{Al}$  exposure age dataset in combination with the stratigraphical record (e.g. Möller *et al.* 1994; Funder *et al.* 1994, 1998) and the climate record from the Renland ice core (Fig. 2; Johnsen *et al.* 1992) a sequential model of Late Pleistocene events in the Jameson Land area is proposed in eleven steps (Fig. 8A-K). The four investigated areas are shown along an approximated transect from the Scoresby Land mountains in the NW to Scoresby Sund in the SE (Figs 1, 8).

- A) Erratics with ‘old’ exposure ages, as seen in the Fynselv area and from the western Central Plateau, were originally deposited on Jameson Land or adjacent areas between  $\sim$ 250 and 430 kyr ago by the Greenland Ice Sheet (Fig. 8A).
- B) During the Saalian glaciation an advance of the Greenland Ice Sheet deposited erratics on the Jacob Severin plateau and in the Fynselv area. Also, some pre-Saalian quartzite boulders (samples UE-2, 4, see Tab. 1) were re-deposited in the till on the Central Plateau (Fig. 8B). The ice sheet margin probably reached the continental shelf break at this time. During deglaciation, glaciofluvial ridges were formed along the edges of the J.P. Koch plateau and also meltwater incised the Central Plateau and formed the Ugleelv valley.
- C) The marine limit following the Saalian deglaciation was  $\sim$ 70 m a.s.l. (Landvik *et al.* 1994). Summer temperatures on Jameson Land were ca 5 °C warmer than at present during the Langelandselv interglacial (MIS 5e, the Eemian) and with  $\sim$ 20 % more precipitation (Johnsen *et al.* 1992). Possible exposure time for surficial boulders during this ice free interval was  $\sim$ 15 kyr (Fig. 8C).
- D) Either during the last part of the Langelandselv interglacial or in the initial phase of the Weichselian glacial cycle, in the Aucella stade (MIS 5d), high precipitation and cooling temperatures led to growth of local ice-caps on major accumulation centres such as the Scoresby Land mountains, Liverpool Land and the J.P. Koch plateau (Fig. 8D). A westward advance from the Liverpool Land ice cap might have reached into the Ugleelv valley. At around the same time, an outlet glacier from the Greenland Ice Sheet expanded in the Scoresby Sund trough and deposited thick subglacial till along the Jameson Land coast (part of the ‘younger drift’, Fig. 1). The Jacob Severin plateau and the

- Fynselv area remained ice free throughout this period lasting for ~10 kyr
- E) During the Huginssø interstade (MIS 5c) maximum summer temperatures nearly reached present values (Johnsen *et al.* 1992). Hence the local ice cap on the J.P. Koch plateau melted away and ice centred on the Scoresby Land mountains and on Liverpool Land retreated resulting in ice-free conditions on interior Jameson Land. The exposure periods on the Jacob Severin plateau and in Fynselv probably lasted for ~15 kyr and slightly less on the J.P. Koch plateau (Fig. 8E).
- F) Temperatures dropped during the Jyllandselv stade (MIS 5b) but precipitation was still high (like during MIS 5d), and again local ice started to build up over the J.P. Koch plateau but this time it also covered the Fynselv area. Ice on the accumulation centre in the Scoresby Land mountains expanded to the Jacob Severin plateau. At around the same time a glacier advanced westward from Liverpool Land, this time depositing subglacial till in the Ugleelv valley and glaciofluvial landforms on the edge of the Central Plateau adjacent to this valley (Adriellsson & Alexanderson 2005). Also an outlet glacier advanced in the Scoresby Sund trough and deposited subglacial till within the ‘younger drift’ zone.
- G) Once again maximum summer temperatures nearly reached present values during the Mønselv interstade (MIS 5a). This period lasted slightly longer than MIS 5c (Fig. 2; Johnsen *et al.* 1992). Local ice on interior Jameson Land melted away resulting in an ice free period of around 15 kyr in all areas except for on the J.P. Koch plateau where ice lingered slightly longer resulting in ~10 kyr of exposure. Also during this period, wind erosion might have eroded drift surfaces.
- H) During the early Flakkerhuk stade (MIS 4) climate was getting colder and drier (Johnsen *et al.* 1992). This prolonged cold period led to slow accumulation of local ice over all plateaus, eventually coalescing into a thin cold-based ice capping interior Jameson Land. Again an outlet glacier advanced in the Scoresby Sund trough. Deltaic sediments were deposited in glacial lakes in marginal positions to the Scoresby Sund-based outlet glacier and paleoflow directions are both from Scoresby Sund and from the rivers draining the Central Plateau (Hansen *et al.* 1999).
- I) During the mid Flakkerhuk stade (MIS 3) temperatures got slightly warmer compared to MIS 4 but precipitation was still relatively low (Johnsen *et al.* 1992). This resulted in that ice on the Central Plateau was starved from accumulation and melted/evaporated away. An ice free period lasting for ~10 kyr followed, when strong winds from the south formed deflation surfaces on the drift and accumulated sand dunes in the upper Ugleelv valley (Adriellsson & Alexanderson, 2005). In contrast ice could linger on the J.P. Koch plateau and in the Fynselv area, where some precipitation was received due to these areas being closer to the coast. The ice cover on the Jacob Severin plateau could also persist through this period because of its proximity to the Scoresby Land mountains. Prior to the LGM ice probably accumulated again on the Central Plateau.
- J) Local cold-based ice on interior Jameson Land coalesced with active ice in the Scoresby Sund trough during the LGM (Fig. 6J). The active ice was buttressed by the local cold-based ice capping interior Jameson Land and was at least 250 m thick at the mouth of the Scoresby Sund fjord (Håkansson *et al.* 2007). At this time the ice margin probably reached a considerable distance onto the continental shelf. Ice on the tor area along the Fynselv River started to melt at earliest around ~17 kyr ago (Håkansson 2008).
- K) Following the deglaciation of interior Jameson Land the youngest erratics were exhumed and subsequently exposed on the drift-covered plateaus. The total post glacial exposure time of interior Jameson Land until the present is suggested to have been about 15 kyr. Ice probably lingered for another couple of thousand years on the J.P. Koch plateau. When adding the duration of all ice-free periods in the presented model, the total exposure of Jacob Severin plateau and Fynselv is ~70 kyr, on the J.P. Koch plateau ~46 kyr and on the Central Plateau the total exposure is ~40 kyr (Fig. 7K).

## Conclusions

Here we present cosmogenic  $^{10}\text{Be}$  and  $^{26}\text{Al}$  exposure ages on erratics from four areas on interior Jameson Land. Our dataset can be divided in three groups (i) “old” erratics with total exposure and burial histories between ~250 and 430 kyr, estimated from discordant  $^{10}\text{Be}$  and  $^{26}\text{Al}$  data (ii)  $^{10}\text{Be}$  ages of erratics on weathered bedrock and till covered surfaces clustering around ~70 kyr and, (iii) exposure ages from erratics on glaciofluvial ridges and adjacent till covered plateaus ranging between 10.7 and 46.6 kyr. The “old” exposure ages are interpreted to represent erratics deposited by the Greenland Ice Sheet several glacial cycles ago. Erratics with exposure ages  $\leq 70$  kyr are suggested to originate from an ice sheet advance during the Saalian glaciation and an advance by the local Liverpool Land ice-cap during the early Weichselian. The fact that the apparent exposure ages are younger than both the Saalian and the early Weichselian is explained by

that following deposition erratics were shielded from cosmic radiation during periods when substantial areas on Jameson Land were covered by cold-based ice. The LGM/Late Glacial exposure ages from glaciofluvial ridges are interpreted to be a result of exhumation and therefore we suggest that the Greenland Ice Sheet did not cover Jameson Land during the LGM. Instead we propose that the area was covered by local cold-based ice during this time but also during substantial periods of the last glacial cycle.

## Acknowledgements

This research was funded by the Helge Ax:son Johnson Foundation, the Swedish Association for Anthropology and Geography (SSAG) and Kungliga Fysiografiska Sällskapet i Lund. The Danish Polar Centre provided logistic support. Elizabeth Thomas is acknowledged for enthusiastic help and great company in the field and Nicolas Young is thanked for helping in the lab. Nicolaj Krog Larsen and Lena Adrielsson are thanked for valuable discussions and constructive comments on this manuscript.

## References

- Adrielsson, L. & Alexanderson, H. 2005: Interactions between the Greenland Ice Sheet and the Liverpool Land coastal ice cap during the last two glacial cycles. *Journal of Quaternary Science* 20 (3), 269-283.
- Balco, G., Stone, J. O., Lifton, N. A. & Dunai, T. J. A complete and easily accessible means of calculating surface exposure ages or erosion rates from  $^{10}\text{Be}$  and  $^{26}\text{Al}$  measurements. *Quaternary Geochronology* (2008)
- Bierman, P. R., Marsella, K. A., Patterson, C., Davis, P. T. & Caffee, M. 1999: Mid-Pleistocene cosmogenic minimum-age limits for pre-Wisconsin glacial surfaces in southwestern Minnesota and southern Baffin Island: a multiple nuclide approach. *Geomorphology* 27, 25-39.
- Björck, S. & Hjort, C. 1984: A re-evaluated glacial chronology for northern East Greenland. *Geologiska Föreningens i Stockholms Förhandlingar* 105, 235-243.
- Briner, J. P. 2003: The last glaciation of the Clyde region, north-eastern Baffin Island, arctic Canada: Cosmogenic isotopes constraints on Laurentide Ice Sheet dynamics and chronology. *PhD thesis, University of Colorado, Boulder Colorado*, 300 pp.
- Briner, J.P. 2007: Moraine pebbles and boulders yield indistinguishable  $^{10}\text{Be}$  ages: A case study from Colorado, USA. *Eos Trans. AGU*, 88(52), Fall Meeting. Suppl., Abstract PP33B-1272
- Briner, J. P., Miller, G., Davies, P. T., Bierman, P. R. & Caffee, M. 2003: Last Glacial Maximum ice sheet dynamics in the Canadian Arctic inferred from young erratics perched on ancient tors. *Quaternary Science Reviews* 22, 437-444.
- Briner, J. P., Miller, G. H., Davis, T. R. & Finkel, R. 2005: Cosmogenic exposure dating in arctic glacial landscapes: implications for the glacial history of northeastern Baffin Island, Arctic Canada. *Canadian Journal of Earth Sciences* 42, 67-84.
- Briner, J. P., Miller, G., Davies, P. T. & Finkel, R. 2006: Cosmogenic radionuclides from fiord landscapes support differential erosion by overriding ice sheets. *GSA Bulletin* 118, 406-430.
- Davis, P. T., Bierman, P. R., Marsella, K. A., Caffee, M. W. & Southon, J.R. 1999: Cosmogenic analysis of glacial terrains in the eastern Canadian Arctic: a test for inherited nuclides and the effectiveness of glacial erosion. *Annals of Glaciology* 28, 181-188.
- Davis, P. T., Briner, J. P., Coulthard, R. P., Finkel, R. W. & Miller, G. H. 2006: Preservation of Arctic landscapes overridden by cold-based ice sheets. *Quaternary Research* 65, 156-163.
- Dowdeswell, J. A., Uenzelmann-Neben, G., Whittington, R. J. & Marienfeld, P. 1994: The Late Quaternary sedimentary record in Scoresby Sund, East Greenland. *Boreas* 23, 294-310.
- Evans, J., Dowdeswell, J. A., Grobe, H., Niessen, F., Stein, R., Hubberten, H. W. & Whittington, R. J. 2002: Late Quaternary sedimentation in Kejsar Franz Joseph Fjord and the continental margin of East Greenland. In Dowdeswell, J. A., Ó Cofaigh, C. (eds.): *Glacier influenced sedimentation on high latitude continental margins*, 149-179. Geological Society of London: Special Publications 203, London, United Kingdom.
- Fabel, D., Stroeven, A. P., Harbour, J., Kleman, J., Elmore, D. & Fink, D. 2002: Landscape preservation under Fennoscandian ice sheets determined from in situ produced  $^{10}\text{Be}$  and  $^{26}\text{Al}$ . *Earth and Planetary Science Letters* 201, 397-406.
- Fink, D. & Smith, A. 2007: An inter-comparison of  $^{10}\text{Be}$  and  $^{26}\text{Al}$  AMS reference standards and the  $^{10}\text{Be}$  half-life. *Nuclear Instruments and Methods in Physics Research B* 259, 600-609.
- Funder, S. 1972: Remarks on the Quaternary geology of Jameson Land and adjacent areas, Scoresby Sund, East Greenland. *Grønlands Geologiske Undersøgelse, report* 48, 93-98.
- Funder, S. 1984: Chronology of the last interglacial/glacial cycle in Greenland: first approximation. In Mahaney, W.C. (ed.): *Correlation of Quaternary chronologies*, 261-279. GeoBooks, Norwich.
- Funder, S. 1989: Quaternary geology of the ice-free areas and adjacent shelves of Greenland; Chapter 13. In Hulton J.F. (ed): *Quaternary geology of Canada and Greenland*, 742-792. Geological Survey of Canada.
- Funder, S. 2004: Middle and late Quaternary glacial limits in Greenland. In Ehlers, J. & Gibbard, P. L. (eds): *Quaternary Glaciations – Extent and Chronology, Part II*, 425-430. Elsevier, Amsterdam.

- Funder, S. & Hansen, L. 1996: The Greenland Ice Sheet – a model for its culmination and decay during and after the last glacial maximum. *Bulletin of the Geological Society of Denmark* 42, 137-152.
- Funder, S. & Hjort C. 1973: Aspects of the Weichselian chronology in central East Greenland. *Boreas* 2, 69-84.
- Funder, S., Hjort, C. & Landvik, J. Y. 1994: The last glacial cycle in East Greenland, an overview. *Boreas* 23, 283-293.
- Funder, S., Hjort, C., Landvik, J. Y., Nam, S.-I., Reeh, N. & Stein, R. 1998: History of a stable ice margin – East Greenland during the middle and upper Pleistocene. *Quaternary Science Reviews* 17, 77-123.
- Gosse, J. C. & Phillips, F. M. 2001: Terrestrial in-situ cosmogenic nuclides; theory and application. *Quaternary Science Reviews* 20, 1275-1560.
- Hansen, L., Funder, S., Murray, A. S. & Mejdal, S. 1999: Luminescence dating of the last Weichselian Glacier advance in East Greenland. *Quaternary Geochronology* 18, 179-190.
- Harbour, J., Stroeven, A. P., Fabel, D., Clarhäll, A., Kleman, J., Li, Y., Elmore, D. & Fink, D. 2006: Cosmogenic nuclide evidence for minimal erosion across two subglacial sliding boundaries of the late glacial Fennoscandian ice sheet. *Geomorphology* 75, 90-99.
- Hjort, C. 1979: Glaciation in northern East Greenland during the Late Weichselian and Early Flandrian. *Boreas* 8, 281-296.
- Hjort, C. 1981: A glacial chronology for northern East Greenland. *Boreas* 10, 259-274.
- Hjort, C. & Salvigsen, O. 1991: The channel and tor landscape in southeastern Jameson Land, East Greenland. *LUNDQUA Report* 33, 23-26.
- Håkansson, L. 2008: The Late Quaternary Glacial History of Northeast Greenland; cosmogenic isotope constraints on chronology and ice dynamics. *LUNQUA thesis* 61.
- Håkansson, L., Briner, J., Alexanderson, H., Aldahan, A. & Possnert, G. 2007: <sup>10</sup>Be ages from coastal northeast Greenland constrain the extent of the Greenland Ice Sheet during the Last Glacial Maximum. *Quaternary Science Reviews* 26, 2316-2321.
- Johnsen, S. J., Clausen, H. B., Dansgaard, W., Gundestrup, N. S., Hansson, M., Jonsson, P., Steffensen, J. P. & Sveinbjörnsdóttir, A. E. 1992: A “deep” ice core from East Greenland. *Meddelelser om Grønland, Geoscience* 29, 22 pp.
- Kaplan, M. R., Coranto, A., Hulton, N. R. J., Rabassa, J.O., Kubik, P. W. & Freeman, S. P. H. T. 2007: Cosmogenic nuclide measurements in southernmost South America and implications for landscape change. *Geomorphology* 87, 284-301.
- Kohl, C.P. & Nishiizumi, K. 1992: Chemical isolation of quartz for measurement of in-situ produced cosmogenic nuclides. *Geochimica et Cosmochimica Acta* 56, 3583-3587.
- Lal, D. 1991: Cosmic ray labeling of erosion surfaces: In-situ nuclide production rates and erosion models. *Earth and Planetary Science Letters* 104, 424-439.
- Landvik, J. Y. 1994: The last glaciation of Germania Land and adjacent areas, northeast Greenland. *Journal of Quaternary Science* 9, 81-92.
- Landvik, J. Y., Lyså, A., Funder, S., Kelly, M. 1994: The Eemian and Weichselian stratigraphy of the Langelandselv area, Jameson Land East Greenland. *Boreas* 23, 412-423.
- Landvik, J. Y., Brook, E. J., Gualtieri, L., Raisbeck, G., Salvigsen, O. & Yiou, F. 2003: Northwest Svalbard during the last glaciation: Ice-free areas existed. *Geology* 31, 905-908.
- Lasca, N. P. 1969. The Surficial Geology of Skeldal, Mesters Vig, North East Greenland. *Meddelelser om Grønland* 176:3, 56 pp.
- Lyså, A. & Landvik, J. Y. 1994: The lower Jyllandselv succession: evidence for three Weichselian glacier advances over coastal Jameson Land, East Greenland. *Boreas* 23, 434-446.
- Marquette, G. C., Gray, J. T., Gosse, J. C., Courchesne, F., Stockli, L., Macpherson, G. & Finkel, R. 2004: Felsenmeer persistence under non-erosive ice in the Torngat Mountains and Kaumajet Mountains, Quebec and Labrador, as determined by soil weathering and cosmogenic nuclide exposure dating. *Canadian Journal of Earth Sciences* 41, 19-38.
- Möller, P., Hjort, C., Adrielsson, L. & Salvigsen, O. 1994: Glacial history of interior Jameson Land, East Greenland. *Boreas* 23, 320-348.
- Nam, S.-I., Stein, R., Grobe, H., & Hubberten, H. 1995: Late Quaternary glacial/interglacial changes in sediment composition at the East Greenland continental margin and their paleocenaographic implications. *Marine Geology* 122, 243-262.
- Nordenskjöld, O. 1907: On the Geology and Physical Geography of East Greenland. *Meddelelser om Grønland* 28, 151-284.
- Ó Cofaigh, C., Dowdeswell, J. A., Evans, J., Kenyon, N. H., Taylor, J., Mienert, J., & Wilken, M. 2004: Timing and significance of glacially influenced mass-wasting in the submarine channels of the Greenland Basin. *Marine Geology* 207, 39-54.
- Putkonen, J. & O’Neil, M. A. 2006: Quaternary degradation of unconsolidated landforms in the western North America. *Geomorphology* 75, 408-419.
- Putkonen, J. & Swanson, T. 2003: Accuracy of cosmogenic ages for moraines. *Quaternary Research* 59, 255-261.
- Ronnert, L. & Nyborg, M. R. 1994: The distribution of different glacial landscapes on southern Jameson Land, East Greenland according to Landsat Thematic Mapper data. *Boreas* 23, 294-311.
- Schunke, E. 1986: Periglazialformen und Morphodynamik im südlichen Jameson Land, Ost-Grønland. *Abhandlungen der Akademie der Wissenschaften in Göttingen. Vanderhoeck & Ruprecht, Göttingen*, 142 pp.
- Stein, R., Nam, S.-I., Grobe, H. & Hubberten, H. 1996: Late Quaternary glacial history and short-term ice rafted debris fluctuations along the east Greenland continental margin. *In*



- Andrews et al. (eds): *Late Quaternary Paleoceanography of the North Atlantic Margins*, Geological Society Special Publication 111, 135-151.
- Stone, J.O. 2000: Air pressure and cosmogenic isotope production. *Journal of geophysical research* 105, 23753-23759.
- Sugden, D. E. 1974: Landscapes of glacial erosion in Greenland and their relationship to ice, topographic and bedrock conditions. *Institute of British Geographers, special publication* 7, 177-195.
- Stroeven, A. P., Fabel, D., Hättestrand, C. & Harbour, J. 2002: A relict landscape in the centre of the Fennoscandian glaciation: cosmogenic radionuclide evidence of tors preserved through multiple glacial cycles. *Geomorphology* 44, 145-154.
- Tveranger, T., Houmark-Nielsen, M., Løvberg, K. & Mangerud, J. 1994: Eemian-Weichselian stratigraphy of the Flakkerhuk ridge, southern Jameson land, East Greenland. *Boreas* 23, 359-384.
- Washburn, A. L. 1965: Geomorphic and vegetational studies in the Mesters Vig district. *Meddelelser om Grønland* 166, 60 pp.
- Wilken, M. & Mienert, W. 2006: Submarine glacial debris-flows, deep-sea channel and past ice stream behaviour of the east Greenland continental margin. *Quaternary Science Reviews* 25, 784-810.

## Appendix IV



# COSMOGENIC $^{10}\text{Be}$ -AGES FROM THE STORE KOLDEWEY ISLAND, NE GREENLAND

BY

LENA HÅKANSSON<sup>1,2</sup>, ANGELA GRAF<sup>3</sup>, STEFAN STRASKY<sup>4</sup>, SUSAN IVY-OCHS<sup>5</sup>,  
PETER W. KUBIK<sup>6</sup>, CHRISTIAN HJORT<sup>1</sup> AND CHRISTIAN SCHLÜCHTER<sup>3</sup>

<sup>1</sup> Department of Geology, Quaternary Sciences, Lund, Sweden

<sup>2</sup> Paleoclimate Laboratory, University at Buffalo NY, USA

<sup>3</sup> Institute of Geological Sciences, University of Bern, Switzerland

<sup>4</sup> Institute of Isotope Geochemistry and Mineral Resources ETH Zürich, Switzerland

<sup>5</sup> Institute of Particle Physics, ETH Zürich, 8092 Zürich, Switzerland

<sup>6</sup> Paul Scherrer Institut c/o Institute of Particle Physics, ETH Zürich, Switzerland

Håkansson, L., Graf, A., Strasky, S., Ivy-ochs, S., Kubik, P.W., Hjort, C. and Schlüchter, C., 2007: Cosmogenic  $^{10}\text{Be}$ -ages from the Store Koldewey island, NE Greenland. *Geogr. Ann.*, 89 A (3): 195–202.

**ABSTRACT.** Earlier work in northeast Greenland has suggested a limited advance of the Greenland Ice Sheet during the Last Glacial Maximum (LGM). However, this concept has recently been challenged by marine geological studies, indicating grounded ice on the continental shelf at this time. New  $^{10}\text{Be}$ -ages from the Store Koldewey island, northeast Greenland, suggest that unscoured mountain plateaus at the outer coast were covered at least partly by cold-based ice during the LGM. It is, however, still inconclusive whether this ice was dynamically connected to the Greenland Ice Sheet or not.

Regardless of the LGM ice sheet extent, the  $^{10}\text{Be}$  results from Store Koldewey add to a growing body of evidence suggesting considerable antiquity of crystalline unscoured terrain near present and Pleistocene ice sheet margins.

*Key words:* Greenland, cosmogenic exposure dating, blockfields

## Introduction

Ice sheets play an important role in the global climate system, affecting, for example, the circulation patterns in the ocean and the global sea-level (e.g. Clark *et al.* 1999; Otto-Bliesner *et al.* 2006). Large and dynamic ice sheets reaching the continental shelves are more interactive with the rest of the climate system compared to less extensive ice sheets terminating on land. Thus, studying extent, thickness and dynamic behaviour of past and present ice sheets is crucial for understanding global climate change.

Along the presently ice-free northeast Green-

land continental margin, interfjord uplands and coastal lowlands are commonly strongly weathered, in contrast with fjord and valley troughs which are characterized by fresh-looking surfaces of glacial erosion. Based on intense bedrock weathering and the lack of deposits from the last glaciation, it has long been thought that interfjord uplands along the northeast Greenland coast have been ice-free throughout the last glacial cycle (Funder and Hjort 1973; Hjort 1979, 1981; Björck and Hjort 1984).

During the most recent decades, considerable effort has been put into both on- and offshore investigations of the Late Quaternary glacial history of northeast Greenland. One large step was taken through the 'Polar North Atlantic Margins' (PON-AM) programme, in which most investigations focused on the Scoresby Sund area (Fig. 1a). This work led to the **Last Glacial Maximum (LGM)** reconstruction of a large outlet glacier, terminating at the mouth of the Scoresby Sund leaving adjacent land areas and the continental shelf free from ice (e.g. Dowdeswell *et al.* 1994; Funder *et al.* 1998).

The concept of a restricted LGM glaciation of northeast Greenland has, however, recently been challenged by new marine studies. Seismic data off the Keiser Franz Joseph Fjord (Fig. 1a) show a prominent moraine c. 50 km from the shelf break interpreted to be a LGM terminal or recessional moraine (Evans *et al.* 2002). Furthermore, O'Co-faigh *et al.* (2004) suggest that submarine channels emanating down the continental slope from the lip of shelf troughs (c. 73–75°N) are generated by glacier ice on the outer shelf or at the shelf break. Radiocarbon dates show that mass wasting

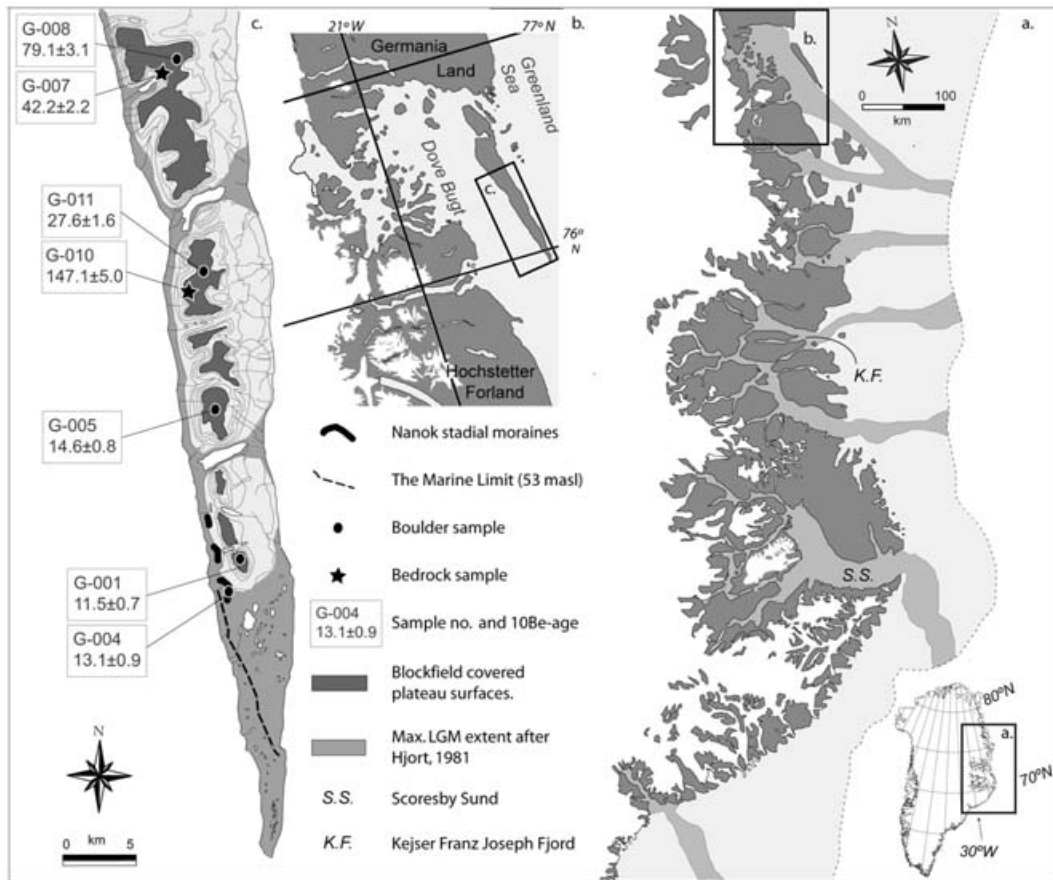


Fig. 1. (a) Overview map of northeast Greenland. The dotted line marks the continental shelf break and darker grey areas show cross-shelf troughs. (b) Map over the Dove Bugt area. (c) Map showing sample positions,  $^{10}\text{Be}$  ages and geomorphological features. Contour intervals are 100 m and dark grey areas show blockfield-covered plateau surfaces, mapped from aerial photographs

in these channels ceased around 13 ka indicating that the last time these channels were active was during the LGM. Both these studies suggest grounded ice on the shelf during the LGM; however, they do not investigate further the extent of ice cover on land.

Here we discuss new  $^{10}\text{Be}$ -ages from the island of Store Koldewey, northeast Greenland, suggesting that unscoured mountain plateaus at the outer coast were covered by cold-based ice during the LGM.

### Geological setting

The island of Store Koldewey (76–77°N) is situated immediately inside the continental shelf, isolating the Dove Bugt embayment in the west from the

open Greenland Sea to the east (Fig. 1). High mountain plateaus (550–800 m a.s.l.) made up by Caledonian crystalline rocks dominate the landscape of this island. On the west coast the terrain rises steeply from close to the shoreline towards the summit plateaus, whereas in the east lowlands of Mesozoic sedimentary rocks are gently rising towards the steep mountain slopes. The Caledonian crystalline rocks are found all around the Dove Bugt Embayment (Henriksen 1997).

Unscoured bedrock outcrops are exposed along the edges of the summit plateaus of Store Koldewey (Fig. 2a). On the central parts of these plateaus the ground is either covered by well developed block fields where the individual blocks have dimensions of 0.5–1 m or by scattered blocks less than 0.5 m tall surrounded by weath-

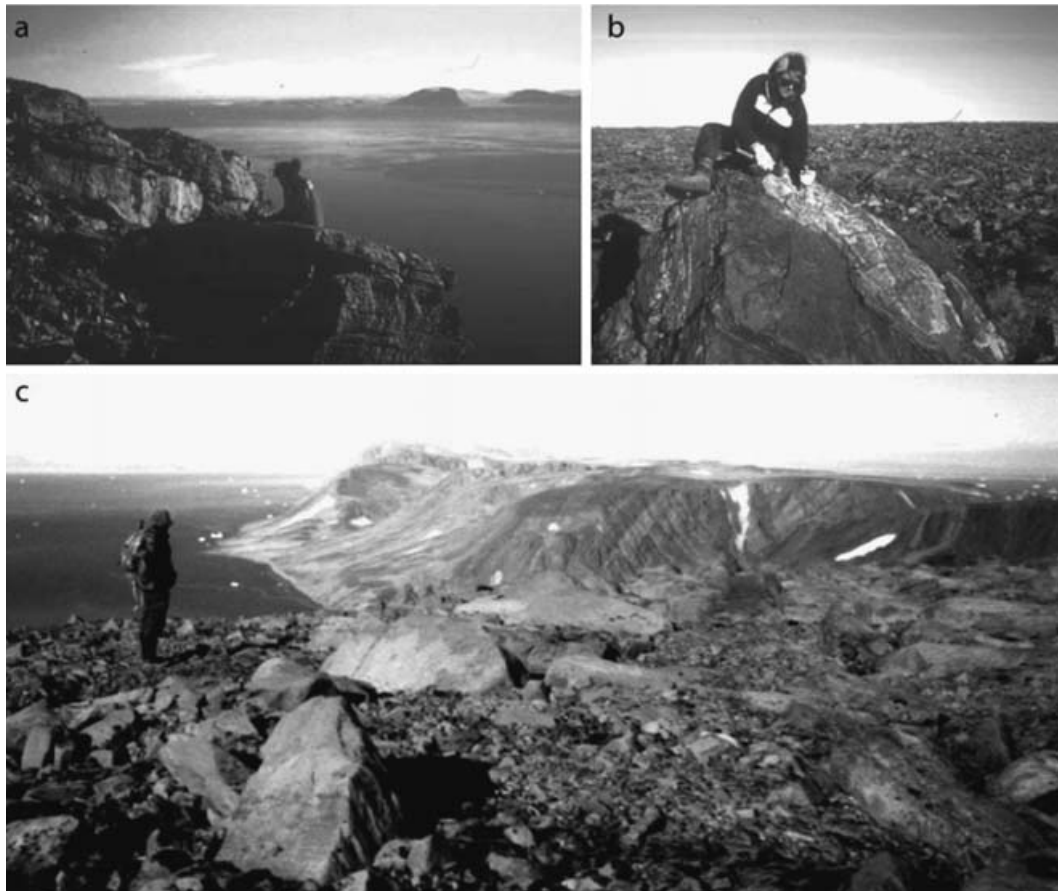


Fig. 2. (a) Sampling of a tor surface along the western plateau edge (G-010). (b) Sampling a boulder (G-005). (c) The blockfield-covered summit plateaus of Store Koldewey towards the north

ered cobble-sized local material (Fig. 2b). These two surface types occur in patches and are equally distributed on both the northern and southern summit plateaus. There is a scattered distribution of larger boulders (0.5–2 m high) and more rarely, erratic quartzite cobbles on both surface types. The larger boulders are generally more rounded compared to the surrounding material (Fig. 2c). U-shaped valleys dissect the high plateaus, cutting through the island from west to east. The southern lowland exhibits a characteristic glacially eroded landscape with numerous rock basins. Sharp-crested moraine ridges at elevations between 80 and 100 m a.s.l. can be followed along the west coast of the island and have been correlated to ice-marginal features at the same altitude on the opposing mainland. Based on earlier stud-

ies it has been suggested that these moraines mark the extent of LGM ice and that they were formed by an advance of a floating ice front, referred to by Hjort (1981) as the Nanok stadial (Fig. 1c). Radiocarbon dates from Hochstetter Forland and the mainland north thereof give minimum deglacial ages of *c.* 9.5  $^{14}\text{C}$  ka BP (Hjort 1981; Björck and Hjort 1984; Björck *et al.* 1994).

Investigations in adjacent areas, on Hochstetter Forland (Björck and Hjort 1984) and Germania Land (Landvik 1994) suggest that northeast Greenland experienced at least one extensive ice advance prior to the LGM, when the Greenland Ice Sheet expanded to the continental shelf break (Fig. 1a). According to these studies, erratics should have been deposited on the unscoured areas during this older glaciation.

Table 1. Sample numbers and  $^{10}\text{Be}$  data for boulder and bedrock samples from Store Koldewey. Surface exposure ages were modelled using a production rate of  $5.1 \pm 0.3 \text{ g}^{-1} \text{ SiO}_2 \cdot \text{a}^{-1}$ , for  $^{10}\text{Be}$  (Stone 2000). Surface erosion rates ( $\epsilon = 0, 1 \text{ mm ka}^{-1}$  and  $2 \text{ mm ka}^{-1}$ ) have been used to calculate  $^{10}\text{Be}$ -ages

Sample	Elevation (m.)	Boulder size (l × w × h) (m.)	$^{10}\text{Be}$ (105 atoms $\text{g}^{-1}$ )	$^{10}\text{Be}$ age (ka) $\epsilon = 0$	$^{10}\text{Be}$ age (ka) $\epsilon = 1 \text{ mm ka}^{-1}$	$^{10}\text{Be}$ age (ka) $\epsilon = 2 \text{ mm/ka}^{-1}$
<i>Moraine boulder</i>						
G.-004	93	0.5 × 1 × 0.6	0.7 ± 0.05	16 ± 1	16 ± 1	17 ± 1
<i>Boulders on unscoured terrain</i>						
G.-001	630	1 × 1 × 0.7	1.05 ± 0.07	14 ± 1	14 ± 1	14 ± 1
G.-005	617	3 × 2 × 1.5	1.28 ± 0.08	18 ± 1	18 ± 1	18 ± 1
G.-008	568	4 × 3 × 0.7	6.74 ± 0.24	97 ± 5	106 ± 11	118 ± 13
G.-011	652	2 × 1.5 × 0.5	2.58 ± 0.13	33 ± 2	34 ± 2	36 ± 2
<i>Unscoured bedrock</i>						
G.-007	686	bedrock	4.05 ± 0.2	51 ± 3	53 ± 4	56 ± 4
G.-010	704	bedrock	13.5 ± 0.41	178 ± 8	214 ± 42	282 ± 78

### Cosmogenic exposure dating

Fieldwork was carried out on Store Koldewey during the summer of 2003 when samples for cosmogenic exposure dating were collected from boulders and bedrock (Fig. 2). Boulder samples were taken from the top surfaces of wide-based boulders, resting on flat, well-drained ground.

Processing of samples was done at the Institute of Geological Sciences, University of Bern, Switzerland. After crushing and sieving, the 0.25–0.4 mm fraction was run through a magnetic separator followed by selective mineral dissolution using nitric and hydrofluoric acid (Kohl and Nishiizumi 1992; Bierman 1994). Beryllium was extracted from dissolved clean quartz following Ochs and Ivy-Ochs (1997), and  $^{10}\text{Be}$  measurements were made at the ETH/PSI tandem facility in Zürich-Hönggerberg. Cosmogenic exposure ages were modelled using a production rate of  $5.1 \pm 0.3 \text{ atoms g}^{-1} \text{ a}^{-1}$  for  $^{10}\text{Be}$ , and production rates were scaled to geographic latitude and altitude (Stone 2000).

In addition, cosmogenic  $^{21}\text{Ne}$  was measured in the same quartz separates used for  $^{10}\text{Be}$  analyses. Unfortunately, high amounts of nucleonic neon were detected in the sampled lithologies. In combination with the relatively low  $^{21}\text{Ne}$  production rates at the sampling sites this made it impossible to distinguish the different neon components, hence to calculate reliable  $^{21}\text{Ne}$  exposure ages. Due to this fact the neon data are not further discussed here.

The calculation of exposure ages from glaciated terrain using cosmogenic isotope concentration relies on the assumptions that the sampled surface (i) lacks isotopes from previous exposures, requiring at least *c.* 2 m of glacial erosion (Davis *et al.* 1999)

and (ii) has experienced only minimal post-glacial surface erosion. Glacially scoured bedrock and erratic boulders often meet these assumptions, whereas strongly weathered bedrock surfaces do not. Thus, exposure ages from unscoured bedrock must be taken as minimum exposure durations (Gosse and Phillips 2001).

### Results

Cosmogenic exposure ages were calculated for four boulder and two bedrock samples from the weathered plateaus and one boulder perched on a sharp-crested moraine ridge on the southwest coast of Store Koldewey. The  $^{10}\text{Be}$ -ages are shown in Table 1 as a function of post-glacial surface erosion rate ( $1 \text{ mm ka}^{-1}$  and  $2 \text{ mm ka}^{-1}$ ).

On the plateaus, sample elevations for boulders range from 568 to 652 m a.s.l. (Table 1). All four sampled boulders consist of gneiss with medium quartz content, the same lithology as the local bedrock. Among the samples from the summit plateaus, the two southernmost boulders give young ages ( $11.5 \pm 0.7$  and  $14.6 \pm 0.8 \text{ ka}$ ), in contrast with the rest of the boulder samples ( $27.6 \pm 1.6$  and  $79.1 \pm 3.1 \text{ ka}$ ). The samples from weathered bedrock ( $42.2 \pm 2.2 \text{ ka}$  and  $147.1 \pm 5.0 \text{ ka}$ ) are sampled on the same plateaus as the older two boulders. (Fig. 1c, Table 1). The boulder from the moraine ridge on the southern lowland yielded an exposure age of  $13.1 \pm 0.9 \text{ ka}$ .

### Discussion

The moraines on the west coast of Store Koldewey have been referred to as part of the Nanok stadial

ice-marginal zone radiocarbon dated to *c.* 9.5  $^{14}\text{C}$  ka BP (Hjort 1981). Only one moraine boulder was dated from the Nanok stadial drift ( $13.1 \pm 0.9$  ka). Since this age overlaps with the two youngest boulders on the Store Koldewey plateaus ( $11.5 \pm 0.7$  and  $14.6 \pm 0.8$  ka) and since the radiocarbon age provides only a minimum estimate of the deglaciation, it may indicate the timing of deglaciation. However, another possibility would be that this moraine marks the marginal position of an early Holocene advance of an outlet glacier into Dove Bugt, implying that the older age is due to the glacier picking up a boulder deposited previously by the LGM advance. Based on only one dated boulder we cannot decide which of these scenarios is the most likely. To accurately estimate the age of a sharp-crested young moraine ridge, it has been recommended to analyse samples from at least three boulders (Putkonen and Swanson 2003).

Previous research suggests two main hypotheses for interpreting the different degrees of weathering in arctic fjord landscapes in terms of ice extent during the LGM. (i) In the Nunatak Hypothesis, highly weathered terrain is interpreted as having been ice-free while freshly eroded troughs held outlet glaciers (Ives 1966; Nesje and Dahl 1990; Ballantyne *et al.* 1998; Rae *et al.* 2004). (ii) In the Selective Glacial Erosion Hypothesis, weathering zones represent differential modification under overriding ice caused by spatial variations in basal thermal regimes (e.g. Sugden 1978; Sollid and Sørbel 1994; Kleman and Hätterstrand 1999; Davis *et al.* 2006). According to the latter hypothesis, weathered areas have been preserved beneath cold-based ice, whereas scoured areas in fjords and valleys have been modified by warm-based ice sliding along its bed. The Nunatak Hypothesis is compatible with earlier terrestrial work in north-east Greenland, suggesting a limited LGM advance of the Greenland Ice Sheet (Fig. 1c; Hjort 1981; Funder *et al.* 1998). In contrast, an extensive, selectively eroding ice sheet advance, covering Store Koldewey during the LGM, might be in line with the interpretations of recent marine studies on the East Greenland shelf (Evans *et al.* 2002; O’Cofaigh *et al.* 2004).

The  $^{10}\text{Be}$ -ages presented here can be interpreted in at least three ways, representing three different LGM scenarios for Store Koldewey and NE Greenland; two of these are in line with earlier investigations suggesting restricted LGM ice whereas one is compatible with an extensive ice sheet advance during the LGM.

- (1) *Ice-free plateaus.* In this scenario the sampled boulders are interpreted as part of the blockfield. The  $^{10}\text{Be}$  ages indicate exposure time since these boulders have been brought to the surface through frost heaving. The young boulder samples ( $11.5 \pm 0.7$  and  $14.6 \pm 0.8$  ka) were taken from the southernmost plateaus (Fig. 1c), which in this scenario would imply periglacial activity on these plateaus during Late Glacial times.
- (2) *Local cold-based ice cap.* Boulders on the Store Koldewey plateaus were brought to their present location during a pre-LGM advance of the Greenland Ice Sheet. The young boulders ( $11.5 \pm 0.7$  and  $14.6 \pm 0.8$  ka) are here interpreted as having been mobilized by a local LGM ice cap. Thus, the southernmost plateaus require local ice cover, whereas the plateaus further to the north where the old boulder and bedrock samples are found might have been ice-free during the LGM.
- (3) *Extensive ice sheet.* The two young boulders ( $11.5 \pm 0.7$  and  $14.6 \pm 0.8$  ka), were brought to the southernmost plateaus during an extensive LGM advance of the Greenland Ice Sheet. The two older boulders ( $27.6 \pm 1.6$  and  $79.1 \pm 3.1$  ka) were either deposited by the same advance, containing inherited cosmogenic isotopes, or during earlier ice sheet advances. Thus, the  $^{10}\text{Be}$ -ages require cold-based ice cover at least on the southernmost plateaus. However, in contrast to scenario (ii) this ice was dynamically connected to the Greenland Ice Sheet and to active ice in the Dove Bugt embayment.

In the last years a wealth of studies, applying cosmogenic isotopes to differentially weathered crystalline terrain, has shown old (pre-LGM) surface exposure ages of blockfield material and tors in Antarctica (Sugden *et al.* 2005), Arctic Canada (Briner *et al.* 2003, 2005, 2006; Staiger *et al.* 2005), the British Isles (Stone *et al.* 1998, Ballantyne *et al.* 2006) and Scandinavia (Brook *et al.* 1996, Stroeve *et al.* 2002). The bedrock ages from the unscoured plateaus of Store Koldewey ( $42.2 \pm 2.2$  ka and  $147.1 \pm 5.0$  ka) add to this growing body of evidence suggesting that crystalline weathered terrain has been stable at least during the end of the last glacial cycle and during the Holocene. We use this reasoning to argue against scenario (i) and that boulders on the Store Koldewey plateaus have been mobilized through periglacial activity. This leaves us with two LGM scenarios; a local cold-based plateau ice-cap or an extensive polythermal ice sheet advance. However,



based on single isotope exposure ages of bedrock no conclusions can be drawn about whether the high isotope concentrations (old ages) of our bedrock samples and G-008 ( $79.1 \pm 3.1$  ka) have been accumulated during one long exposure period or during multiple exposure periods interrupted by cold-based non-erosive ice. Thus it is still inconclusive whether the northern plateaus where the old  $^{10}\text{Be}$ -ages are found were nunataks or covered by cold-based ice during the LGM. To reconcile between ice-free and cold-based ice-covered scenarios for unscoured terrain, recent studies have used paired isotope data ( $^{10}\text{Be}$  combined with  $^{26}\text{Al}$ ) from weathered bedrock (Fabel *et al.* 2002; Briner *et al.* 2003; Davis *et al.* 2006; Phillips *et al.* 2006).

Briner *et al.* (2005) demonstrate that in differentially weathered fjord landscapes it is expected to find scattered exposure ages from erratics resting on unscoured terrain that has been covered by cold-based ice. In contrast samples from glacially scoured terrain give consistently young (LGM) ages. They emphasize the importance of large numbers of exposure ages from unscoured terrain when reconstructing the extent and dynamics of ice advances in differentially weathered fjord zones.

The scattered distribution and the few values of the present data set restrain us from choosing between a local cold-based plateau ice-cap and an extensive polythermal ice sheet advance.

### Conclusions

The present study approaches the glacial history of northeast Greenland by using cosmogenic exposure dating. Here we suggest that unscoured mountain plateaus at the outer coast were covered at least partly by cold-based ice during the LGM. Since the dataset is small and all sampled boulders consist of the same lithology as the local bedrock, it is, however, still inconclusive whether this ice was dynamically connected to the Greenland Ice Sheet. Regardless of the LGM ice sheet extent, the present study adds to a growing body of evidence suggesting considerable antiquity of crystalline unscoured terrain proximal to great ice sheets.

### Acknowledgements

AWI Bremerhaven is acknowledged with appreciation and especially Wilfried Jokat, the leader of the Polarstern cruise ARK XIX. This study was

supported by the Swedish Research Council (VR), The Swedish Society for Anthropology and Geography (SSAG). Analytical costs were funded by the Swiss National Science Foundation, grant number 200020–105220. The Swedish Polar Research Secretariat helped with providing field equipment and The Danish Polar Centre helped provided permits to work in the National Park. Ole Bennike, Nadja Hultsch, Martin Klug, Svenja Kobabe, Holger Cremer and Bernd Wagner are thanked for great help and wonderful company in the field. The manuscript benefited greatly from comments and discussions with Yarrow Axford, Jason Briner, Ole Humlum and Johan Kleman.

*Lena Håkansson, Department of Geology, Quaternary Sciences. GeoBiosphere Centre, Sölvegatan 12, 223 62 Lund, Sweden and Paleoclimate Laboratory, University at Buffalo, 876 NSC, Buffalo, NY 14260, USA.*

*E-mail: Lena.Hakansson@geol.lu.se*

*Angela Graf, Institute of Geological Sciences, University of Bern, Baltzerstrasse 1–3, 3012 Bern, Switzerland*

*Stefan Strasky, Institute of Geological Sciences, University of Bern, Baltzerstrasse 1–3, 3012 Bern, Switzerland*

*Susan Ivy-Ochs, Paul Scherrer Institut c/o Institute of Particle Physics, ETH Zürich, Clausiusstrasse 25, 8092 Zürich, Switzerland*

*Peter Kubik, Paul Scherrer Institut c/o Institute of Particle Physics, ETH Zürich, Clausiusstrasse 25, 8092 Zürich, Switzerland*

*Christian Hjort, Department of Geology, Quaternary Sciences. GeoBiosphere Centre, Sölvegatan 12, 223 62 Lund, Sweden*

*Christian Schlüchter, Institute of Geological Sciences, University of Bern, Baltzerstrasse 1–3, 3012 Bern, Switzerland*

### References

- Ballantyne, C.K., McCarroll, D., Nesje, A. and Dahl, S.O., 1998: The last ice sheet in North-West Scotland: Reconstruction and implications. Quaternary Science Reviews, 17: 1149–1184.*  
*Ballantyne, C.K., McCarroll, D. and Stone, J.O., 2006: Vertical dimensions and age of the Wicklow Mountains ice dome,*

- Eastern Ireland, and implications for the extent of the last Irish ice sheet. *Quaternary Science Reviews*, 25: 2048–2058.
- Bierman, P.R., 1994: Using in situ cosmogenic isotopes to estimate rates of landscape evolution: A review from the geomorphic perspective. *Journal of Geophysical Research*, 99: 13885–13896.
- Björck, S. and Hjort, C., 1984: A re-evaluated glacial chronology for northern East Greenland. *Geologiska Föreningens i Stockholms Förhandlingar*, 105: 235–243.
- Björck, S., Wohlfahrt, B., Bennike, O., Hjort, C. and Persson, T., 1994: Revision of the early Holocene lake sediment based chronology and event stratigraphy on Hochstetter Forland, NE Greenland. *Boreas*, 23: 513–523.
- Briner, J.P., Miller, G., Davies, P.T., Bierman, P.R. and Caffee, M., 2003: Last Glacial Maximum ice sheet dynamics in the Canadian Arctic inferred from young erratics perched on ancient tors. *Quaternary Science Reviews*, 22: 437–444.
- Briner, J.P., Miller, G.H., Davis, T. and Finkel, R.F., 2005: Cosmogenic exposure dating in arctic glacial landscapes: implications for the glacial history of northeastern Baffin Island, Arctic, Canada. *Canadian Journal of Earth Sciences*, 42: 67–84.
- Briner, J.P., Miller, G., Davies, P.T. and Finkel, R., 2006. Cosmogenic radionuclides from fiord landscapes support differential erosion by overriding ice sheets. *GSA Bulletin*, 118: 406–430.
- Brook, E.J., Nesje, A., Lehman S.J., Raisbeck, G.M. and Yiou, F., 1996: Cosmogenic nuclide exposure ages along a vertical transect in western Norway: implications for the height of the Fennoscandian ice sheet. *Geology*, 34: 207–210.
- Clark, P.U., Alley, R.B. and Pollard, D., 1999: Northern hemisphere ice-sheet influences on global climate change. *Science*, 286: 1104–1111.
- Davis, P.T., Bierman, P.R., Marsella, K.A., Caffee, M.W. and Southon, J.R., 1999: cosmogenic analysis of glacial terrains in the eastern Canadian arctic: a test for inherited nuclides and the effectiveness of glacial erosion. *Annals of Glaciology*, 28: 181–188.
- Davis, P.T., Briner, J.P., Coulthard, R.P., Finkel, R.W. and Miller, G.H., 2006: Preservation of Arctic landscapes overridden by cold-based ice sheets. *Quaternary Research*, 65: 156–163.
- Dowdeswell, J.A., Uenzelmann-Neben, G., Whittington, R.J. and Marienfeld, P., 1994: The Late Quaternary sedimentary record in Scoresby Sund, East Greenland. *Boreas* 23: 294–310.
- Evans, J., Dowdeswell, J.A., Grobe, H., Niessen, F., Stein, R., Hubberten, H.W. and Whittington, R.J., 2002: Late Quaternary sedimentation in Kejsar Franz Joseph Fjord and the continental margin of East Greenland. In: Dowdeswell, J.A. and O’Cofaigh, C. (eds): Glacier influenced sedimentation on high latitude continental margins. Geological Society. London. Special Publications 203. 149–179.
- Fabel, D., Stroeven, A.P., Harbor, J., Kleman, J., Elmore, D. and Fink, D., 2002: Landscape preservation under Fennoscandian Ice Sheets determined from in-situ produced <sup>10</sup>Be and <sup>26</sup>Al. *Earth and Planetary Science Letters*, 201: 397–406.
- Funder, S. and Hjort, C., 1973: Aspects of the Weichselian chronology in central East Greenland. *Boreas*, 2: 69–84.
- Funder, S., Hjort, C., Landvik, J.Y., Nam, S.-I., Reeh, N. and Stein, R., 1998: History of a stable ice margin – East Greenland during the middle and upper Pleistocene. *Quaternary Science Reviews*, 17: 77–123.
- Gosse, J.C. and Phillips, F.M., 2001: Terrestrial in-situ cosmogenic nuclides: theory and application. *Quaternary Science Reviews*, 20: 1275–1560.
- Henriksen, N., 1997: Geological Map of Greenland 1:500 000, Dove Bugt, Sheet 10. Copenhagen: Geological Survey of Denmark and Greenland.
- Hjort, C., 1979: Glaciation in northern East Greenland during the Late Weichselian and Early Flandrian. *Boreas*, 8: 281–296.
- Hjort, C., 1981: A glacial chronology for northern East Greenland. *Boreas*, 10: 259–274.
- Ives, J.D., 1966: Block fields, associated weathering forms on mountain tops and the Nunatak hypothesis. *Geografiska Annaler*, 48A: 220–223.
- Kleman, J. and Hättestrand, C., 1999: Frozen-bed Fennoscandian and Laurentide ice sheets during the Late Glacial Maximum. *Nature*, 402: 63–66.
- Kohl, C.P. and Nishizumi, K., 1992: Chemical isolation of quartz for measurement of in-situ produced cosmogenic nuclides. *Geochimica et Cosmochimica Acta*, 56: 3585–3587.
- Landvik, J.Y., 1994: The last glaciation of Germania Land and adjacent areas, northeast Greenland. *Journal of Quaternary Science*, 9: 81–92.
- Nesje, A. and Dahl, S.O., 1990: Autochthonous block fields in southern Norway – implications for the geometry, thickness an isostatic loading of the Late Weichselian Scandinavian ice sheet. *Journal of Quaternary Science*, 5: 225–234.
- O’Cofaigh, C., Dowdeswell, J.A., Evans, J., Kenyon, N.H., Taylor, J., Mienert, J. and Wilken, M., 2004: Timing and significance of glacially influenced mass-wasting in the submarine channels of the Greenland Basin. *Marine Geology*, 207: 39–54.
- Ochs, M. and Ivy-Ochs, S., 1997: The chemical behavior of Be, Fe, Ca and Mg during AMS target preparation from terrestrial silicates modeled with chemical speciation calculations. *Nuclear Instruments and Methods in Physics Research*, B123: 235–240.
- Otto-Bliesner, B.L., Marshall, S.J., Overpeck, J.T., Miller, G.H., Hu, A. and CAPE Last Interglacial Project members, 2006: Simulating arctic climate warmth and icefield retreat in the last interglaciation. *Science*, 311: 1751–1753. DOI: 10.1126/science.1120808.
- Phillips, W.M., Hall, A.M., Mottram, R., Fifield, L.K. and Sugden, D.E., 2006: Cosmogenic <sup>10</sup>Be and <sup>26</sup>Al exposure ages of tors and erratics, Cairngorm Mountains, Scotland: Timescales for the development of a classic landscape of selective linear glacial erosion. *Geomorphology*, 73: 222–245.
- Putkonen, J. and Swanson, T., 2003: Accuracy of cosmogenic ages for moraines. *Quaternary Research*, 59: 255–261.
- Rae, A.C., Harrison, S., Mighall, T. and Dawson, A.G., 2004: Periglacial trimlines and nunataks of the last glacial maximum: the Gap of Dunloe, southwest Ireland. *Journal of Quaternary Science*, 19: 87–97.
- Sollid, J.L. and Sørbel, L., 1994: Distribution of glacial landforms I Southern Norway in relation to the thermal regime of the last continental ice sheet. *Geografiska Annaler*, 76 (A): 25–36.
- Staiger, J.K.W., Gosse, J.C., Johnson, J.V., Fastook, J., Gray, J.T., Stockli, D.F., Stockli, L. and Finkel, R., 2005: Quaternary relief generation by polythermal glacier ice. *Earth Surface Processes and Landforms*, 30: 1145–1159. DOI: 10.1002/esp.1267.
- Stone, J.O., Ballantyne, C.K. and Fifield, L.K., 1998: Exposure dating and validation of periglacial weathering limits, Northwest Scotland. *Geology*, 26: 587–590.
- Stone, J.O., 2000: Air pressure and cosmogenic isotope production. *Journal of Geophysical Research*, 105: 23753–23759.
- Stroeven, A.P., Fabel, D., Hättestrand, C. and Harbour, J., 2002: A relict landscape in the centre of the Fennoscandian glaciation: cosmogenic radionuclide evidence of tors preserved

HÅKANSSON, L., GRAF, A., STRASKY, S., IVY-OCHS, S., KUBIK, P.W., HJORT, C. AND SCHLÜCHTER, C.

- through multiple glacial cycles. *Geomorphology*, 44: 145–154.
- Sugden, D.E., 1978: Glacial erosion by the Laurentide ice sheet. *Journal of Glaciology*, 83: 367–391.
- Sugden, D.E., Balco, G., Cowdery, S.G., Stone, J.O. and Sass, III L.C., 2005: Selective glacial erosion and weathering zones in the coastal mountains of Mary Bird Land, Antarctica. *Geomorphology*, 67: 317–334.
- Manuscript received Jan. 2007, revised and accepted June 2007.

